ACS EARTH AND SPACE CHEMISTRY

Review

Cite This: ACS Earth Space Chem. 2018, 2, 168−202

The Role of Organic Aerosol in Atmospheric Ice Nucleation: A Review

Daniel A. Knopf,*,† Peter A. Alpert,‡ and Bingbing Wang§

†Institute for Terrestrial and Planetary Atmospheres/School of Marine and Atmospheric Sciences, Stony Brook University, Stony Brook, New York 11794-5000, United States

‡Laboratory of Environmental Chemistry, Paul Scherrer Institute, 5232 Villigen, Switzerland

§State Key Laboratory of Marine Environmental Science, College of Ocean and Earth Sciences, Xiamen University, Xiamen 361102, China

ABSTRACT: Predicting the formation of ice in the atmosphere presents one of the great challenges in physical sciences with important implications for the chemistry and composition of the Earth's atmosphere, the hydrological cycle, and climate. Among atmospheric ice formation processes, heterogeneous ice nucleation proceeds on aerosol particles ranging from a few nanometers to micrometers in size, commonly referred to as ice nucleating particles (INPs). Research over the last two decades has demonstrated that organic matter (OM) is ubiquitous in the atmosphere, present as organic aerosol (OA) particles or as coatings on other particle types. The physicochemical properties of OM make predicting how OM can contribute to the INP population challenging. This review focuses on the role of OM in INPs, summarizing and highlighting recent advances in our understanding of the ice nucleation process gained from theoretical, laboratory, and field studies. Examination of ice residuals and INPs with analytical techniques demonstrates that OM participates in atmospheric ice crystal formation. Molecular dynamic simulations provide insight into the microscopic processes that initiate ice nucleation. The amorphous phase state of OM in the supercooled and metastable regime is identified as a key factor in assessing the particles' nucleation pathways and rates. A theoretical model is advanced, based on particle water activity, to holistically predict amorphous phase changes and ice nucleation rates of particles coated by OM. The goal of this review is to synthesize our current understanding and propose future research directions needed to fully evaluate how OA particles contribute to INPs in the atmosphere.

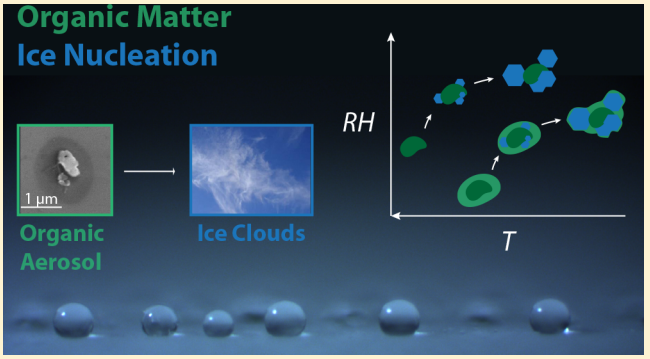

KEYWORDS: *Organic Aerosol, Ice Nucleation, Organic Matter, Amorphous Phase State, Molecular Dynamics Simulation, Laboratory Experiments, Field Measurements, Organic Coating*

INTRODUCTION

Water and its solid crystalline form, ice, are ubiquitous on land and in the air. Ice has not only been observed on Earth but also on planets[1,2] and moons[3−5] throughout the solar system, making it a particularly interesting subject because its melted form can provide the means for life.[6] The formation of ice in the Earth's atmosphere changes the radiative properties of clouds by modulating their interaction with incoming shortwave and outgoing longwave radiation, thereby impacting the radiative balance and thus, climate.[7−12] Greater than 50% of Earth's precipitation originates via the ice phase,[13] and hence, atmospheric ice nucleation plays a key role in the global hydrological cycle.[14] Ice crystals formed in the upper troposphere and lower stratosphere (UT/LS) can sediment, resulting in water removal and causing dehydration of the UT/LS.[15,16] This has consequences for water vapor distribution and thus the radiation budget considering that water vapor is the strongest greenhouse gas.[17,18] Ice particles at the tropopause control water transport into the LS affecting stratospheric chemical composition. Surfaces of ice crystals can serve as heterogeneous sites for reactions resulting in ozone destruction and act as a sink of HNO_3.[19−21] Despite recognition of the importance of atmospheric ice formation, our predictive understanding is still insufficient for its representation in climate models.[7,22]

Cloud droplet and primary ice crystal nucleation proceed on aerosol particles, which are suspensions of liquid or solid matter having sizes of a few nanometers to hundreds of micrometers. Ice multiplication mechanisms may proceed after some initial ice is present.[23−26] Whereas mineral dust particles and sea spray aerosol (SSA) account for the greatest aerosol mass concentrations, organic aerosol (OA) makes up a significant fraction of the ambient global tropospheric aerosol.[7,27−35] OA can contribute 20−90% by mass to the submicrometer aerosol.[27] OA can be directly emitted from sources such as

Received: October 24, 2017
Revised: January 17, 2018
Accepted: January 19, 2018
Published: January 19, 2018

DOI: 10.1021/acsearthspacechem.7b00120
ACS Earth Space Chem. 2018, 2, 168−202

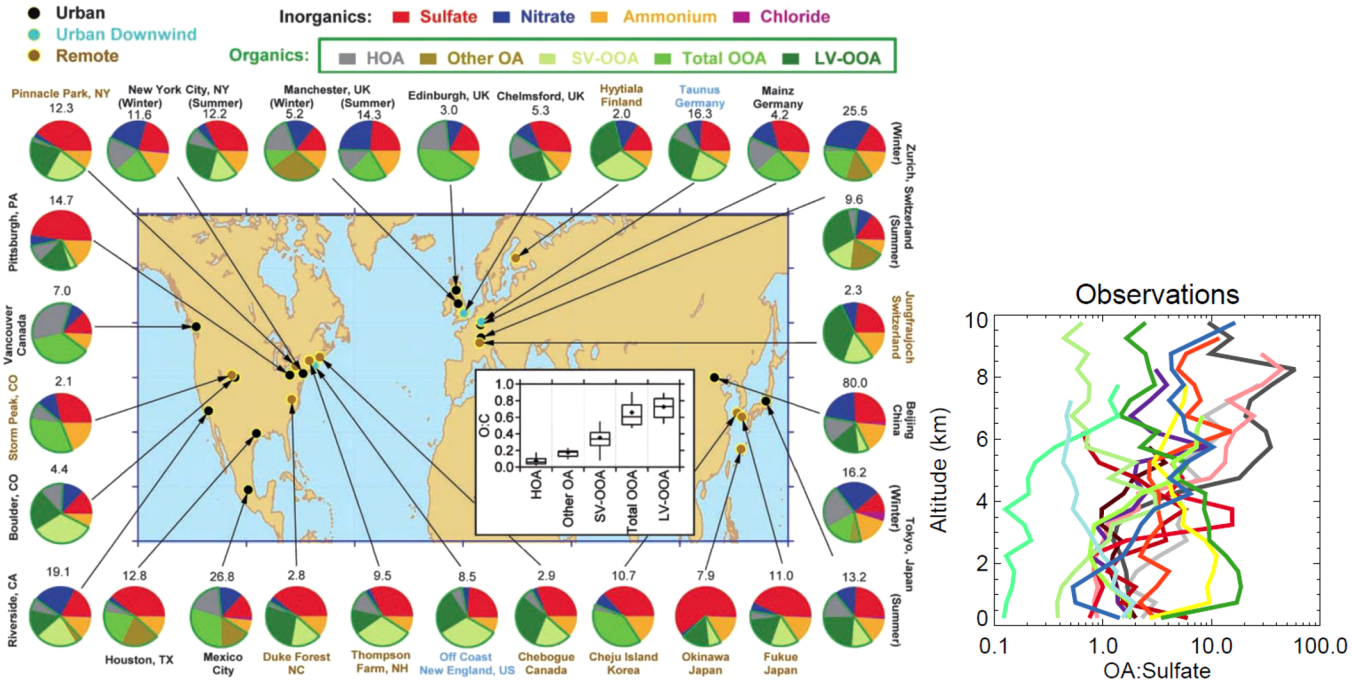

Figure 1. (left panel) Total mass concentration (in $\mu g\ m^{-3}$) and mass fractions of nonrefractory inorganic species and organic components in submicrometer aerosols and oxidation level expressed as oxygen to carbon ratio (O:C) measured with the aerosol mass spectrometer at multiple surface locations in the Northern Hemisphere. (right panel) Organic aerosol (OA) to sulfate ratio (OA:sulfate) as a function of altitude derived from 17 field campaigns. (left) Reprinted from Jimenez et al. (2009).[29] (right) Reprinted from Heald et al. (2011).[59]

fossil fuel combustion and biomass burning, termed primary OA (POA), whereas secondary organic aerosol (SOA) stems from the oxidation of volatile organic compounds (VOCs), the latter contributing significantly to the global OA burden.[28,36−39] The impact of organic matter (OM) generally on atmospheric ice nucleation is not well understood because its widespread atmospheric presence has been only thoroughly established with advancements of novel aerosol particle analytical techniques.[27−29,31,33] In contrast, biological particles (excluded from our definition of OM) and insoluble inorganic material such as mineral dust have been studied for their ice forming propensity for a much longer time.[40−47] The focus of this review is on the role of OM in atmospheric ice nucleation, concentrating on the last one to two decades of research that have linked OA particles with ice nucleation. It builds upon previous reviews that provide excellent overviews of various ice nucleation data sets including inorganic (e.g., mineral dust) and biological particle types and associated theoretical data representations.[10,48−57]

This review is organized as follows. The presence of OA in the atmosphere is first briefly surveyed followed by a discussion of the unique physicochemical properties of OM and OA and their effects on atmospherically relevant ice formation pathways. Then, the current microscopic understanding of homogeneous and heterogeneous ice nucleation is summarized. This is followed by a description of selected field measurements that include chemical speciation of the ice nucleating particles (INPs) and ice residuals (IRs). An INP represents a material or object that is assumed to be the agent responsible for observed heterogeneous ice nucleation,[58] and an IR represents the particle left over after the ice is sublimated. We further discuss recent laboratory studies examining atmospheric OA and OM surrogates for ice nucleation. Then, the current theoretical descriptions of ice nucleation data are summarized, and a new ice nucleation model is suggested to predict ice nucleation by inorganic particles coated by amorphous OM. Finally, a summary and suggestions for future research directions responding to open questions on the contributions of OM and OA to atmospheric INPs are presented.

Composition of Organic Aerosols. OA particles are ubiquitous and have been observed in natural remote and anthropogenically impacted regions as displayed in Figure 1.[29] Sulfate compounds in significant amounts can be associated with OA particles (Figure 1).[59] The condensed-phase OM is typically discriminated as hydrocarbon-like OA (HOA), semivolatile (SV-) and low-volatile oxygenated OA (LV-OOA), and extremely LV-OOA (ELV-OOA). Volatility decreases as species' oxidation level increases (O:C).[60−62] For example, POA from fossil fuel combustion and other urban sources typically falls in the class of HOA.[31] SOA forms as the oxidation products of anthropogenically or biogenically emitted VOCs partition to the condensed phase.[60,63] OA can also form via aqueous-phase chemical reactions between dissolved OM and soluble trace gases within cloud droplets and subsequent evaporation of the droplets.[64−68]

Atmospheric aerosol particles resemble a complex chemical mixture of compounds.[69−79] Gas−particle interactions and coagulation of different particle types yield aerosol particles that can be multicompositional and multiphase. Inorganic species such as sulfates and nitrates can condense on particles, leading to chemical modification, changes in hygroscopicity, and changes in ice nucleation propensity.[53,80−88] The mixing state of a particle population is a quantitative measure of the number of particles composed of one or any mixture of components. It therefore describes the particles' heterogeneous composition and has important effects on the radiative scattering and absorption cross sections.[89−92] The particle mixing state is also a crucial parameter for ice nucleation, yielding information

DOI: 10.1021/acsearthspacechem.7b00120
ACS Earth Space Chem. 2018, 2, 168−202

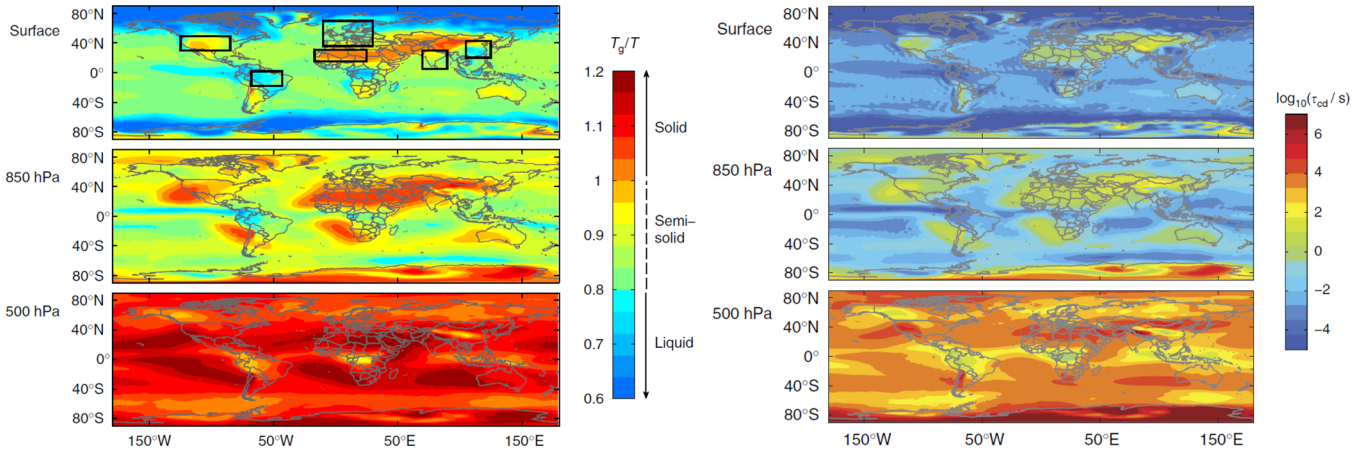

Figure 2. Modeled SOA phase state in the global atmosphere (a) and characteristic mixing time scales of water (b) in SOA particles at the surface, 850 hPa, and 500 hPa. Reprinted and adapted from Shiraiwa et al. (2017).[122]

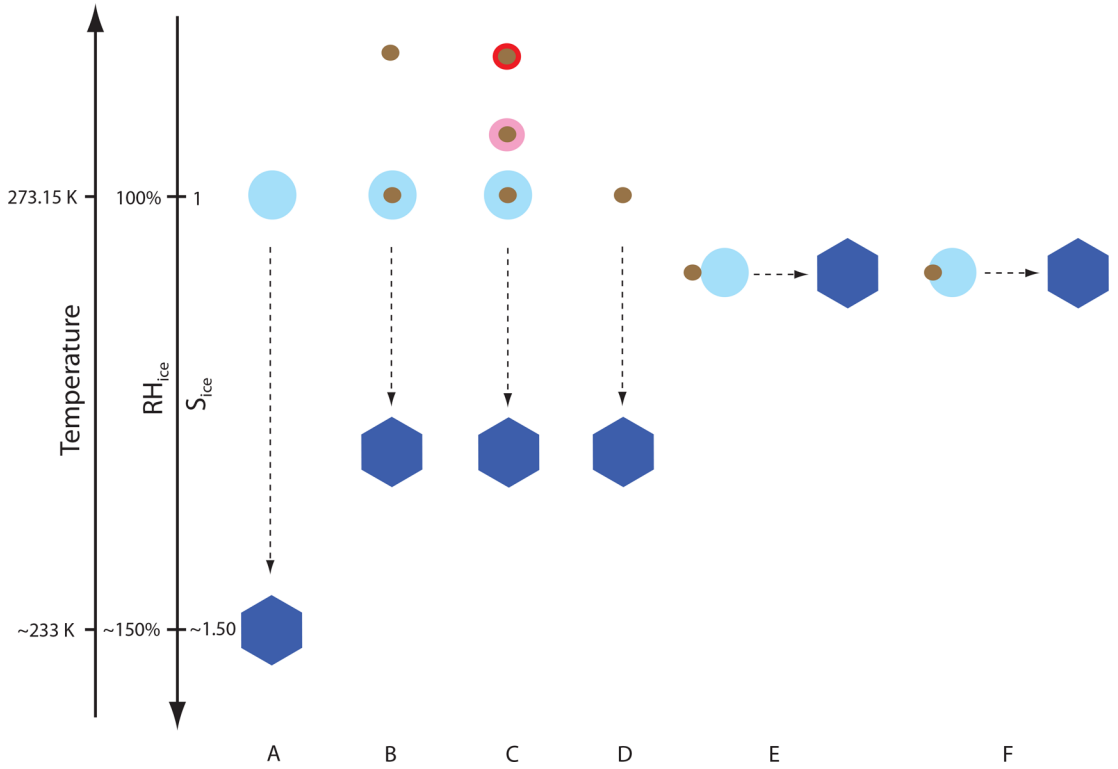

Figure 3. Schematic overview of different ice nucleation pathways, exemplary given as a function of temperature, relative humidity, and supersaturation with respect to ice (RH_{ice} and S_{ice}, respectively). (A) Homogeneous ice nucleation, (B) immersion freezing, (C) deliquescence and water uptake followed by immersion freezing, (D) deposition ice nucleation, (E) contact ice nucleation, (F) inside-out freezing. Symbol forms and sizes not to scale.

about the specific chemical species on the particle surface, which will interact with a supercooled aqueous solution or water vapor that is supersaturated with respect to ice. Chemical analysis of IRs has shown the physicochemical complexity of INPs.[54,93,94] The recent advances in single particle microspectroscopic analyses of aerosol particle populations further demonstrate the complex morphology and composition of ambient aerosol.[70] In photochemically active environments where oxidation of VOCs can occur or after long-range transport, aerosol particles have been observed to be dominated or coated by OM.[69−74,79,95−102] In such dynamic processes, it is expected that atmospheric aging could continuously alter the chemical complexity of OM and its ice nucleation propensity.

Phase State of OM in the Atmosphere. It is commonly assumed that INPs contain insoluble and/or solid substrates that facilitate ice nucleation.[40] However, it has been shown that OM with varying phases, macromolecules, and organic monolayers can initiate ice nucleation.[103−112] A unique feature of OA particles is that they can be amorphous and can exist in different phases, including liquid, semisolid, and solid (or glassy) states in response to changes in temperature (T) and relative humidity (RH).[113−116] This is in contrast to particles comprised of inorganic salts that have a thermodynamically defined phase transition from crystalline solid to liquid (deliquescence),[117] for instance. Phases of OA reflect different particle viscosities and thus different substrate hardnesses, all of

DOI: 10.1021/acsearthspacechem.7b00120
ACS Earth Space Chem. 2018, 2, 168−202

which potentially impact ice nucleation.[105,118,119] A characteristic parameter is the glass transition temperature, T_g, that describes the viscosity of a liquid on the order of 10^{12} Pa s, where the molecular motion is so slow that it can be considered a solid.[113,120,121] Species with very low T_g, such as sulfuric acid or water, can act as a plasticizer that significantly decreases T_g of a particle if present among other components.[113,114] At low temperatures, e.g., in the UT/LS where the atmospheric temperature can be as low as 180 K, it is conceivable that the majority of OM can be present in a solid state.[113] This has been evaluated by a recent global modeling study of the SOA phase state.[122]

Figure 2a displays global simulations of the annual average of T_g/T that is taken as representative of the SOA phase state for different altitudes.[122] Although there are regions where SOA can be solid in the surface boundary layer, the model results suggest that most of the SOA particles are solid above 500 hPa (~5 km), whereas middle (440−700 hPa) and high (<440 hPa) clouds can contain ice crystals and are present 18 and 33% of the time globally, respectively.[123,124] In the cold polar regions, mixed-phase clouds that contain supercooled water droplets and ice crystals can exist at much lower altitudes.[125−128]

The organic phase state impacts water diffusivity and typical condensed-phase mixing time scales (Figure 2b) that ultimately govern the time that solid OM needs to transition to a more liquid state and come into equilibrium with water vapor.[119,129] This organic solid-to-liquid transition is termed humidity-induced amorphous deliquescence.[130] Figure 2b shows that mixing time scales, τ_{cd}, of OA particles with water can range from several minutes to days at temperatures low enough for ice formation. Thus, τ_{cd} can be longer than typical cloud activation time periods (governed by the updraft velocity), potentially inhibiting full deliquescence and allowing the OA to serve as a substrate for ice nucleation.

Ice Nucleation Pathways. Figure 3 introduces the basic ice nucleation modes[40,58,131,132] for exemplary values of RH and supersaturation with respect to ice (RH_{ice} and S_{ice}, respectively), where the temperature and humidity trajectories do not necessarily depict all atmospheric conditions that allow for ice formation. The purpose of Figure 3 is to provide a differentiation between the nucleation modes and to introduce which ice nucleation pathways are discussed in this review. These definitions are based on a macroscopic viewpoint and may not reflect the actual microscopic or molecular processes at the particle interface.[40,58] A supercooled water or aqueous solution droplet can freeze by homogeneous ice nucleation (Figure 3A). The presence of an insoluble particle such as a mineral dust can act as INP when immersed in a supercooled droplet (Figure 3B). Deliquescence of salts[117] and water uptake can precede immersion freezing (Figure 3C). Water condensation immediately prior to ice nucleation, termed condensation freezing, is assumed to resemble the situation of immersion freezing.[55,133] Immersion freezing is suggested to be the dominant ice nucleation pathway in the atmosphere.[134−137] Pathways B and C can also occur at supercooled temperatures. Pathway D displays deposition ice nucleation where ice forms on an INP from the supersaturated gas phase. Processes not discussed here that can also take place in the atmosphere are contact ice nucleation (Figure 3E),[53,131] inside-out evaporation freezing (Figure 3F),[132,138] and ice multiplication.[23,24] Contact ice nucleation occurs when an INP collides or comes into contact with a supercooled water or aqueous solution droplet.[139] Inside-out freezing occurs when an INP is in contact with the liquid−air interface, establishing three interfaces (i.e., gas, solid, liquid), at supercooled conditions. Ice multiplication refers to the generation of ice crystals via fracturing processes during droplet freezing or riming of ice by supercooled droplets or from ice-ice collisions.

Impact of Organic Matter on Ice Nucleation Pathway. When amorphous OA or OM are involved in ice nucleation, the condensed-phase diffusion processes within OA particles will ultimately govern the ice nucleation pathway.[105,113,118,119,121,140,141] Because amorphous OM does not display a sharp deliquescence point, a layer of complexity to above-described nucleation modes is added when predicting the thermodynamic conditions under which ice nucleation proceeds. A demonstration of this is given by Berkemeier et al. (2014),[119] who applied a numerical kinetic molecular flux model to quantify the relationship between the ice nucleation pathway and OA viscosity governed by diffusivity of both the organic species and water. Figure 4 illustrates the different

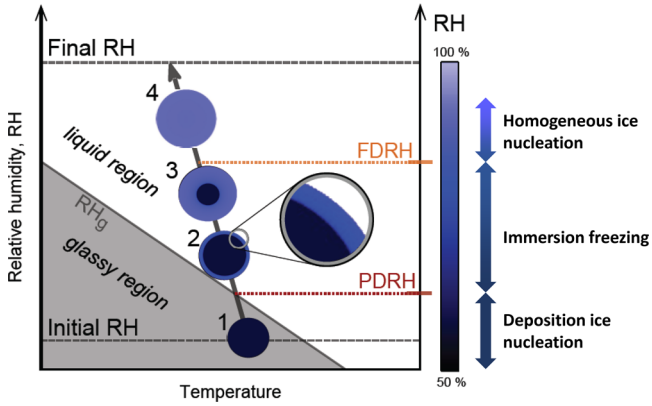

Figure 4. Transition of the amorphous organic phase upon increasing RH from a solid (glassy) state via partial deliquescence relative humidity (PDRH) to a liquid state at full deliquescence relative humidity (FDRH). Potential ice nucleation pathways are indicated. Adapted and reprinted from Berkemeier et al. (2014).[119]

stages during deliquescence of an amorphous OA particle as full deliquescence relative humidity (FDRH) is approached.[119] The water activity, a_w, of the aqueous solution surrounding the solid organic particle core at FDRH is in equilibrium with the water partial pressure. The formation of ice depends on the propensity of the solid organic core to initiate ice nucleation in the supercooled aqueous solution as depicted in Figure 4. The existence of a glass transition and FDRH leads to the following potential scenarios of atmospheric ice nucleation that are uniquely attributable to the presence of amorphous OM:[112,119] (1) Ice formation in the glassy region may be due to ice nucleation on the solid organic particle, i.e., deposition ice nucleation. (2) During partial deliquescence (PD), a residual solid core is coated by an aqueous shell, and immersion freezing may proceed. (3) At FDRH, only homogeneous freezing will occur at temperatures below ~238 K. (4) The presence of a glassy phase in disequilibrium with surrounding water vapor (e.g., cloud activation at fast updrafts as discussed below) may suppress or initiate ice nucleation beyond the homogeneous ice nucleation limit.

Figure 5 presents atmospheric ice nucleation pathways considering the ice nucleation modes discussed and the presence of inorganic and amorphous organic aerosol particles. It shows, in a more complete manner compared to Figure 3,

DOI: 10.1021/acsearthspacechem.7b00120
ACS Earth Space Chem. 2018, 2, 168−202

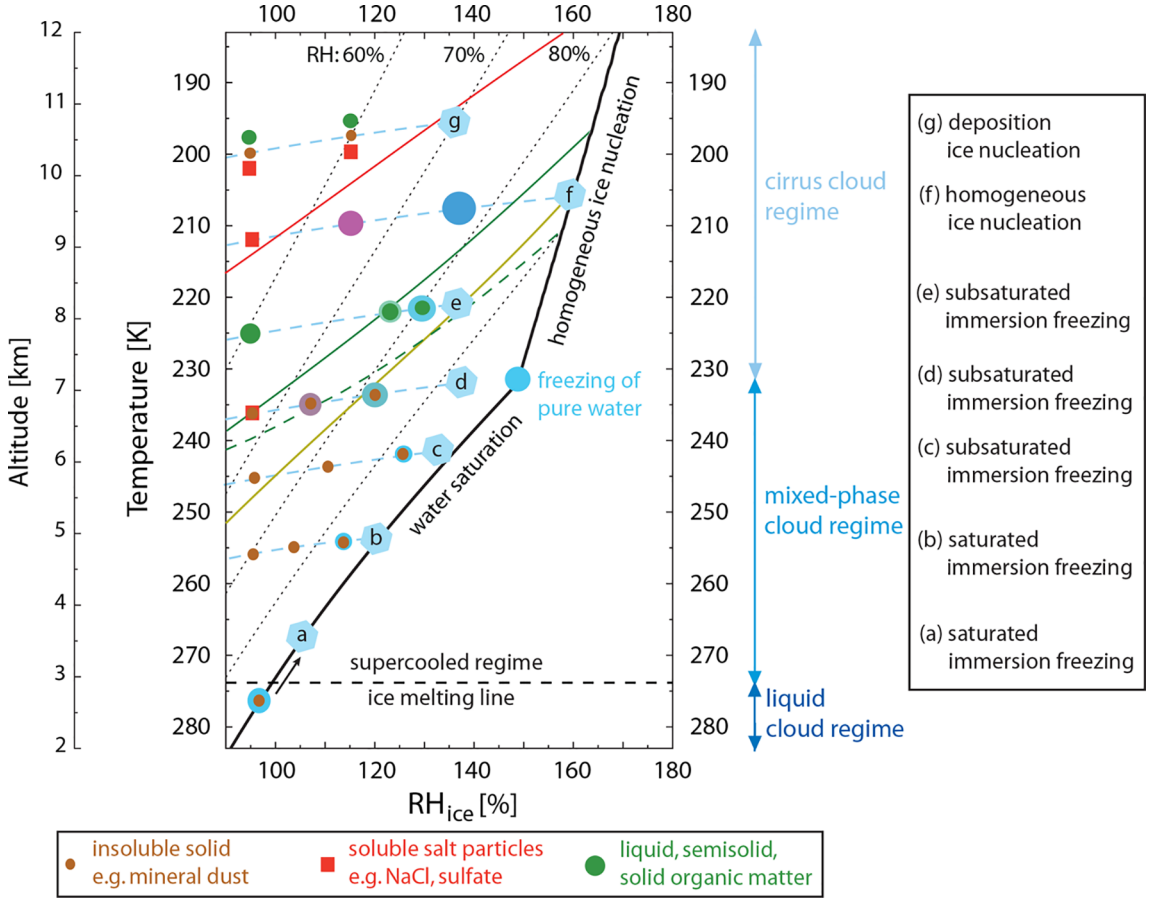

Figure 5. Potential immersion freezing and deposition ice nucleation under atmospheric thermodynamic conditions for particles of different chemical compositions. Dotted lines give conditions of constant relative humidity with respect to water. Altitude is given as an estimate using a dry adiabatic lapse rate of 10 K km^{-1}. Particle trajectories are given as blue dashed lines. Red, green, and golden solid lines represent the glass transition temperature for α-pinene SOA with and without the presence of sulfates (Charnawskas et al., 2017[112]) and naphthalene SOA (Wang et al., 2012[105]), respectively. The green dashed line represents the full deliquescence relative humidity of α-pinene SOA (Charnawskas et al., 2017[112]). The symbol forms and sizes do not reflect actual particle size and morphology changes but rather indicate the particles' phase states. Trajectories d and f involve deliquescence of the inorganic material followed by water uptake.

how particle composition impacts the formation of ice as a response to changes in thermodynamic conditions expressed as T, RH, and RH$_{ice}$. Figure 5 displays the thermodynamic conditions of the condensed phase. In other words, if the condensed phase is in disequilibrium with the gas phase, ice nucleation may proceed at different T and RH. Immersion freezing is depicted in pathways a−e (Figure 5). This nucleation pathway can occur under condensed phase water-subsaturated (Figure 5, pathway c−e) or -saturated conditions (Figure 5, pathways a and b), where particle water activity, a_w < 1 or a_w = 1, respectively. Deposition ice nucleation can proceed under ice-supersaturated gas phase and water-subsaturated conditions (Figure 5, pathway g).

Three cloud phase regimes can be discriminated in the atmosphere as indicated in Figure 5. At temperatures warmer than the ice melting line of 273.15 K, only liquid clouds exist. At temperatures cooler than the ice melting line and warmer than the homogeneous freezing temperature of supercooled water, mixed-phase clouds may form with coexisting supercooled droplets and ice crystals. Only ice crystals form at temperatures colder than the homogeneous freezing of pure water and RH larger than the homogeneous freezing limit, which is typical of cirrus clouds. This review highlights observations from laboratory and field studies of ice nucleation by OA/OM under conditions of RH and T similar to cirrus and mixed phase clouds while emphasizing the challenges in predicting OA acting as INPs.

The physicochemical characteristics of the INPs in these cloud regimes will govern the ice nucleation pathways. Figure 5 displays the equilibrium T and RH under which immersion freezing or deposition ice nucleation proceed but also exemplifies how initial chemical composition of the particle can affect ice formation routes. The composition of liquid droplets is constrained by the water saturation line where a_w = 1 by definition, which represents pure water. Cloud droplet solute concentration is typically low, on the order of 10^2 μM,[142] for which $a_w \approx 1$ is a reasonable assumption. An increase in humidity beyond liquid saturation leaves droplet a_w = 1 unchanged. For colder temperatures, the homogeneous freezing limit defines the humidity region above which only ice exists (any solution droplet present will freeze). The Kelvin effect leading to increased water vapor pressure[143] is important to consider for particles smaller than 0.2 μm but can be neglected in this discussion because ambient INPs are typically larger.[40,53]

Mineral dust is a common particle type in the atmosphere and serves as a large source of INPs.[49,50] Dust particles may take up water under subsaturated conditions and act also as cloud condensation nuclei (CCN),[144−155] in particular when

DOI: 10.1021/acsearthspacechem.7b00120
ACS Earth Space Chem. 2018, 2, 168−202

coated with hygroscopic material due to aging processes.[156,157] Dust particles may initiate immersion freezing under subsaturated[158,159] and saturated conditions[49] (Figure 5, pathways a–c). Dissolvable inorganic species present as coatings or as a particle deliquesce promptly upon changes in RH[117] followed by water uptake (see Figure 5, pathways d and f). However, amorphous OM can exhibit humidity-induced amorphous deliquescence[130] above the T_g or corresponding RH_{ice} (e.g., the red, green, or golden lines in Figure 5, pathway e) until full deliquescence (FD) occurs (Figure 5, dashed green line). Also note how the presence of sulfates in SOA (Figure 5, red line) decreases T_g as shown for the case of α-pinene SOA (Figure 5, green line).[112] These phase state changes present a challenge for predictions of ice nucleation kinetics because of the competition and relationship between the ice nucleation rate and changes in organic phase state. When a single organic species deliquesces, the solid OM surface area decreases as the surrounding a_w of the aqueous solution increases, both affecting the ice nucleation rate as discussed in the next section.

Specific Effects of Organic Matter on Ice Nucleation. Cooling and humidification rates of air masses complicate the predictions of ice formation from amorphous OA particles. These rates can change T_g and FDRH, which depend on particle viscosity or diffusivity and thus are kinetic parameters. This contrasts with typical thermodynamic parameters, e.g., the melting temperature of a solid. Therefore, the atmospheric conditions under which phase transitions occur depend also on the updraft velocity, which directly impacts cooling and humidification rates. A slower updraft velocity allows for more time for deliquescence to proceed, potentially resulting in full deliquescence of the OA particle at warmer and drier conditions compared to when a faster updraft is active. Therefore, the same OM can be present in different phase states under the same atmospheric thermodynamic conditions (i.e., T and RH_{ice}), resulting in different ice nucleation pathways and corresponding ice nucleation rates. OA particle size or coating thickness can also impact the rate and atmospheric altitude of the organic phase change, as larger particles or thicker coatings require more time to reach full deliquescence.

Another peculiarity of amorphous OM concerns the potential change in particle morphology upon nucleation of ice from an aqueous organic solution droplet. As water crystallizes, a freeze-induced phase separation into pure ice and a freeze-concentrated solution can occur.[140,160−164] Hence, ice nucleation may not necessarily result in a pure ice crystal but an ice crystal with inclusions or one that is partially or fully coated by the freeze-concentrated solution. This can have implications for water vapor pressure, multiphase chemical kinetics when the frozen particles act as reactive substrates, and the particles' radiative properties. The remaining highly concentrated aqueous organic solution can also form a glass.[140,165] Subsequent ice sublimation can leave a highly porous solid organic particle behind with implications for particle radiative properties and cloud formation.[165,166] In addition, these cloud cycling processes may allow for preactivation of the OA particles, thereby enhancing the particle's ice nucleation rate in subsequent ice activation cycles.[167−169]

Upon solidification and crystallization, OM can display different polymorphisms[170−172] when undergoing temperature changes.[173,174] The expected interfacial changes upon transition from one to another polymorphic phase have not yet been examined with regard to water interaction, e.g., via interfacial hydrogen bonding. Temperature can influence organic mixtures where, e.g., mixtures of fatty acids[175,176] can be miscible at ambient conditions but immiscible at lower temperature, resulting in demixing.[177] However, as pointed out by Marcolli et al. (2004),[178] in the presence of a sufficiently high number of miscible organic and inorganic components, a liquid (or amorphous solid) is the thermodynamically stable phase. The authors observed a decrease of the deliquescence RH with an increasing number of components present in the solution. This in turn would decrease the particle's ability to act as an INP. However, it has also been observed that, in complex inorganic/organic particles, efflorescence (liquid-to-solid transition) can occur upon increasing humidity.[179] How these phase transitions proceed at supercooled temperatures or in the metastable regime is not known.

Lastly, the occurrence of liquid–liquid phase separation (LLPS) in inorganic–organic particles[180−183] and OM[184−186] upon changes in humidity has been observed. LLPS can impact droplet surface tension and as such potentially cloud droplet activation.[187] However, the occurrence of LLPS at temperatures relevant for ice nucleation has not been investigated, except for a study by You et al. (2015),[181] and its impact on ice nucleation in aerosol particles or cloud droplets in terms of organic phase, interfacial tension, and water activity has not yet been examined.

MICROSCOPIC DESCRIPTIONS OF ICE NUCLEATION

Homogeneous Ice Nucleation. Homogeneous ice nucleation in aqueous solution is considered to be a stochastic process that depends on the volume of the solution and the time that it remains supercooled as well as $S_{ice} > 1$.[40] The presence of inorganic and/or organic solutes depresses the freezing point from the one of pure water, resulting in freezing temperatures lower than ∼238 K.[188−190] The homogeneous ice nucleation rate coefficient, J_{hom}, of pure water as a function of temperature is still under investigation with a recent study suggesting a maximum value of $J^{max}_{hom} \approx (2 \times 10^{12} \pm 10^2)$ cm^{-3} s^{-1} at ∼229 K.[191] A change in the ice nucleation rate may impact the evolution of clouds for temperatures as warm as 243 K.[192] Recently, Lupi et al. (2017)[193] showed that the ice nucleation rate can depend strongly on the prevalent ice polymorph, i.e., hexagonal ice, cubic ice,[194] or a mixture of the two referred to as stacking disordered ice.[195] They found that stacking-disordered critical crystallites at 230 K are more stable than hexagonal ones by ∼14 kJ mol^{-1} of crystallite, which corresponds to nucleation rates more than 3 orders of magnitude larger than those predicted by classical nucleation theory (CNT) assuming only hexagonal ice. When analyzing experimental ice nucleation rates, assuming the presence of hexagonal critical crystallites instead of stacking-disordered critical crystallites will result in underestimation of the ice-liquid interfacial free energy.

It has been shown experimentally that J_{hom} and median freezing temperature can be predicted using solution a_w as the ice nucleation determinant independent of the solute's nature.[140,190,196−199] Theoretical studies have corroborated the applicability of a_w to describe homogeneous ice nucleation.[200−202] The temperature dependence of a_w in aqueous inorganic or organic solutions is only established for few solutes and remains a matter of current research.[140,190,196,198,203−211] An additional unanswered question concerns the role of the vapor–liquid interface in initiating

DOI: 10.1021/acsearthspacechem.7b00120
ACS Earth Space Chem. 2018, 2, 168−202

homogeneous ice nucleation based on arguments of partial wettability following Young's equation.[212−215] Initial molecular dynamics (MD) simulations indicated that nucleation does not actually occur at the vapor−liquid interface but close to it (i.e., the subsurface).[216,217] A recent computational study using a nanofilm found that ice nucleation initiates away from the air−water interface in a region that is more favorable to the formation of cubic ice.[218]

Heterogeneous Ice Nucleation. The basic requirements for a particle to initiate ice nucleation heterogeneously are that[40,58] (i) it must be insoluble, (ii) it must be larger than the critical ice nucleus germ, estimated to be >0.1 μm, (iii) its surface must have chemical bonds that can interact with and arrange water molecules, (iv) it must have a crystallographic match representing geometrical arrangement of bonds, or (v) there must be active sites representing localized phenomena on the substrate surface of varying quality. Despite advances in instrumentation that allow for visualization of substrate locations at which ice forms,[219,220] in situ observations of ice nucleation on the nanometer and subnanometer scale have not yet been achieved. Recall that the ice nucleation pathways[40,58] are macroscopically defined and the underlying microscopic processes are not well understood. For example, it has been suggested that deposition ice nucleation is the result of homogeneous ice nucleation of water residing in nanosize pores, the latter causing a strong "negative" Kelvin effect thereby reducing the water vapor pressure and impacting S_{ice}.[221] This is in line with a so-called two-step nucleation mechanism[222] where a liquid condensate forms prior to nucleation, which can explain nucleation of a solid phase initiated by pockets and at wedges on substrate surfaces.[223−226]

When interpreting heterogeneous ice nucleation on the molecular scale, one should keep in mind that substrate surfaces can be readily covered by organic gases. For example, after ∼1 s exposure to SV-VOCs at concentrations in the range of ∼1 ppb, an organic layer can form on a substrate, which is directly proportional to the uptake coefficient of the adsorbing gas,[227] termed adventitious carbon in surface science.[228] Surface tension studies on levitated single droplets demonstrate surface contamination in minutes, even when purging with high purity N_2 gas.[229] Under very careful experimental conditions, VOCs, ammonia, or amines can still be present and partition to the condensed phase.[230−232] The use of cold traps for carrier gases to generate humidified gas flows can minimize contamination by trace gas species.[233] The choice of water source may also impact cleanliness of INP surfaces, where the most commonly applied water is Millipore water (resistivity of >18.3MΩ cm) throughout various studies, but triple-distilled water[234] or a combination of Millipore water with an ion exchange column[231] are also used. How carbon contamination of surfaces present as a monolayer or several monolayers affects ice nucleation has not yet been systematically assessed. Hence, microscopic interpretation of ice nucleation experiments should be performed with caution.

Currently, computer experiments such as MD simulations[235] and Monte Carlo calculations provide the best means to improve our molecular understanding of heterogeneous ice nucleation on a scale not yet feasible to examine in laboratory experiments. Focus in these simulations has been placed on the role of inorganic substrates such as mineral dusts or AgI acting as INPs.[236−246] In addition, how the presence of an electric field and different surface geometries impact ice nucleation has been examined.[247−250] Despite these and other studies,[242,243,251,252] a clear picture of which substrate features represent key physicochemical parameters for description of heterogeneous ice nucleation has not yet emerged. For example, a good ice lattice match with the substrate seems not to be required,[251−253] whereas the degree of hydrophobicity and surface morphology may play important roles.[243,252] The ice nucleation propensity can be lost if adsorption of water is too great.[243] The formation of an ice embryo may be favored away from the liquid−solid interface, i.e., in the second overlayer of water from the substrate and not on the substrate itself.[244,252] Potentially, a combination of all these factors could define the ice nucleation propensity of any particular substrate, but the lack of defining parameters makes developing theoretical descriptions of heterogeneous ice nucleation challenging.

Fitzner et al. (2017)[254] recently investigated precritical water cluster formation from two substrates, either rough or smooth, having the same ice nucleation rate. The rough surface yielded pure hexagonal ice, and additionally, precritical cluster formation mimicked homogeneous freezing. This can be understood given that if hetero- and homogeneous ice nucleation yield the same ice polymorph (hexagonal ice), then condensation and evaporation of precritical clusters should proceed similarly. In contrast, precritical clusters formed within 5 Å of the smooth surface prior to ice nucleation lead to stacking disordered ice (cubic and hexagonal ice) and polymorphism. This implies that, when assessing the enhancement of heterogeneous ice nucleation compared to homogeneous freezing, knowledge of the formed polymorph is crucial. In other words, the crystal face unique to a respective polymorph templated by the substrate may be more important than the actual substrate structure itself in understanding what does or does not make an ice nucleator.[254]

Computer simulations of ice nucleation initiated by carbonaceous or organic substrates have just begun to gain attention. Molinero and co-workers[255−258] and Cabriolu[259] have used MD simulations to study heterogeneous ice nucleation on graphene or graphite substrates. These studies found that ice nucleation follows classical nucleation theory (CNT)[259] and that the transition from liquid to crystal occurs in a single activated step mainly controlled by the size of the ice nucleus.[255] In addition, they observed that the hydrophilicity of the graphitic surface is not a good predictor of ice nucleation ability, but that ordering of liquid water in contact with the substrate plays an important role in the heterogeneous ice nucleation mechanism.[257] This could help explain the experimentally observed insignificant increase in ice nucleation by O_3 oxidized Lamp Black 101 soot, a reference material for soot.[260] Hydrophobic and hydrophilic atomically rough surfaces do not induce layering and thus do not promote heterogeneous nucleation of ice.[258] Figure 6 shows the structure of interfacial water on a graphitic surface that has been modified by adding OH groups every 1 nm, thereby enhancing surface hydrophilicity determined from an MD simulation.[257] Hexagonal patches can be identified in the first and second layer of water molecules. The authors suggest that the rare formation of bilayer patches of hexagons (i.e., the fluctuations in the second layer) may be associated with the nucleation of ice. However, the water does not show a specific alignment or structure associated with given OH surface features (Figure 6). This finding is similar to recent simulations showing for different hydroxylated substrates that neither the symmetry of the OH

DOI: 10.1021/acsearthspacechem.7b00120
ACS Earth Space Chem. 2018, 2, 168−202

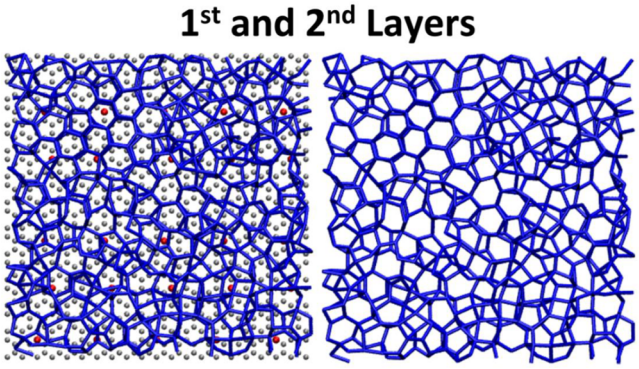

Figure 6. Structure of interfacial water in contact with a modified graphitic surface with OH placed in 1 nm distances. Carbon atoms of the surface are shown with gray spheres, OH-like groups with red spheres, and water as blue sticks that connect neighbors within 0.35 nm. Both first and second layers are shown to highlight the presence of bilayer hexagonal patches (showing the surface in the left panel and hiding it for clarity in the right panel). There is no apparent alignment between the water molecules and the surface atoms, indicating that the surface does not template the formation of ice. Reprinted from Lupi et al. (2014).[257]

patterns nor the similarity between a substrate and ice correlate well with the ice nucleation ability.[261]

It is well-known from experimental studies that organic monolayers with alcohol head groups act as ice nucleating surfaces, being more efficient at nucleating ice than monolayers with the same chain length but with carboxyl head-groups.[106−109,111,262,263] A recent MD simulation study captured these observed freezing trends and attributed the variation in ice nucleation temperatures to spatial fluctuations in the monolayer and lattice mismatch.[264]

Another microscopic model of ice nucleation by a solid in contact with a liquid and surrounding gas phase is the three-phase contact line concept.[132,138,265−274] Under partial wetting, the gas, solid, and liquid phases exist in contact with each other, establishing a contact line in three dimensions. CNT can explain why ice nucleation is preferred and faster at the contact line compared to nucleation in the bulk.[266] The free energy cost of creating the interface around the nucleus is lowest at the point of the three pre-existing interfaces compared to, e.g., creating an interface within the liquid phase.[266,268] The contact line concept was applied to help explain inside-out freezing[132,138] and the superior ability of proteins from the bacterium *Pseudomonas syringae* to freeze water.[271] Interface-specific sum frequency generation (SFG) spectroscopy coupled with MD simulations indicated that the protein features a hydrophilic−hydrophobic−hydrophilic pattern.[271] This pattern imposes structural changes in the adjacent water, alternating between liquid- and vaporlike water interfaces in contact with the protein, thereby resembling a contact line.

Computer simulations on the order of nanometers and nanoseconds will benefit our fundamental understanding of ice nucleation but have yet to be validated by experimental observations, which are typically on larger scales and proceed over longer time periods. Relevant physicochemical parameters and constraints to predict ice formation in clouds that spread kilometers in size and take minutes to hours to evolve must be acquired from ice nucleation studies performed in the field and laboratory. Interface-specific experimental techniques such as SFG and second-harmonic generation (SHG) spectroscopy can yield information on water structure at supercooled temperatures.[271,275,276] Experimental observations of changes in interfacial water structure as ice nucleation is approached allows for comparison and interpretation by MD simulations.[271,276]

FIELD MEASUREMENTS OF ICE RESIDUALS AND ICE NUCLEATING PARTICLES

Field measurements in the past decades have resulted in a wealth of determined INP number concentrations and examination of IRs.[40,53,54,277−285] In this review, we focus on recent field measurements that were accompanied by techniques allowing for chemical speciation of INPs and IRs. Furthermore, those of which that demonstrated any potential or lack thereof of OA, carbonaceous particles, or OM to act as INPs are included.[93,94,96,98,101,102,219,278,286−303] In the following, we will discuss selected studies in more detail.

Cziczo et al. (2013) examined IRs from cirrus clouds using a Counterflow-Virtual-Impactor (CVI) coupled to Particle Ablation by Laser Mass Spectrometry (PALMS) and found a dominance of dust particles and a smaller portion of organic containing particles, particularly organics associated with sulfates, making up IRs.[93] These findings corroborate earlier observations by DeMott et al. (2003) also indicating that IRs consisted of organics and sulfates.[278] Froyd et al. (2010)[290] examined the composition of IRs in subvisible cirrus clouds as displayed in Figure 7. They found that internal mixtures of

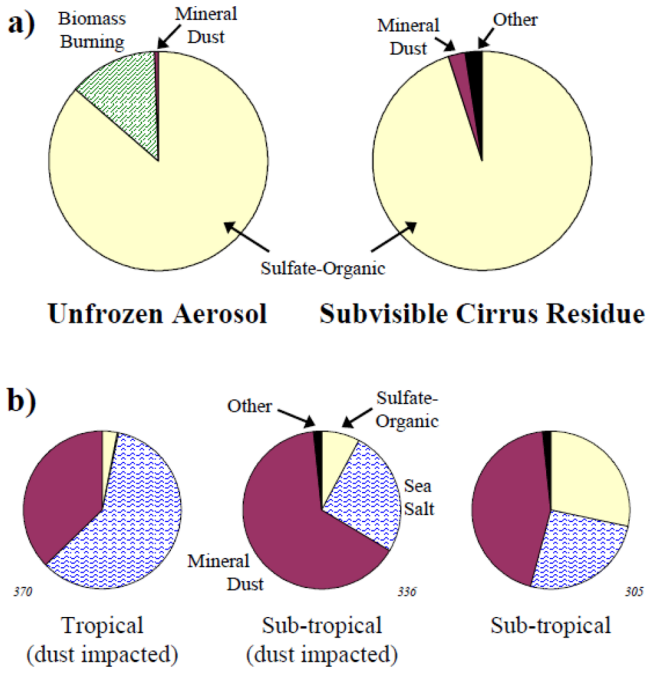

Figure 7. Particle types in the tropical tropopause region. (a) Subvisible cirrus residues at 16.0−17.4 km are compared to unfrozen aerosols. (b) Residues from several anvil cirrus encounters at lower altitudes, 12−14 km. Reprinted from Froyd et al. (2010).[290]

neutralized sulfate with OM dominated the IRs and were similar in size and chemically indistinguishable from their unfrozen sulfate-organic aerosol counterparts. Mineral dust particles were not enhanced in these subvisible cirrus IRs, and biomass burning particles were depleted in the IRs (Figure 7a). These organosulfate compounds, present in the free troposphere, have been identified as the sulfate ester of 2,3-epoxy-2-

DOI: 10.1021/acsearthspacechem.7b00120
ACS Earth Space Chem. 2018, 2, 168−202

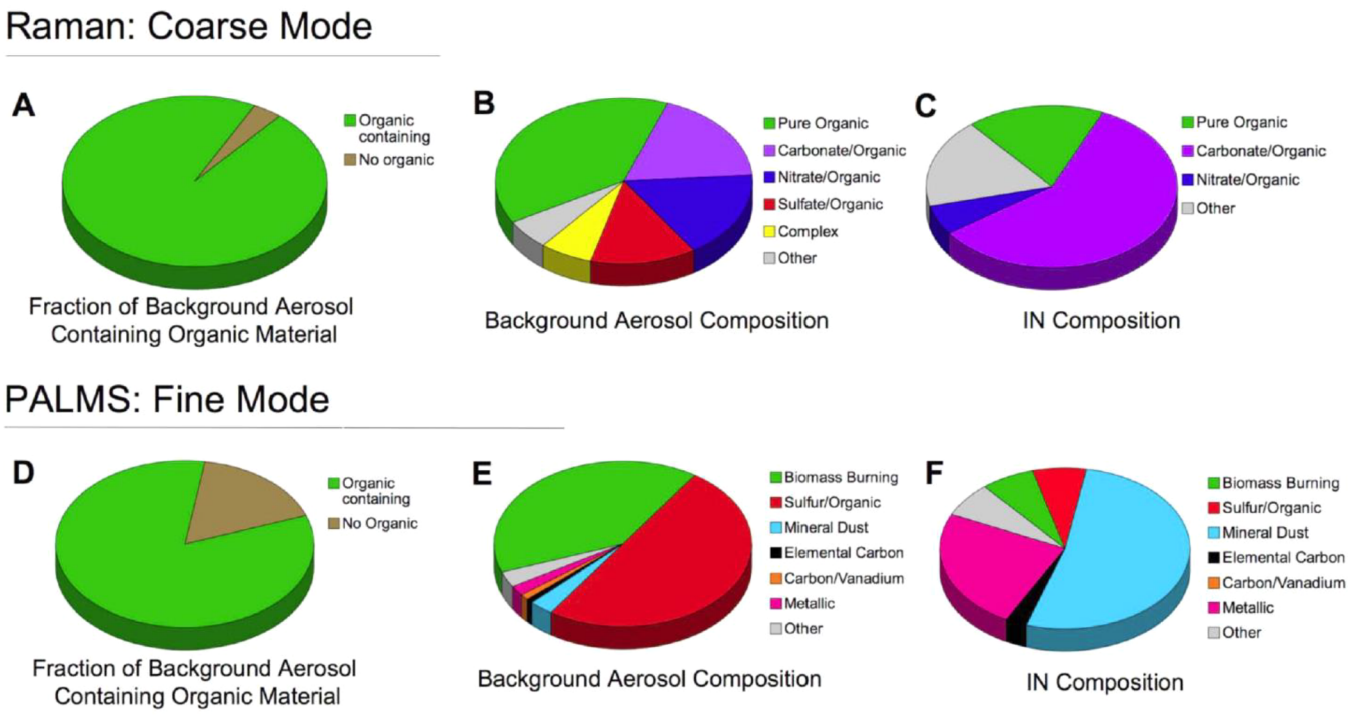

Figure 8. Compositional summary of coarse (>2 μm) and fine (<2 μm) mode background aerosol particles and INPs collected at Storm Peak Laboratory using both particle analysis by laser mass spectrometry (PALMS) and Raman analyses. Reprinted from Baustian et al. (2012).[287]

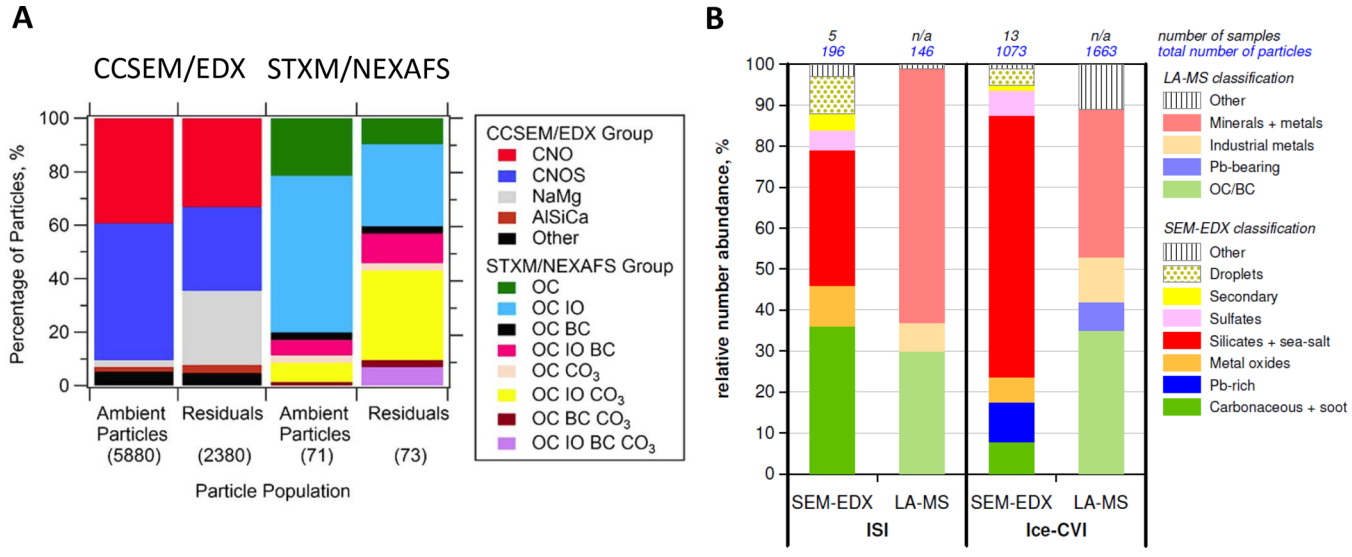

Figure 9. (A) ISDAC field campaign: Particle groups of ambient particles and in-cloud residual particles. CCSEM/EDX groups particles according to major elemental composition. For STXM/NEXAFS analyses, the colors indicate particle classes distinguished by different combinations of organic carbon (OC) and internally mixed with other components: inorganics (IO), black carbon (BC), and carbonates (CO_3). The numbers in parentheses represent the total number of particles analyzed. (B) High Alpine Research Station Jungfraujoch: Relative number abundance of particle groups determined by SEM/EDX and laser ablation mass spectrometry (LA-MS) for IRs sampled by ice selective inlet (ISI) and ice counterflow-virtual-impactor (Ice-CVI). (A) Adapted from Hiranuma et al. (2013).[288] (B) Reprinted from Worringen et al. (2015).[301]

methyl-1,4-butanediol (IEPOX, $C_5H_{10}O_3$),[304] a second generation oxidation product of isoprene[305−307] corroborating the role of SOA in cloud ice formation.

During the Megacity Initiative: Local And Global Research Observations (MILAGRO) field campaign,[308] air masses were tracked and sampled at various sites downwind from Mexico City. From analysis of individual particles with scanning transmission X-ray microscopy (STXM) coupled with near-edge X-ray absorption fine structure spectroscopy (NEXAFS) and computer-controlled scanning electron microscopy with an energy-dispersive X-ray analyzer (CCSEM/EDX), Moffet et al. (2010)[74] showed that, as the aerosol plume evolved from the city center, the organic mass per particle increased, the fraction of carbon−carbon double bonds decreased, and organic functional groups were enhanced indicative of photochemical aging.[29,61] These anthropogenic-dominated OA and SOA particles initiated immersion freezing and deposition ice nucleation, however, at different particle temperature and

DOI: 10.1021/acsearthspacechem.7b00120
ACS Earth Space Chem. 2018, 2, 168−202

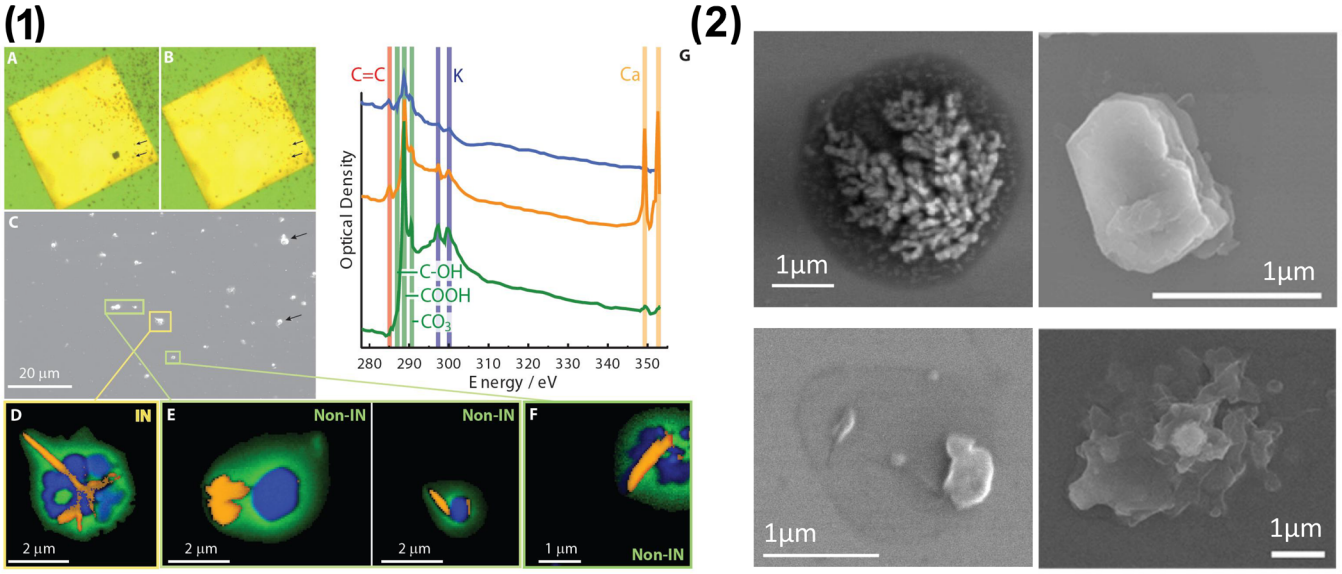

Figure 10. (1) INP identification and STXM/NEXAFS chemical imaging of INP and non-INPs. (1A, 1B) The ice formation and ice sublimation event observed in the experiment, respectively. (1C) SEM image of the same sample area at higher magnification. (1D) Identified INP and (1E, 1F) non-INP component images emphasizing the contrast between noncarbonaceous inorganic species (blue), organic carbon (green), and calcium (orange). (1G) NEXAFS spectra of the particles with the major functionalities highlighted. (2) The two SEM images on each the left and right-hand side represent identified INPs with organic coatings. (1) Reprinted from Knopf et al. (2014).[96] (2) Reprinted and adapted from Knopf et al. (2014)[96] and China et al. (2017),[102] respectively.

humidity conditions than those of most particles studied in laboratory experiments.[101] These findings highlighted the potential of chemically complex, anthropogenically impacted OA and SOA particles to participate in ice cloud formation. An improved sampling procedure was used during the California Research at the Nexus of Air Quality and Climate Change (CalNex) campaign,[309] where ice nucleation experiments and single particle analyses by STXM/NEXAFS and CCSEM/EDX were conducted on concurrent particle samples.[98] In this photochemically active region, all examined particles possessed OM, and the INPs were among those determined at a statistically significant level, further corroborating the role of OM in ice nucleation.

At the Storm Peak Laboratory (Steamboat Springs, Colorado, elevation of 3210 m), Baustian et al. (2012) sampled ambient aerosol in the fine and coarse mode for particles acting as INPs using PALMS and Raman spectroscopy.[287] In fine mode, the INPs were dominated by mineral dust, though a fraction of organic particles acted as INPs as well (Figure 8). In contrast, INPs in the coarse mode were dominated by OM. This difference in INP composition emphasizes the importance of assessing the physicochemical properties of the entire aerosol population, encompassing both accumulation and coarse mode particles. Furthermore, the organic INPs of the coarse mode showed exceptional ice nucleation propensity for temperatures below 230 K, activating at significant rates close to RH_{ice} of 100%.

McCluskey et al. (2014)[292] sampled laboratory prescribed burns and wildfires, showing that biomass burning leads to the release of particles that are active as immersion freezing INPs at temperatures from 241 to 261 K using the Continuous Flow Diffusion Chamber (CFDC) technique.[310] The authors applied transmission electron microscopy/energy-dispersive X-ray (TEM/EDX) to examine morphology and composition of IRs, observing that INPs from wildfires consisted largely of carbonaceous particles such as tar balls or minerals rather than soot particles. The authors hypothesized that either secondary processes resulting in carbonaceous particles or uplifting of soil matter could explain why these two particle types made up the majority of INPs. Although a decrease in INP numbers was observed in some experiments when removing refractory black carbon (rBC) using laser ablation[311,312] during prescribed burns of some fuels, that does not explain why during wildfires BC was a deficient INP type.

During the Indirect and Semi-Direct Aerosol Campaign (ISDAC) field campaign[313] conducted over Alaska near Barrow, aerosol particles were examined for composition and cloud formation including ice nucleation using CCSEM/EDX, STXM/NEXAFS, and CFDC by means of a CVI[288] (Figure 9A). In general, the authors found, in agreement with other studies,[96,98,101,102] that all ambient particles and cloud residuals contain some OM.[288] The analyzed IRs possessed an inorganic or soot core and were coated by OM dominated by carboxylic groups indicative of chemical aging. This study suggests that particle size, composition, and chemical processing impact the particles' cloud nucleating ability. Worringen and co-workers sampled IRs and INPs using three different techniques at the High Alpine Research Station Jungfraujoch (Switzerland).[301] Their measurements indicated that Ca-rich particles, carbonaceous material, and metal oxides made up the major fraction of INPs and IRs (Figure 9B). This study emphasizes that carbonaceous particles play a role in mixed-phase cloud formation and that different sampling techniques such as the ice selective inlet (ISI) and ice-CVI yield different particle type contributions to ambient INPs and IRs. The application of SEM with high-resolution instruments was found to be particularly suited for investigation of INPs and IRs. At the same site, Kupiszewski et al. (2017)[302] observed that larger (up to 1 μm in diameter) BC-containing IRs increased the activated frozen fraction of particles. Furthermore, BC-containing IR were found to have a thick coating, emphasizing the importance of atmospheric particle aging for ice nucleation.

DOI: 10.1021/acsearthspacechem.7b00120
ACS Earth Space Chem. 2018, 2, 168−202

Knopf et al. (2014)[96] examined particles for their physicochemical properties and ice nucleation propensity during the Carbonaceous Aerosols and Radiative Effects Study (CARES) campaign located in Central California.[314] A novel experimental procedure allowed identification of individual INPs among hundreds or thousands of collected particles not acting as INPs. Furthermore, the identified INPs were chemically imaged and compared with the compositional signature of the non-INPs present in the same air mass (Figure 10). This study found that all analyzed particles contained OM though different particle type classes were identified. The identified INPs belonging to a certain particle type class were indistinguishable from the particles of the same class that did not act as INPs. The authors suggested that this may be due to the underlying stochastic nature of nucleation processes necessitating knowledge about the entire particle population to predict ice nucleation. This finding is similar to observations by Froyd et al. (2010)[290] and Wang et al. (2012).[98] The same technique was applied to examine free tropospheric particles as potential INPs, sampled in the Azores (Figure 10B).[102] At this remote location, all particles possessed OM as partial or full coating and initiated heterogeneous ice nucleation in the immersion mode at saturated and subsaturated conditions for temperatures between 235 and 246 and in the deposition mode at ~120% RH_{ice} and 222 K. These long-range transported and chemically aged free tropospheric particles showed very similar ice nucleation propensities among the different samples collected at the Pico Mountain Observatory. It was hypothesized that this is due to the similar nature of the organic coating acquired by these particles.

These recent studies indicate that particle size and associated particle composition are crucial parameters governing ice nucleation. For example, limiting the sampled particle size range may skew the identified numbers of ambient INPs. Though chemical speciation was not achieved on individual INPs, Mason and co-workers examined ambient aerosol particles collected on substrates using an impactor for immersion freezing in a size-segregated fashion spanning particle sizes from 180 nm to 10 μm (determined by the cut-points of the 10 impactor stages) and probed freezing temperatures between 243 and 258 K.[315−317] Correlations between the INP concentration and measurements of total particles, fluorescent bioparticles, BC, sodium, methanesulfonic acid, and wind speed were performed. Employing this technique at a marine coastal site, the greatest INP concentrations were found in the supermicrometer size range between 1.8 and 5.6 μm in diameter with less than half of the INPs numbers at lower and larger particle sizes.[315] Key findings were that primary biological aerosol particles were likely the major source of INPs at 248 to 258 K, mineral dust may have also had an important contribution to INPs active at 243 K, and BC and marine particles were negligible contributors. A complementary study by these authors including sites in North America and Europe indicated a similar trend where supermicrometer particles yielded the highest INP numbers.[317] In fact, it was concluded that, if either supermicrometer or coarse-mode particles were not sampled at those ground sites, approximately 78 and 53% of immersion-mode INPs, respectively, may have been missed.[317] Similar findings of higher correlation of INP numbers with supermicrometer-sized particles were observed during mountain-site INP measurements.[318−320]

LABORATORY MEASUREMENTS OF ORGANIC ICE NUCLEATING PARTICLES

Laboratory studies have tremendously aided in our understanding of ice nucleation by allowing ice formation to be observed under controlled conditions of T and RH_{ice}, identifying previously unknown and atmospherically relevant INPs, and relating particle chemical composition and mixing state to ice nucleation propensity.[49,50,53] Experiments have linked amorphous OA particle phase states with ice nucleation ability.[105,112,321−327] Other studies have emphasized a reduction in the uncertainties of relevant physical parameters including T, S_{ice}, INP surface area and nucleation time to improve ice nucleation descriptions.[328−333] Novel technical approaches have been applied to quantify the molecular interplay and water structure at an ice nucleating interface[271,276,334] and monitor ice nucleation at submicrometer resolution.[219,220,335,336] Despite current progress, there still exists a knowledge gap to explain ice nucleation on a fundamental and molecular level when considering amorphous OM.

Organic particle types that have recently gained more attention for their ice nucleation ability are marine-derived particles,[279,337] ice nucleating macromolecules (INMs),[104,110,338−344] soil OM,[345−349] plant-derived OM,[350−352] dissolved organic species,[140,198,199,353−356] OA,[103,162,168,233,312,322−324,357−366] and SOA particles.[105,112,167,325−327,367]

Ice Nucleation by SOA Particles. Previous studies have observed ice nucleation on laboratory-generated SOA particles.[105,167,321,325−327,367] For illustrating the challenging task of predicting ice nucleation from SOA, Figure 11 shows a compilation of experimentally obtained frozen fraction values

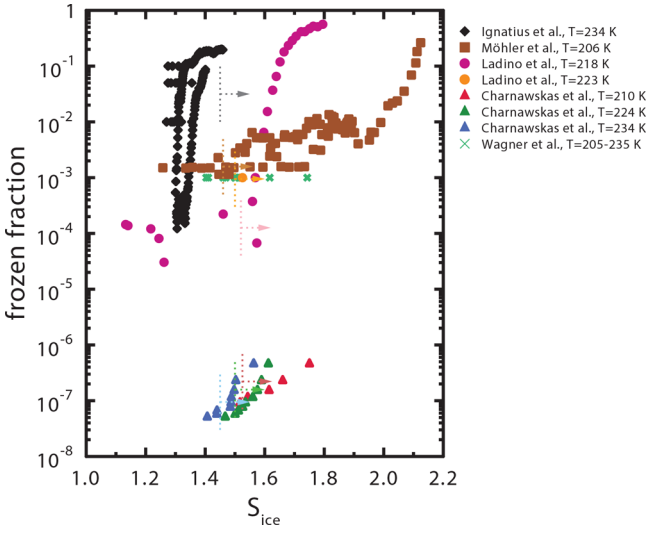

Figure 11. Compilation of frozen particle fractions as a function of ice supersaturation, S_{ice}, for laboratory-generated α-pinene SOA particles generated from α-pinene reaction with O_3 and OH in the presence of UV light (black, Ignatius et al., 2016[327]), α-pinene reaction with O_3 (brown, Möhler et al., 2008;[321] light green, Wagner et al., 2017;[368] and purple and orange, Ladino et al., 2014[326]) and α-pinene reaction with OH (red, green, and blue, Charnawskas et al., 2017[112]). Vertical dotted lines indicate the homogeneous freezing limit for particle sizes used in each study (Koop et al., 2000[197]). Lighter-colored arrows for all data sets point toward conditions in which homogeneous freezing becomes drastically more favorable. Arrows for Wagner et al. (2017[368]) are omitted for clarity.

DOI: 10.1021/acsearthspacechem.7b00120
ACS Earth Space Chem. 2018, 2, 168−202

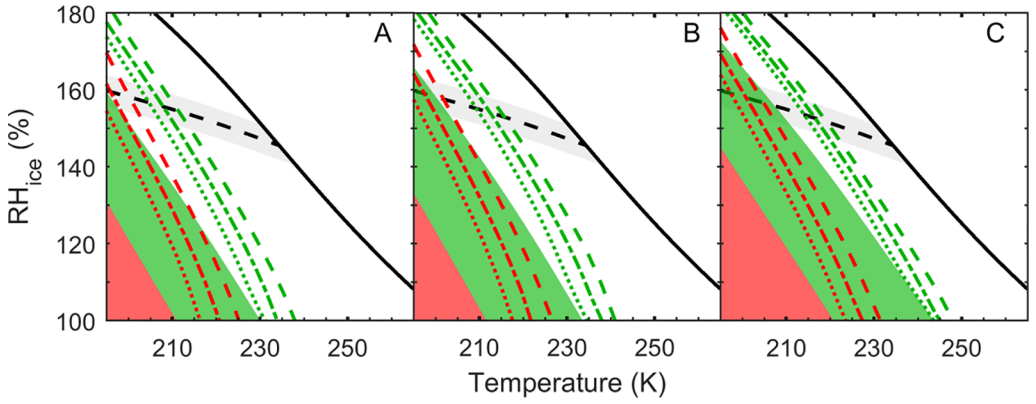

Figure 12. Simulated T_g (solid lines) for isoprene (A), a-pinene (B), and naphthalene (C) SOA with (red) and without sulfate (green) and corresponding FDRH for different updraft velocities of 0.03, 0.28, and 2.8 m s^{-1} as dotted, dash-dotted, and dashed lines, respectively. Black solid and dashed lines represent water saturation and the homogeneous freezing limit,[195] respectively. Reprinted from Charnawskas et al. (2017).[112]

(f_{ice} = number of nucleated ice crystals/aerosol particle number) for ice nucleating SOA particles derived from α-pinene as a precursor gas as a function of S_{ice}. The homogeneous freezing regime is included as dotted lines for each data set dependent on T and RH. We note that these studies all utilized particles with diameters on the order of 10^2–10^3 nm. Ice formation by α-pinene SOA particles from ozonolysis was investigated by Möhler et al. (2008)[321] in a cloud chamber over activation time scales of ∼90 s, representing cooling rates of ∼1.5 K min^{-1}. They observed that only a few ice nucleation events occurred in the heterogeneous freezing regime, whereas most were observed at homogeneous freezing conditions. Cloud chamber data over a wider temperature range of 205–235 K for the same particle system are presented in Wagner et al. (2017),[368] revealing that ice nucleation occurred at or above homogeneous freezing conditions. Similarly, Ladino et al. (2014)[326] found α-pinene SOA particles with different O:C generated at room temperature to form ice in the homogeneous freezing regime when using a CFDC having a 12 s residence time, resulting in very short activation times (i.e., a cooling rate of 300 K min^{-1}). However, when precooling the SOA particles, an increased ice nucleation propensity was observed attributed to the transitioning of the particles into a more viscous phase state. When using OH as the main oxidant for α-pinene, Charnawskas et al. (2017)[112] demonstrated that biogenic SOA from the OH reaction with isoprene, α-pinene, and longifolene formed ice only at the homogeneous freezing limit, i.e., S_{ice} of 1.45–1.65 for temperatures between 210 and 235 K. This study applied typical cloud activation time scales on the order of ∼20 min (or cooling rates of 0.1 K min^{-1}) and observed the least favorable conditions for ice formation as seen in Figure 11. The cooling rate applied to SOA particles is likely a significant parameter that affects observation of freezing and allows for accessing lower frozen fractions.[102,112] Application of slower rates enhances the likelihood that particles reach thermodynamic equilibrium resulting in PD or FD, both of which may reduce SOA ice nucleation efficiency leading to observed lower frozen fractions. Ignatius et al.[327] generated SOA particles by exposure of α-pinene to O_3 and OH radicals at various temperatures between 235 and 268 K. In contrast to previous studies, exceptional heterogeneous ice nucleation efficiency was observed, where all freezing events took place below homogeneous freezing conditions. A possible explanation is that the SOA particles changed into a highly viscous glassy phase state prior to CFDC sampling as they were transported through tubing at a warmer T than the particles' formation temperature,[327] potentially leading to drying of the particles. The residence time in the CFDC was 10 s, likely probing the ice nucleation ability of solid SOA particles because the time for reaching FD was too short.[112,119] This case illustrates that, if SOA in a glassy state are exposed to thermodynamic conditions in which they should be liquid, residence times that are too short may result in those particles maintaining their glasslike state and initiating deposition or immersion freezing. On the other hand, particles that are liquid and are too quickly exposed to conditions favoring a glassy phase (e.g., from room temperature to a lower temperature with too short residence time) may not have sufficient time to equilibrate and solidify. In this latter case, no ice nucleation or homogeneous ice nucleation would be expected to occur. Although the α-pinene SOA particles summarized in Figure 11 may have different chemical compositions, the most significant parameter that changes the ice nucleation propensity expressed as f_{ice} is hypothesized to be the particle phase state prior to ice nucleation. When starting the ice nucleation experiment with liquid α-pinene SOA particles, the particles do not show significant ice nucleation propensity. However, if the SOA particles are highly viscous or solid when entering an ice nucleation experiment, higher f_{ice} values may be observed. In summary, unless the experimental T and RH trajectories or history are well-known and compare close to atmospherically relevant cloud activation conditions, it will be difficult to ascertain the role of biogenically or anthropogenically derived SOA in atmospheric ice formation processes.

Evaluation of the effect of different updraft velocities, which will govern the particles' RH and T trajectories, on the SOA particle phase state was conducted by Charnawskas et al. (2017).[112] The authors modeled SOA particle phase and water uptake for different updraft velocities resulting in different humidification rates for the purposes of constraining heterogeneous ice nucleation regimes in the RH and T parameter space as shown in Figure 12. These results were derived using a numerical diffusion model that includes kinetics of gas-phase diffusion, reversible adsorption, surface-to-bulk transfer, and bulk diffusion of water through particles constrained by observations of particle hygroscopicity and viscosity as a function of RH and T.[119] Figure 12 shows the thermodynamic conditions at which lofted isoprene, α-pinene, and naphthalene SOA particles experience glass transition and full deliquescence

DOI: 10.1021/acsearthspacechem.7b00120
ACS Earth Space Chem. 2018, 2, 168–202

as a function of air parcel updraft velocity with implications for the potential ice nucleation pathways. The simulation results indicate that, for slow updraft velocities (lower humidification rates, dotted green lines), the potential heterogeneous freezing regime (RH_{ice} > 100%) starts at T < ~230, ~235, and ~240 K for isoprene, α-pinene, and naphthalene SOA particles, respectively. Faster updrafts shift these conditions by 5−8 K to warmer temperatures. Figure 12 also demonstrates the impact of sulfates on the SOA phase state, resulting in significantly lower glass transition points and FDRH,[113,114] thus limiting the conditions where heterogeneous ice nucleation can proceed. The simulations suggest that the investigated biogenic SOA (Figure 12A, B) does not act as INP for mixed-phase cloud conditions and likely will serve as INP only at lower temperatures and faster updraft velocities. This is qualitatively in agreement with previous studies that based this conclusion on derived water diffusion coefficients in α-pinene SOA particles.[118,141] Naphthalene SOA shows the highest FDRH values and as such has the greatest potential to act as an INP under mixed-phase cloud conditions. However, the simulations of naphthalene SOA neglect the potential of condensed-phase oligomerization reactions that can proceed in SOA formation.[369,370] This may be the reason for the disagreement with experimental data by Wang et al. (2012),[105] who showed that naphthalene SOA can act as INP in immersion mode for temperatures up to 240 K and close to water saturation. Wang et al. (2012)[105] experimentally demonstrated that the glass transition point modulates the ice nucleation pathway, resulting in either immersion freezing or deposition ice nucleation. The authors compared their laboratory data with ice nucleation observations from the MILAGRO and CalNex campaigns.[98,101] These ambient particles were all dominated by OM, likely due to SOA formation in these photochemically active regions, and the T and S_{ice} at which either deposition ice nucleation or immersion freezing occurred were constrained by predicted naphthalene SOA glass transition as a function of a_w.[105] In summary, SOA derived from heavier precursor gases such as naphthalene show higher glass transition points and therefore can act as INPs over a greater range of T and RH. This is in line with condensed-phase material with higher molecular weight showing warmer glass transition temperatures.[113] Furthermore, the SOA particle oxidation state and the presence of plasticizing material such as sulfates have a significant impact on the conditions at which heterogeneous ice nucleation can proceed.[112−114,119,122]

Humic-like Substances as INPs. Humic acids (HAs) and humic-like substances (HULIS) are common Earth and atmospheric constituents.[371] It has been demonstrated that those compounds can nucleate ice in the deposition and immersion modes[233,372] where the latter pathway follows a water activity description.[360,373] In the case of immersion freezing, no correlation with droplet volume was observed.[360] Chemical aging[374,375] due to ozone exposure of the HULIS compound Leonardite resulted in a decrease in deposition ice nucleation ability.[233] The authors hypothesized that this was due to alterations of hydrophobic and hydrophilic functional groups on particle surfaces.[233] Investigations of solid ice nucleating soil organic particles (such as HULIS) were reviewed previously and in general agree that heat treatment and hydrogen peroxide exposure of soils decreases their ice nucleation ability, which is thought to be a result of the organic digestion, i.e., chemical modification or dissolution and removal of biogenic or organic from the soil particle surface.[53] However, it is important to note that ambient atmospheric HULIS may take up organic vapors such as toluene and benzyl alcohol in the presence of water vapor[376] and that chemical aging by OH radicals can impact HULIS particle composition by molecular fragmentation with consequences for particle hygroscopicity.[377] Smaller-sized oxidized molecules, like C2−C6 carboxylic acids dissolved in water, have not been found to affect ice nucleation[353] similar to previous studies employing dicarboxylic acids.[354]

Ice Nucleating Macromolecules. In contrast to ice nucleating solid organic substrates hundreds of nanometers to micrometers in size, INMs are on the order of 10^2 kDa or ~3 nm in diameter.[44,104,110,338−341,343,344,378−380] Pummer et al. (2012)[340] demonstrated that the water in which pollen was previously suspended retains ice nuclei after the pollen grains were removed and provided evidence that the responsible ice nucleating agents are polysaccharide macromolecules. Other studies have since confirmed this finding for the same type of pollen.[339,343,378] Observation of pollen and pollen-derived components such as sugars and sugar-alcohols in atmospheric particles have been made,[381−383] highlighting the potential relevance of INMs for atmospheric ice cloud formation. However, other biogenic particles such as fungal spores and bacteria can serve as a source of INMs,[104,344,379] which may imply that INMs in general are derived from a variety of biological or biogenic particles. Figure 13 adapted from

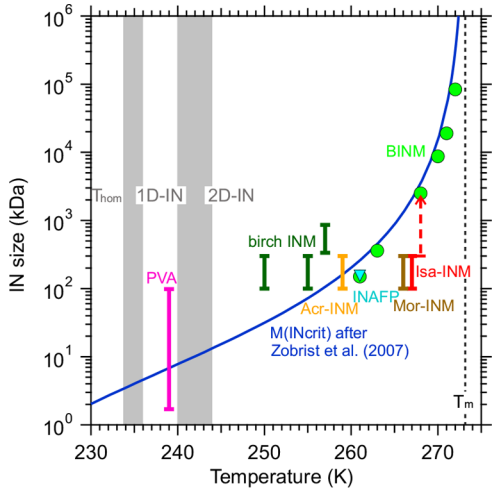

Figure 13. Size of ice nucleating macromolecules (INM) derived from poly(vinyl alcohol) (PVA, magenta), birch INM (green), bacterial INM (BINM, lime), bacterial ice nucleating/antifreeze proteins (INAFP, cyan), and fungal spores from *Acremonium implicatum* (Acr-INM, orange), *Isaria farinose* (Isa-INM, red), and *Mortierella alpine* (Mor-INM, brown) as a function of the observed median ice nucleation temperature. The blue line is the size of the critical ice nucleus from classical nucleation theory.[108] Assumed regions in one and two dimensions of water molecular templating to form ice (1D-IN and 2D-IN, respectively) are shown. Melting and homogeneous freezing temperature of pure water, T_m and T_{hom}, respectively, are given. Reprinted from Pummer et al. (2015).[104]

Pummer et al. (2015)[104] compiled INM size as a function of observed ice nucleation temperature and found that their relationship follows closely the prediction of the critical ice cluster size given by CNT parametrized by Zobrist et al. (2007).[108] It may be that the size of a single INM determines the temperature for it to nucleate ice. However, it should be

DOI: 10.1021/acsearthspacechem.7b00120
ACS Earth Space Chem. 2018, 2, 168−202

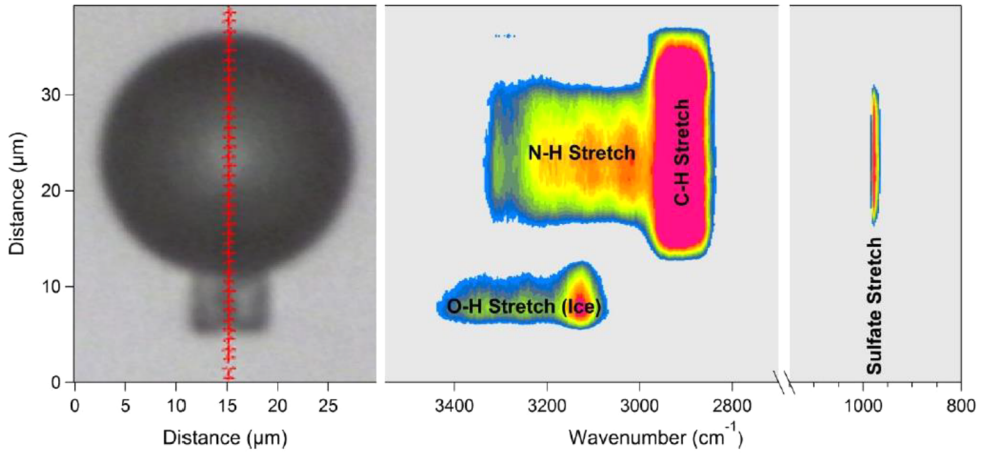

Figure 14. Optical microscope images and Raman spectroscopy line scans (red hashed line) of a glassy organic particle with an ammonium sulfate core nucleating ice at 215 K. Reprinted from Schill and Tolbert (2013).[324]

noted that, due to possibly different chemical properties of INMs or aggregation from filtration, total concentration of INMs is uncertain and leads to a range of ice nucleation temperatures.[104] For example, suspensions of INM at ≤1000 kDa derived from either the pollen *Betula pendula* or the fungus *Fusarium avenaceum* were observed to nucleate ice from 253 to 258 K and 248−267 K, respectively,[344] indicating that ice nucleation temperatures should also depend on the total concentration of INMs present.[104,344] Dreischmeier et al. (2017)[110] observed not only heterogeneous ice nucleation from pollen washing water but simultaneous ice binding properties, both initiated by polysaccharides bearing carboxylate groups where the former is due to macromolecules >100 kDa and the latter <100 kDa. Polysaccharides may be an atmospheric ice nucleating agent due to their ubiquity in organic and biogenic matter. X-ray microspectroscopic evidence has shown that ice nucleation can occur on atmospheric particles coated by OM[96] that has a similar chemical signature to that of atmospheric marine polysaccharide-like particles.[384]

Marine-Derived INPs. SSA particles composed of sea salts and OM may dominate the number of INPs in regions where atmospheric dust loadings are relatively low.[337,385,386] Fragments of marine phytoplankton cells, intact cells, and associated exudate material nucleate ice, where immersion freezing followed solution water activity.[337,387−390] Immersion freezing did not show a correlation with droplet volume.[387] Cellulose is a common constituent of cell walls in plants and algae in both the marine and terrestrial environment and was recently shown to nucleate ice as efficiently as desert dust.[352] The authors also claim that, although airborne cellulose is less abundant than atmospheric minerals, it could play a role in cloud formation. Wilson et al.[337] found that droplets prepared from water sampled from the sea surface microlayer (the uppermost 1−1000 μm of the ocean surface) froze heterogeneously and provided evidence based on particle size, heat treatment, and X-ray microspectroscopy that the likely ice nucleating substrate stemmed from phytoplankton exudate material. This material, which can be polysaccharidic and proteinacoues,[391] retained its ice nucleation propensity when filtering through a 0.2 μm filter, adding to the class of water-soluble INMs similar to findings of INMs derived from fungi, bacteria, and pollen.[104,340,378−380] DeMott et al.[279] and McCluskey et al.[392] showed that aerosolized particles from a laboratory wave flume containing cultures of phytoplankton and bacteria can also nucleate ice and suggested that numbers of INPs over remote marine regions may be linked to biological processes in the water.

Organic Matter Mixed with Mineral Dust, Ammonium Sulfate, and Soot. During atmospheric transport, mineral dust can be coated by inorganic material or OM. Recent experimental studies generally agree that coated mineral dust (e.g., coated with sulfates, ammonium sulfate, ammonium bisulfate, nitric acid, levoglucosan, or succinic acid) show decreased ice nucleation ability below water saturation.[85,87,321,361,393−402] By increasing RH toward 100%, thereby diluting the coating material, ice nucleation temperatures approach those of uncoated mineral particles, indicative of typical freezing point depression behavior.[188,197,356,373,395,399] Modification of particle surfaces due to chemical reaction can significantly alter the ice nucleation behavior as shown, e.g., for sulfuric acid-coated feldspar[394] and kaolinite.[88,399] These laboratory studies demonstrate that aging of particles that acquire coatings can alter physical (solute effect) and chemical (surface site) particle properties resulting in different ice nucleation characteristics.

In a 2013 study by Schill and Tolbert,[324] heterogeneous ice nucleation was directly observed for mixed organic and ammonium sulfate particles in which the organic was present as a glass coating the inorganic core. Figure 14 shows optical images of ice nucleation with Raman spectra acquired along a cross section of the organic particle and ice crystal. Two organic components, 2,2,6,6-tetrakis(hydroxymethyl)cyclohexanol and 1,2,6-hexanetriol referred to as C10 and C6, respectively, were mixed with ammonium sulfate. The optical microscopy image shows that ice nucleated on the surface of the mixed C6/C10 particle coating present in a glasslike state engulfing the ammonium sulfate core (Figure 14, left panel). The Raman spectra show that the N−H and sulfate stretching modes are localized at the core whereas the C−H stretching modes encompasses the particle, indicating that the organic is completely coating the inorganic particle core (Figure 14, right panel). Ice (O−H stretching mode) is located on the glassy organic surface (C−H stretching mode). These observations directly demonstrate that a highly viscous organic surface can act as a substrate requirement for heterogeneous ice nucleation. Surrogate SOA material such as sucrose, citric acid, raffinose, and 4-hydroxy-3-methoxy mandelic acid among

DOI: 10.1021/acsearthspacechem.7b00120
ACS Earth Space Chem. 2018, 2, 168−202

others can be glassy at UT temperatures and have been shown to nucleate ice.[168,322−324,358] Murray et al.[322] observed that aqueous citric acid aerosol can be solid under typical cirrus conditions inducing heterogeneous ice nucleation. The authors suggest that ice nucleation by organic-rich particles may explain observed low ice crystal numbers and high in-cloud humidity in the tropical tropopause layer.

Soot or BC is ubiquitous in the atmosphere as a result of biomass burning and fossil fuel combustion,[403] and its ability to nucleate ice has been previously discussed in detail.[49,50,53] During atmospheric transport, soot can acquire OM, impacting particle morphology and mixing state.[404−407] Recently, Ullrich et al. (2017)[408] evaluated the ice nucleation propensity of different types of soot using a cloud chamber. They observed that soot particles with higher OC content (>20%) showed lower deposition ice nucleation efficiency than that of soot with lower OC content (<20%). Soot can be a more efficient INP compared to the investigated desert dust in deposition mode at temperatures between 215 and 235 K. Only a few studies have investigated the ice nucleation propensity of organic-coated soot particles.[112,409−412] Kulkarni et al. (2016)[411] emphasizes that despite the wealth of observations the effect of different atmospheric aging processes on the propensity of soot to nucleate ice is not well established. Aging processes will be discussed in more detail in the following section.

Biomass Burning Aerosol as INPs. Previous studies observed that INPs were present in only some prescribed laboratory burns of different biomass fuels reflecting southeastern and western U.S. flora.[364,365] Ice nucleation was observed at temperatures lower than 233 K but only at the homogeneous freezing limit of aqueous solution.[364] These findings are similar to experimental ice nucleation results applying biomass burning surrogate species.[198,199] Levin et al. (2016) observed measurable INP concentrations at 243 K from combustion emissions from 13 of 22 different biomass fuel types.[366] When removing rBC via laser-induced incandescence,[311,312] they observed significant reductions in INP numbers, emphasizing the role of rBC in INP for some biomass fuels.

The Effects of Atmospheric Aging, Coating, and Oxidation State on Ice Nucleation. Friedman et al. (2011)[409] investigated the effect of coatings of adipic, malic, and oleic acid on soot on ice nucleation. In addition, oleic acid-coated soot particles were exposed to ozone to simulate atmospheric oxidation. The authors did not observe heterogeneous freezing at 253 and 243 K and only homogeneous freezing at 233 K. Oxidation of oleic acid-coated soot particles by ozone did not have a significant effect on ice nucleation. Chou et al. (2013)[410] did not observe changes in the ice nucleation efficiency of soot particles from a vehicle diesel engine that had been photochemically aged. However, addition of α-pinene at 238 K led to a thicker organic coating with higher organic carbon (OC) to BC ratio, increased particle size, and enhanced ice nucleation. Schill et al. (2016)[412] studied immersion freezing at 243 K from particles emitted by a diesel engine fueled with either petrodiesel and biodiesel. The exhaust was aged up to 1.5 photochemically equivalent days using an oxidative flow reactor. The authors found that aging of the diesel exhaust did not impact INP numbers and that exhaust of both fuels is not likely to contribute to atmospheric INP concentrations under mixed-phase cloud conditions. Kulkarni et al. (2016)[411] investigated the ice nucleation ability of fresh and aged diesel soot particles for temperatures between 223 and 233 K. They employed transmission electron microscopy (TEM), X-ray photoelectron spectroscopy (XPS), and single particle mass spectrometry to track morphological and compositional changes of the soot particles. Bare, hydrated, and compacted soot particles induced ice formation below the homogeneous freezing threshold, whereas soot particles coated with α-pinene SOA nucleated ice at homogeneous freezing conditions in agreement with the study by Charnawskas et al. (2017).[112] However, soot particles coated with a similar SOA formed at ∼80% RH conditions (high RH) had an ice nucleation efficiency that was similar to that of bare soot particles.[411] This may be because the α-pinene SOA coating under those initial high RH conditions was chemically different compared to that of the α-pinene SOA coating generated under dry conditions. Another reason may be due to SOA volatility. Previous research has found that RH and T can impact SOA volatility,[33,413−418] implying that if SOA coatings were to evaporate from soot particles, then their bare surface may be exposed after some time, rendering their ice nucleation efficiency like that of bare soot particles. This may point again to the importance of the SOA generation conditions and corresponding SOA phase state for understanding the potential ice nucleation pathways.

During atmospheric transport, particles can age by condensation of inorganic compounds and OM and by multiphase chemical reactions involving, e.g., atmospheric oxidants and radicals such as O_3 and OH.[374,375,419−424] The impact of heterogeneous or multiphase chemical oxidation of some organic substrates on ice nucleation has been previously investigated.[103,233,260,409,425] Exposure of soot surrogate material Lamp Black 101 to O_3 simulating ∼2 weeks of atmospheric residence did not change the ice nucleation propensity in a temperature range from 242 to 257 K.[260] Friedman et al. (2011)[409] exposed bare soot and soot coated with oleic acid to O_3 simulating 3.5 days of atmospheric aging and did not observe a difference in the ice nucleation capability of either particle type. Wang and Knopf (2011)[233] exposed Leonardite, a humic acid, and Suwannee River fulvic acid (SRFA) to O_3 simulating ∼2 weeks residence under remote conditions. In that study, they observed that O_3 oxidation led to a decrease in deposition nucleation efficiency and to water uptake at lower temperatures for Leonardite particles and to an increase in the lowest temperature at which deposition nucleation was observed for the SRFA particles. Brooks et al. (2014)[425] investigated ice nucleation in the contact mode using fresh and oxidized soot and polycyclic aromatic hydrocarbon (anthracene, pyrene, and phenanthrene) particles. O_3 exposure was conducted at ∼80 ppm for 24 h. Exposure to ozone facilitated ice nucleation, on average, at 2−3 K warmer temperatures. For similar O_3 exposures, Collier and Brooks (2016)[103] examined the ice nucleating propensity of organic hydrocarbons including octacosane, squalane, and squalene in contact with water. The oxidized octacosane initiated contact freezing at 1.1 K warmer temperatures than the fresh one, and the difference between these temperatures was determined to be statistically significant. Oxidized squalane initiated freezing at ∼2 K lower temperatures than the fresh one, whereas freezing initiated by oxidized squalene did not differ from application of fresh squalene particles.

In all these experiments, chemical aging was conducted at room temperature under which the organic phase is likely semisolid or liquid. However, particles acting as INPs are likely to be found at higher altitudes and thus lower temperatures

DOI: 10.1021/acsearthspacechem.7b00120
ACS Earth Space Chem. 2018, 2, 168−202

where particle oxidation may dominantly occur on solid organic phases. Chemical aging by oxidation of a solid particle versus that of a liquid particle will proceed differently[426−429] with different implications for the oxidized particles' cloud formation potential. Chemical processing of a solid organic particle by atmospheric oxidants may be limited to the uppermost particle surface layers[420,428] and may proceed via different reaction pathways, e.g., leading to higher degrees of molecular fragmentation[377,426,430,431] thereby impacting hygroscopicity.[84,377,432,433] This in turn affects water uptake, which is necessary for immersion freezing to proceed.

A few studies have examined SOA formation from precursor gases cyclohexene, α-pinene, and limonene reacting with O_3 for temperatures as low as 243 K.[434−437] In general, these studies found that the SOA yield increases at lower temperatures due to lower vapor pressures and different particle chemical compositions. For example, SOA particles from the ozonolysis of α-pinene at 253 K had increased mass fraction of carboxylic acids and lower O:C compared to SOA formed at 293 K.[437] Furthermore, it was observed that dimer ester production was suppressed at lower temperatures. These observations point to different chemical compositions of SOA at lower formation temperatures that will likely impact particle hygroscopcity, viscosity, and reactivity toward atmospheric oxidants, which in turn will affect ice nucleation. Considering that during atmospheric transport OA is continuously exposed to atmospheric oxidants and to condensing secondary OM, both potentially altering the physicochemical properties of the particle, more experimental and theoretical studies conducted at atmospherically relevant temperatures investigating the impact of chemical aging under atmospherically relevant oxidant exposures and SOA formation on INPs are warranted.

Not explicitly discussed when describing the ice nucleation potential of SOA particles or coatings is the fact that, depending on the chemical formation pathway, SOA material has different O:C ratios.[29,33,62,420,438−440] Although T_g is dominated by the molecular weight of the species,[113] O:C also impacts T_g.[122] Numerical diffusion modeling suggests that, for α-pinene SOA, increases of O:C increase T_g, whereas for naphthalene SOA, an increase in O:C results in a lower T_g.[112,119] The reason for this trend is based on the produced condensed-phase products accounted for in the model.[119] Composition-determined changes in T_g will also impact FDRH and thus the regime of potential ice nucleation pathways. Furthermore, a solid SOA particle phase state at room temperature is not a guarantee that this particle initiates ice nucleation at lower temperatures as observed for the case of longifolene SOA.[112] A greater particle hygroscopicity likely accelerates the amorphous deliquescence and thus decreases the window in which immersion freezing can proceed. Clearly, the chemical composition, phase state, and hygroscopicity of SOA particles under typical mixed-phase and cirrus cloud conditions must be well characterized to predict their potential to act as atmospheric INPs.

■ ANALYSES OF ICE NUCLEATION DATA

Current State of Ice Nucleation Data Analysis. How best to analyze heterogeneous ice nucleation data is currently being debated with more studies focusing on immersion freezing[49,50,328,332,373,441,442] than deposition ice nucleation.[221,233,333,443] Commonly, two approaches to explain the data are used: a stochastic description based on CNT and a deterministic or singular description. The stochastic description assumes that cluster formation leading up to ice nucleation occurs randomly over time on a substrate yielding a heterogeneous ice nucleation rate coefficient, $J_{het}(T)$.[40,108]

By measuring J_{het}, CNT allows contact angles to be derived that can be parametrized in different ways to reflect the substrate's propensity to nucleate ice. Different parametrizations, however, result in different interpretation of the underlying nucleation mechanism.[40,108,328,360] Theoretical calculation of any contact angle requires not only J_{het} observations but also a choice in free energy of ice nucleus activation. This in turn necessitates knowledge of thermodynamic and kinetic parameters relating to the critical water cluster and parameters such as supersaturation and temperature. A recent nonclassical method to calculate free energy of critical cluster formation has been proposed based on changes in entropy as water molecules transition from the bulk to the ice cluster, rearranging their hydrogen bonding environment.[331]

In contrast, the singular hypothesis assumes that there are a number of surface active sites on a particle, each of which has a different ice nucleating efficiency depending on temperature only. This explanation neglects ice nucleation kinetics, i.e., fluxes of water molecules and fluctuations of ice embryo formation, and currently lacks a physical basis of the observed events.[328,444] The concept of ice active sites has been used to parametrize ice nucleation data and implemented in CNT-based analyses. These include the multicomponent model,[445] the time-dependent freezing rate parcel model,[446] parametrizations of INPs per liter of air,[277] the probability density function (PDF) model,[447,448] the active site model,[447,448] the surface site-based stochastic model,[442] the singular or modified-singular description,[387,388,445,449−451] and the so-called soccer ball model.[444] However, because of the lack of observational characterization as discussed above, it remains to be seen whether active site distributions, though intriguing conceptually, are more than a mathematical construct to describe data. Furthermore, fitting parameters for these schemes applied to large-scale atmospheric models are always implicitly dependent on the choice of laboratory-defined thermodynamic and kinetic parameters.[441] In cloud-resolving models, the role of time, particle size, ice nucleation schemes, or contact angle distributions on ice cloud formation have been investigated and are currently under scrutiny as to which are or are not appropriate to implement when predicting ice nucleation.[452−456]

In the atmosphere, the aerosol population is physicochemically diverse, and the chemical complexity of an entire aerosol population may need to be considered to predict ice nucleation.[96] A nucleation probability dispersion function has been applied in a previous study that describes the deviation of individual particle ice nucleation coefficients from that of the average particle population, which was successful to represent laboratory freezing data and capable of predicting atmospheric ice nucleation.[333] Field measurements have indicated that INPs can belong to a major particle type class, where the few particles acting as INPs are chemically indistinguishable from the remaining inactive same particle types.[96,98,290] This may be explained by the stochastic nature inherent to nucleation according to CNT or specific particle features unresolvable with current techniques.

During cloud activation that includes droplet activation and ice nucleation, OA particles can experience amorphous phase transition (e.g., see Figure 4), where the outer shell experiences changes in a_w.[119,130] Therefore, immersion freezing models that

DOI: 10.1021/acsearthspacechem.7b00120
ACS Earth Space Chem. 2018, 2, 168−202

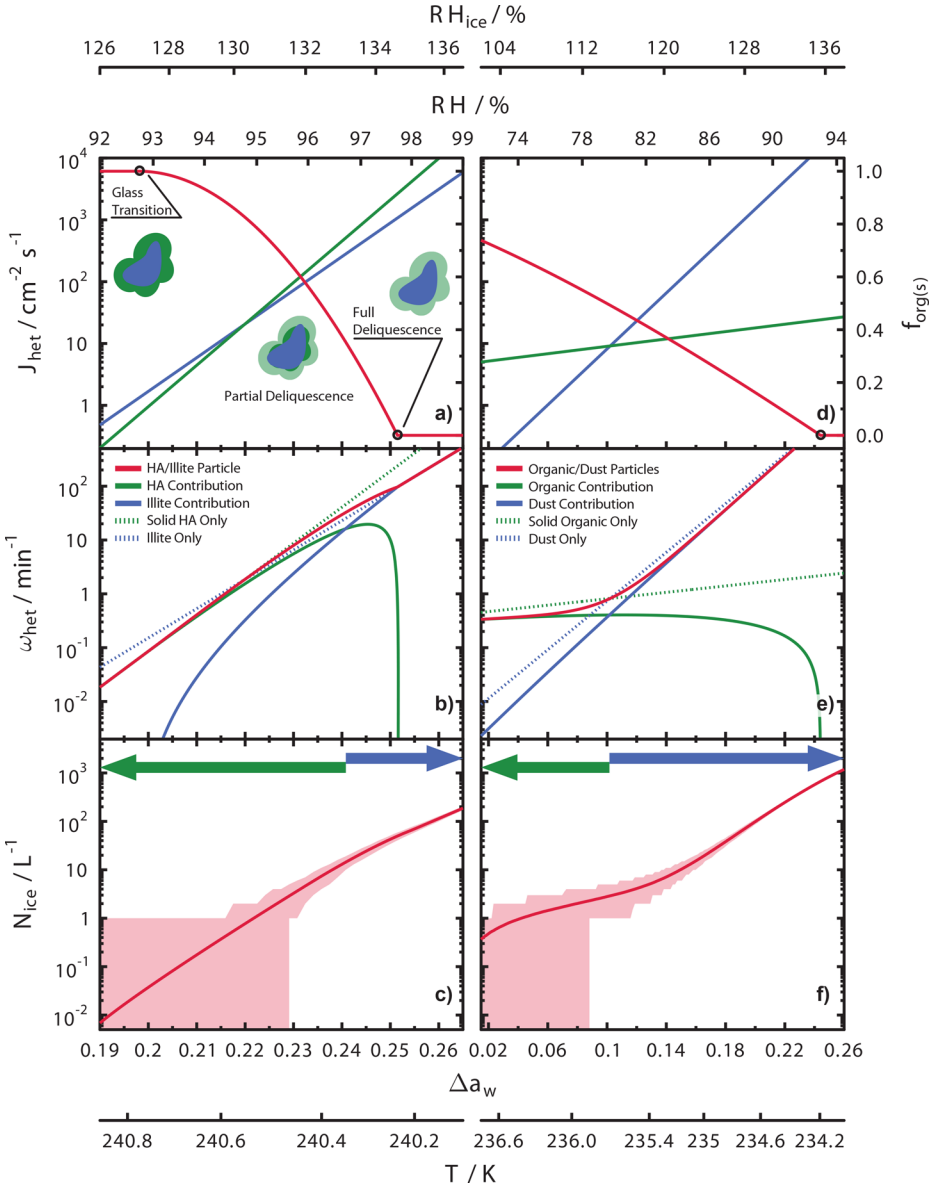

Figure 15. Representation of immersion freezing from Illite dust particles coated by humic acid (HA) (a–c) and mixed ambient OM containing particles and natural mineral dust (d–f). (a, d) The fraction that solid OM coats the mineral dust, $f_{org(s)}$, is shown as red lines. A visual representation is illustrated under glasslike and partial and fully deliquesced conditions where blue is the mineral, dark green is the solid OM, and light green is the deliquesced OM. Heterogeneous ice nucleation rate coefficients, J_{het}, as a function Δa_w for the solid OM and mineral dust are shown as green and blue lines, respectively. (b, e) Calculated heterogeneous ice nucleation rates, ω_{het}, for mixed organic/dust particles (red) and the contribution from either OM (green) or mineral dust (blue). ω_{het} calculated from only OM or mineral dust particles are shown as dotted green and blue lines, respectively. (c, f) Simulated ice concentration, N_{ice}, per liter of air. The shaded area represents the combined random error from stochastic freezing and random sampling of particle size. Green and blue arrows indicate the range at which ice nucleation rates are dominated by solid OM or mineral dust, respectively.

can account for changes in particle a_w would be desirable to implicitly account for amorphous phase changes. The majority of parametrizations and models that apply the active sites concept do not consider particle a_w, though attempts have been made using fit functions.[399] Introduction of solution a_w[355,356,373] renders J_{het} independent of the nature of the solute in the aqueous solution and interfacial energies. Thus, application of a_w avoids the capillary approximation, which is the main weakness of CNT.[40] Currently, the water activity-based immersion freezing model (ABIFM)[328,373] might present one approach to describe immersion freezing induced by amorphous OA particles.

Illustration of Water Activity-Based Model for Immersion Freezing. Previous reviews have discussed in detail various ice nucleation parametrizations.[49,50,53] Here, we briefly demonstrate predictions of the change in immersion freezing rate of inorganic particles coated by amorphous OM using ABIFM[373] as an alternative. These calculations only serve the purpose to demonstrate the prediction of INP numbers by immersion freezing, implicitly accounting for amorphous deliquescence of the organic coating. Other cloud microphysical effects,[9,457,458] including homogeneous ice nucleation, liquid droplet growth, water vapor depletion due to the Bergeron–Wegener–Findeisen process,[459–461] ice crystal growth, entrainment and mixing, and ice crystal sedimentation

DOI: 10.1021/acsearthspacechem.7b00120
ACS Earth Space Chem. 2018, 2, 168–202

are neglected. J_{het} is parametrized as a function of Δa_w,[197,373] where Δa_w is the difference between droplet solution a_w and the ice melting point, $a_w(T) - a_{w,ice}(T)$.[355] In equilibrium between gas- and condensed-phase, a_w equals ambient RH.[197] It is assumed that during amorphous deliquescence a solid organic phase coexists with an aqueous organic solution.

We simulate a particle population composed of Illite mineral dust particles coated with Leonardite, an HA, serving as a surrogate of an amorphous HULIS depicted in Figure 15a–c. For both components, J_{het} has been determined in the laboratory.[360,373,462] Upon continuous cooling with 0.1 K min^{-1}, we assume that the HA in these mixed particles will pass the glass transition similar to a fulvic acid[105] at RH = 93% at T = 240 K and reach FDRH similar to other studied OA particle systems.[112,113,119,377] Prior to the glass transition, ice formation is only possible via deposition ice nucleation on the solid (glassy) HA coating the Illite dust. Beyond the FDRH, ice formation is only possible via immersion freezing on the mineral surface. Between T_g and FDRH, an aqueous solution, some glassy HA, and Illite surface are present, and immersion freezing can occur on both organic and inorganic surfaces. The fractional coverage of solid HA, $f_{org(s)}$, is parametrized with a quadratic equation (see Figure 13a, red line), where $f_{org(s)} = 1$ prior to glass transition and $f_{org(s)} = 0$ at FDRH = 98%. J_{het} is calculated for Illite and Leonardite following ABIFM,[373] displayed as blue and green lines, respectively, in Figure 15a. The heterogeneous ice nucleation rate, ω_{het}, for a population of HA/Illite dust particles is shown in Figure 15b as a red line, where $\omega_{het} = J_{het,org} A_{org} + J_{het,dust} A_{dust}$. This two-component system uses $f_{org(s)}$ to calculate surface area, where the exposed solid HA surface area is $A_{org} = A_p f_{org(s)}$, the exposed Illite dust surface area is $A_{dust} = A_p(1 - f_{org(s)})$, and the particle surface area is A_p. We employ A_p on the order of 10^{-3} cm^2, the total particle surface area in 1 L of air for assumed bimodal log-normally distributed spherical particles with mode parameters, $N_1 = 95$ cm^{-3}, $\mu_1 = 100$ nm, $\sigma_1 = 0.5$ and $N_2 = 5$ cm^{-3}, $\mu_1 = 800$ nm, $\sigma_1 = 1.0$. This distribution is according to typical aerosol sizes and numbers in the troposphere having an enhanced accumulation mode with few coarse mode particles,[463−465] but the choice of aerosol size distribution will not affect the model findings. Figure 15b shows the contribution of the HA and Illite dust to ω_{het} in addition to upper limits of the nucleation rate due to a particle population consisting of only solid organic or mineral dust.

At a humidity slightly higher than the glass transition, the solid HA and Illite dust surface exposed to aqueous solution can nucleate ice with a combined rate $\omega_{het} = 0.09$ min^{-1} at $\Delta a_w = 0.2$. At this condition, $f_{org(s)} = 0.999$ and HA dominates ω_{het} despite having lower J_{het} compared to Illite as shown by the green and blue lines, respectively. At $\Delta a_w = 0.24$, the contributions of HA and Illite to ω_{het} become equal as indicated by the intersection of the green and blue lines. For $\Delta a_w > 0.245$, the contribution of the solid HA sharply decreases until FDRH is reached at $\Delta a_w > 0.25$, at which point no solid HA is present to nucleate ice. Overall, Figure 15b shows that when $\Delta a_w < 0.24$, the solid HA acts as the INP, and for $\Delta a_w > 0.24$, the Illite dust acts as INP. Knowledge of J_{het} and $f_{org(s)}$ allows calculation of the number of ice crystals produced, N_{ice}, given in Figure 15c. We assume individual binomial distributions to simulate freezing for all 10^5 particles present in 1 L of air and time step of 10 s. If a particle induces ice nucleation, it is removed from the distribution, and a record is kept of how many ice particles froze in the simulated volume, or N_{ice}, with units of L^{-1}. Figure 15c shows N_{ice} as a function of Δa_w. Freezing is simulated with a frost point, $T_f = 243.5$ K. At conditions where solid HA dominates immersion freezing, indicated by the green arrow, N_{ice} increases from 10^{-2} to 10 L^{-1}. When Illite particles dominate, as indicated by the blue arrow, N_{ice} continues to rise, surpassing 100 L^{-1} due to continued cooling and increasing J_{het} and ω_{het}. We note that homogeneous ice nucleation is negligible here and becomes important only at $\Delta a_w > 0.313$.[197,355]

Repeating these simulations, each time sampling freezing from a binomial distribution and particle size from the bimodal log-normal distribution, yields 10th and 90th percentiles of N_{ice} to assess uncertainty ranges[328] shown as the shaded region in Figure 15c. Stochastic freezing and random sampling of aerosol particle size distribution were the only contributors to this uncertainty estimate. At warm and dry conditions, e.g., $\Delta a_w <$ 0.21, the uncertainty in N_{ice} is more than 2 orders of magnitude because only a few ice nucleation events occurred giving rise to a large statistical uncertainty. At colder and more humid conditions, more ice nucleation events are observed resulting in less uncertainty.

We use the above model to evaluate another immersion freezing system where natural dust particles are coated by OM as shown in Figure 15d–f. Ice nucleation experiments performed by China et al. (2017)[102] employed ambient particles that were predominantly dust coated by OM. The authors suggested that the organic coating nucleated ice due to the fact it was the only common constituent among those particles individually identified and that all samples with organic coatings nucleated ice at similar RH and T. As an analogue to Figure 15a–c, we assume $J_{het}(\Delta a_w)$ from China et al. (2017)[102] in Figure 13d–f as representative of ambient organic coatings. Natural dust[466] and its corresponding parametrization for $J_{het}(\Delta a_w)$[328] is used for simulating ice nucleation by the dust core. Figure 15d displays J_{het} of the OM-coated dust and natural dust particles where T_g and FDRH are assumed to proceed at 50 and 90% RH, respectively, based on water uptake measurements by China et al. (2017).[102] Figure 13e shows that OM dominates ω_{het} until ∼80% RH. Figure 15f displays the resulting N_{ice} as a function of Δa_w, RH, RH_{ice}, and T having applied $T_f = 237$ K and the same aerosol population (size and concentration) as in panels b and c. The particles with OM dominate ice nucleation up to $N_{ice} = 3$ L^{-1} in the range indicated by the green arrow in Figure 15f. This region also exhibits the most stochastic uncertainty due to a low number of freezing events. At more humid conditions (RH > 80%), natural dust dominates ice nucleation indicated by the blue arrow, and the stochastic uncertainty is greatly reduced for N_{ice} = 10−10^3 L^{-1}.

Although the simulations in Figure 15 do not represent real cloud or aerosol processes, the uncertainty estimate can yield understanding of observed ice nucleation. The uncertainty estimates imply that instrumental uncertainty in T or RH may play a greater role than stochastic uncertainty when large numbers of INPs are measured. However, stochastic freezing uncertainty should be considered when interpreting data in the case of low N_{ice}. For example, when ice crystals form in the atmosphere with $N_{ice} = 0.2$ L^{-1}, then 80% of the time, due to randomly occurring freezing events and variability of particle size, actual N_{ice} varies between 10^{-3} and 10 L^{-1} (Figure 15c and f), which is a typical reported range in field measurements.[53,277] Given that observed INP concentrations are commonly <10 L^{-1} and concentrations are often near the detection limit,[467]

DOI: 10.1021/acsearthspacechem.7b00120
ACS Earth Space Chem. 2018, 2, 168−202

resulting N_{ice} concentrations should be expected to suffer from stochastic (nucleation theory) and random (aerosol statistics) uncertainty. Increasing the observed number of freezing events and improving particle surface area measurements could contribute to a resolution of this issue.[328] Although the simulations presented in Figure 15 are highly idealized, they demonstrate that capturing the freezing efficiency, the glass transition, FDRH, and freezing point depression of OM should be important for quantifying atmospheric ice nucleation from chemically complex aerosol particles.

■ SUMMARY AND FUTURE RESEARCH DIRECTIONS

Recognizing the abundance of OM in the atmosphere, this article summarized recent findings dealing with the role of airborne OM as a potentially significant contributor of ice nucleating substrates. Considering the wide range of thermodynamic conditions present in the Earth's atmosphere, OM will impact atmospheric ice nucleation in different ways compared to "classically" regarded INPs such as insoluble mineral dust particles. Despite the great advancements in understanding ice nucleation processes, many challenges remain to assess the importance of OM and OA particles in atmospheric cloud glaciation. We highlighted the peculiar physicochemical features of OM, which are modulated by changes in ambient temperature and humidity, the current lack of molecular level understanding of ice nucleation, the challenges in analyses and measurements of INPs and IRs, and the necessity of descriptive physical and chemical approaches that include OM specific processes. A multidisciplinary approach is necessary covering molecular, laboratory, field, and modeling scales to improve our predictive understanding of atmospheric ice nucleation by OM. We have identified the following key points that, we feel, warrant future research to fill knowledge gaps in ice nucleation by OM:

1. Gain a sufficiently comprehensive molecular understanding of the interaction between liquid water and water vapor with organic substrates of varying composition, morphology, viscosity, and surface functional groups to confidently predict OM nucleating behavior. Establish the physical and chemical interfacial features that initiate and govern the nucleation process. Molecular dynamic simulations and Monte Carlo and density functional theory calculations have been shown to be promising approaches. Further validation of those model results by carefully designed experiments, and applying controlled, artificial substrates will be required to confirm the insights gained on ice nucleation mechanisms.

2. Further develop techniques to rapidly image the dynamic ice nucleation process and instrumentation to probe and characterize the interfaces that initiate ice nucleation at the subnanoscale. Complementary to current SEM and SFG methods, further development of instruments capable of measurements of the ice nucleating sites with high temporal (because nucleation occurs rapidly) and spatial resolution is necessary. INP measurements will benefit from improvements in the detection limit, temporal resolution of the ice nucleation event, and increases in the sampled number of ice nucleation events.

3. Expand direct measurements of OM and SOA viscosity and associated phase changes including liquid−liquid phase separation processes under thermodynamic conditions relevant for mixed-phase and cirrus clouds and relate those parameters to ice nucleation. Evaluate the competition between diffusion governed OM and SOA phase changes, ice nucleation pathways, and ice nucleation kinetics. This requires a rigorous humidity and temperature trajectory assessment in experiments and will need to be applicable to actual cloud activation time scales.

4. Establish a better understanding of how chemical aging of OM by atmospheric oxidants and different SOA formations pathways (e.g., low or high NO_x conditions, oligomerization reactions, SOA precursor gases with higher molecular weight, etc.) impact ice nucleation by a combination of oxidant exposure ice nucleation experiments, theoretical model simulations, and field campaigns.

5. Expand measurements of INP spectra, i.e., for the entire particle size distribution covering the supermicrometer mode, including the physicochemical characterization of ambient INPs containing OM in the planetary boundary layer and free troposphere in different environments and geological locations. Assess the INPs' chemical complexity and mixing state. Identification of ice nucleating macromolecules in nanometer sizes and observation of high INP number concentrations in supermicrometer particle sizes emphasize the need to expand the measured INP size spectrum.

6. Continue to develop uncertainty assessment methodologies for any employed measurement technique sufficient to rigorously establish statistical significance of gathered data. Low INP concentrations relative to detection limits are associated with a large data scatter irrespective of instrument accuracy. In general, stochastic freezing and aerosol size variability can be meaningfully reduced when probing a larger number of INPs. Furthermore, best practices should be developed with regard to potential contamination issues by trace gas exposure and applied water sources.

7. Further develop and evaluate descriptive approaches to ice nucleation (immersion, deposition, and contact modes) considering the insufficient knowledge about the physicochemical features of active sites. Theoretical models should represent the amorphous phase changes of OM and the varying ice nucleation kinetics as OA particles are advected in a cloud system. Considering the kinetically driven amorphous OM phase changes, evaluate the application of the time-independent and time-dependent ice nucleation models. The kinetic flux model and a water activity-based freezing description show promise for a comprehensive representation of the amorphous phase-ice nucleation relationship. Approaches also will depend on the applied scale, i.e., cloud microphysics vs large-scale atmospheric models and thus will differ in complexity. Future field measurements would benefit from being explicitly focused on constraining global model predictions over a wide range of T and RH, ideally over the full range of INP sizes.

8. Better establish how important cloud recycling of organic INPs and associated particle morphological changes and preactivation are as contributors to ice nucleation in the atmosphere. Establish the degree to which preactivation and associated changes in ice nucleation propensity may occur using laboratory particle surrogates. Identify atmospheric conditions under which those effects are expected and can be confirmed in field observations.

We hope that these suggestions spur novel and exciting research, ultimately resolving how OM can act as ice nucleating substrate in the atmosphere. There are likely many more discoveries to be made when probing multicomponent and multiphase OM or OA particles at supercooled temperatures and metastable conditions for their interaction with water.

DOI: 10.1021/acsearthspacechem.7b00120
ACS Earth Space Chem. 2018, 2, 168−202

AUTHOR INFORMATION

Corresponding Author

*E-mail: Daniel.Knopf@stonybrook.edu.

ORCID

Daniel A. Knopf: 0000-0001-7732-3922

Notes

The authors declare no competing financial interest.

ACKNOWLEDGMENTS

This work was funded by the U.S. Department of Energy, Office of Science (BER), Atmospheric System Research (DE-SC0016370) and U.S. National Science Foundation grants AGS 1446286 and AGS 1232203. P. A. acknowledges support from the European Union's Horizon 2020 research and innovation program under the Marie Skłodowska-Curie grant agreement No. 701647. B. W. acknowledges the support by the National Natural Science Foundation of China (No. 41775133), the Fundamental Research Funds for the Central Universities (No. 20720160111), and the Recruitment Program of Global Youth Experts of China. The authors are grateful to J. Aller and A. Fridlind for reading the manuscript and providing helpful comments.

NOMENCLATURE

ABIFM	water activity-based immersion freezing model
A_{dust}	surface area of mineral dust, [cm^2]
A_p	surface area of particle, [cm^2]
A_{org}	surface area of organic compound, [cm^2]
a_w	water activity
$a_{w,ice}$	ice melting point as a function of water activity
CalNex	California Research at the Nexus of Air Quality and Climate Change
CARES	Carbonaceous Aerosols and Radiative Effects Study
CCSEM/EDX	computer-controlled scanning electron microscopy with energy-dispersive X-ray analysis
CFDC	continuous flow diffusion chamber
CNT	classical nucleation theory
CVI	counterflow-virtual-impactor
Δa_w	water activity criterion
ELV-OOA	extremely LV-OOA
FD	full deliquescence
FDRH	full deliquescence relative humidity
f_{ice}	number of nucleated ice crystals/aerosol particle number
$f_{org(s)}$	fractional coverage of solid
HA	humic acid
HOA	hydrocarbon-like OA
HULIS	humic-like substances
Ice-CVI	ice counterflow-virtual-impactor
INM	ice nucleating macromolecule
INP	ice nucleating particle
ISDAC	Indirect and Semi-Direct Aerosol Campaign
ISI	ice selective inlet
J_{het}	heterogeneous ice nucleation rate coefficient, [cm^{-2} s^{-1}]
$J_{het,dust}$	heterogeneous ice nucleation rate coefficient of mineral dust, [cm^{-2} s^{-1}]
$J_{het,org}$	heterogeneous ice nucleation rate coefficient of organic compound, [cm^{-2} s^{-1}]
J_{hom}	homogeneous ice nucleation rate coefficient, [cm^{-3} s^{-1}]
LLPS	liquid−liquid phase separation
LV-OOA	low-volatile oxygenated OA
MD	molecular dynamics
MILAGRO	The Megacity Initiative: Local and Global Research Observations
μ_1, μ_2	location parameter of log-normal distribution
N_1, N_2	particle numbers in bimodal log-normal size distribution
N_{ice}	number of ice crystals, [L^{-1}]
O:C	atomic oxygen to carbon ratio
OA	organic aerosol
OC	organic carbon
OM	organic matter
ω_{het}	heterogeneous ice nucleation rate, [s^{-1}]
PALMS	particle ablation by laser mass spectrometry
PD	partial deliquescence
PDF	probability density function
POA	primary organic aerosol
rBC	refractory black carbon
RH	relative humidity, [%]
RH_{ice}	relative humidity with respect to ice, [%]
σ_1, σ_2	scale parameter of log-normal distribution
SFG	sum frequency generation spectroscopy
SHG	second-harmonic generation spectroscopy
S_{ice}	supersaturation with respect to ice
SOA	secondary organic aerosol
SRFA	Suwannee River fluvic acid
SSA	sea spray aerosol
STXM/NEXAFS	scanning transmission X-ray microscopy coupled with near-edge X-ray absorption fine structure spectroscopy
SV-OA	semivolatile OA
τ_{cd}	characteristic time scale of bulk diffusion
TEM	transmission electron microscopy
TEM/EDX	transmission electron microscopy/energy-dispersive X-ray analysis
T	temperature, [K]
T_f	frost point, [K]
T_g	glass transition temperature
UT/LS	upper troposphere and lower stratosphere
VOC	volatile organic compound
XPS	X-ray photoelectron spectroscopy

REFERENCES

(1) Smith, P. H.; Tamppari, L. K.; Arvidson, R. E.; Bass, D.; Blaney, D.; Boynton, W. V.; Carswell, A.; Catling, D. C.; Clark, B. C.; Duck, T.; DeJong, E.; Fisher, D.; Goetz, W.; Gunnlaugsson, H. P.; Hecht, M. H.; Hipkin, V.; Hoffman, J.; Hviid, S. F.; Keller, H. U.; Kounaves, S. P.; Lange, C. F.; Lemmon, M. T.; Madsen, M. B.; Markiewicz, W. J.; Marshall, J.; McKay, C. P.; Mellon, M. T.; Ming, D. W.; Morris, R. V.; Pike, W. T.; Renno, N.; Staufer, U.; Stoker, C.; Taylor, P.; Whiteway, J. A.; Zent, A. P. H2O at the Phoenix Landing Site. *Science* **2009**, *325* (5936), 58−61.

(2) Whiteway, J. A.; Komguem, L.; Dickinson, C.; Cook, C.; Illnicki, M.; Seabrook, J.; Popovici, V.; Duck, T. J.; Davy, R.; Taylor, P. A.; Pathak, J.; Fisher, D.; Carswell, A. I.; Daly, M.; Hipkin, V.; Zent, A. P.; Hecht, M. H.; Wood, S. E.; Tamppari, L. K.; Renno, N.; Moores, J. E.; Lemmon, M. T.; Daerden, F.; Smith, P. H. Mars Water-Ice Clouds and Precipitation. *Science* **2009**, *325* (5936), 68−70.

DOI: 10.1021/acsearthspacechem.7b00120
ACS Earth Space Chem. 2018, 2, 168−202

(3) Carr, M. H.; Belton, M. J. S.; Chapman, C. R.; Davies, A. S.; Geissler, P.; Greenberg, R.; McEwen, A. S.; Tufts, B. R.; Greeley, R.; Sullivan, R.; Head, J. W.; Pappalardo, R. T.; Klaasen, K. P.; Johnson, T. V.; Kaufman, J.; Senske, D.; Moore, J.; Neukum, G.; Schubert, G.; Burns, J. A.; Thomas, P.; Veverka, J. Evidence for a subsurface ocean on Europa. *Nature* **1998**, *391* (6665), 363−365.
(4) Scipioni, F.; Schenk, P.; Tosi, F.; D'Aversa, E.; Clark, R.; Combe, J. P.; Ore, C. M. D. Deciphering sub-micron ice particles on Enceladus surface. *Icarus* **2017**, *290*, 183−200.
(5) Fisher, E. A.; Lucey, P. G.; Lemelin, M.; Greenhagen, B. T.; Siegler, M. A.; Mazarico, E.; Aharonson, O.; Williams, J. P.; Hayne, P. O.; Neumann, G. A.; Paige, D. A.; Smith, D. E.; Zuber, M. T. Evidence for surface water ice in the lunar polar regions using reflectance measurements from the Lunar Orbiter Laser Altimeter and temperature measurements from the Diviner Lunar Radiometer Experiment. *Icarus* **2017**, *292*, 74−85.
(6) Ball, P. *Life's Matrix: A Biography of Water*, 1st ed; University of California Press, 2001.
(7) Boucher, O.; Randall, D.; Artaxo, P.; Bretherton, C.; Feingold, G.; Forster, P.; Kerminen, V.-M.; Kondo, Y.; Liao, H.; Lohmann, U.; Rasch, P.; Satheesh, S. K.; Sherwood, S.; Stevens, B.; Zhang, X. Y. Clouds and Aerosols. In *Climate Change 2013: The Physical Science Basis. Contribution of Working Group I to the Fifth Assessment Report of the Intergovernmental Panel on Climate Change*; Stocker, T. F., Qin, D., Plattner, G.-K., Tignor, M., Allen, S. K., Boschung, J., Nauels, A., Xia, Y., Bex, V., Midgley, P. M., Eds.; Cambridge University Press: Cambridge, United Kingdom and New York, NY, USA, 2013.
(8) Storelvmo, T.; Jeanloz, R.; Freeman, K. H. Aerosol Effects on Climate via Mixed-Phase and Ice Clouds. *Annu. Rev. Earth Planet. Sci.* **2017**, *45*, 199−222.
(9) Baker, M. B.; Peter, T. Small-scale cloud processes and climate. *Nature* **2008**, *451* (7176), 299−300.
(10) Baker, M. B. Cloud microphysics and climate. *Science* **1997**, *276* (5315), 1072−1078.
(11) Lohmann, U.; Feichter, J. Global indirect aerosol effects: a review. *Atmos. Chem. Phys.* **2005**, *5*, 715−737.
(12) Rosenfeld, D.; Sherwood, S.; Wood, R.; Donner, L. Climate effects of aerosol-cloud interactions. *Science* **2014**, *343* (6169), 379−380.
(13) Lau, K. M.; Wu, H. T. Warm rain processes over tropical oceans and climate implications. *Geophys. Res. Lett.* **2003**, *30* (24), 2290.
(14) Mulmenstadt, J.; Sourdeval, O.; Delanoe, J.; Quaas, J. Frequency of occurrence of rain from liquid-, mixed-, and ice-phase clouds derived from A-Train satellite retrievals. *Geophys. Res. Lett.* **2015**, *42* (15), 6502−6509.
(15) Brewer, A. W. Evidence for a world circulation provided by the measurements of helium and water vapour distribution in the stratosphere. *Q. J. R. Meteorol. Soc.* **1949**, *75* (326), 351−363.
(16) Holton, J. R.; Haynes, P. H.; McIntyre, M. E.; Douglass, A. R.; Rood, R. B.; Pfister, L. Stratosphere-troposphere exchange. *Rev. Geophys.* **1995**, *33* (4), 403−439.
(17) Lohmann, U.; Roeckner, E.; Collins, W. D.; Heymsfield, A. J.; McFarquhar, G. M.; Barnett, T. P. The role of water vapor and convection during the Central Equatorial Pacific Experiment from observations and model simulations. *J. Geophys. Res.* **1995**, *100* (D12), 26229−26245.
(18) Held, I. M.; Soden, B. J. Water vapor feedback and global warming. *Annu. Rev. Energy Env.* **2000**, *25*, 441−475.
(19) Krämer, M.; Schiller, C.; Voigt, C.; Schlager, H.; Popp, P. J. A climatological view of HNO3 partitioning in cirrus clouds. *Q. J. R. Meteorol. Soc.* **2008**, *134* (633), 905−912.
(20) Popp, P. J.; Marcy, T. P.; Watts, L. A.; Gao, R. S.; Fahey, D. W.; Weinstock, E. M.; Smith, J. B.; Herman, R. L.; Troy, R. F.; Webster, C. R.; Christensen, L. E.; Baumgardner, D. G.; Voigt, C.; Karcher, B.; Wilson, J. C.; Mahoney, M. J.; Jensen, E. J.; Bui, T. P. Condensed-phase nitric acid in a tropical subvisible cirrus cloud. *Geophys. Res. Lett.* **2007**, *34* (24), L24812.
(21) Voigt, C.; Schlager, H.; Ziereis, H.; Karcher, B.; Luo, B. P.; Schiller, C.; Kramer, M.; Popp, P. J.; Irie, H.; Kondo, Y. Nitric acid in cirrus clouds. *Geophys. Res. Lett.* **2006**, *33* (5), L05803.
(22) Forster, P.; Ramaswamy, V.; Artaxo, P.; Berntsen, T.; Betts, R.; Fahey, D. W.; Haywood, J.; Lean, J.; Lowe, D. C.; Myhre, G.; Nganga, J.; Prinn, R.; Raga, G.; Schulz, M.; Van Dorland, R. Chapter 2: Changes in Atmospheric Constituents and in Radiative Forcing. In *Climate Change 2007: The Physical Science Basis. Contribution of Working Group I to the Fourth Assessment Report of the Intergovernmental Panel on Climate Change*; Solomon, S., Qin, D., Manning, M., Chen, Z., Marquis, M., Averyt, K. B., Tignor, M., Miller, H. L., Eds.; Cambridge University Press: Cambridge, United Kingdom and New York, NY, USA, 2007; pp 129−234.
(23) Field, P. R.; Lawson, P.; Brown, R. A.; Lloyd, G.; Westbrook, C.; Moisseev, D.; Miltenberger, A.; Nenes, A.; Blyth, A.; Choularton, T.; Connolly, P.; Buehl, J.; Crosier, J.; Cui, Z.; Dearden, C.; Demott, P.; Flossmann, A.; Heymsfield, A.; Huang, Y.; Kalesse, H.; Kanji, Z. A.; Korolev, A.; Kirchgaessner, A.; Lasher-Trapp, S.; Leisner, T.; Mcfarquhar, G.; Phillips, V.; Stith, J.; Sullivan, S. Secondary Ice Production: Current State of the Science and Recommendations for the Future. In *Ice Formation and Evolution in Clouds and Precipitation: Measurement and Modeling Challenges*; American Meteorological Society, 2017; Vol. *58*, pp 7.1−7.20.
(24) Hallett, J.; Mossop, S. C. Production of secondary ice particles during riming process. *Nature* **1974**, *55* (6), 679−679.
(25) Ladino, L. A.; Korolev, A.; Heckman, I.; Wolde, M.; Fridlind, A. M.; Ackerman, A. S. On the role of ice-nucleating aerosol in the formation of ice particles in tropical mesoscale convective systems. *Geophys. Res. Lett.* **2017**, *44* (3), 1574−1582.
(26) Fridlind, A. M.; Li, X. W.; Wu, D.; van Lier-Walqui, M.; Ackerman, A. S.; Tao, W. K.; McFarquhar, G. M.; Wu, W.; Dong, X. Q.; Wang, J. Y.; Ryzhkov, A.; Zhang, P. F.; Poellot, M. R.; Neumann, A.; Tomlinson, J. M. Derivation of aerosol profiles for MC3E convection studies and use in simulations of the 20 May squall line case. *Atmos. Chem. Phys.* **2017**, *17* (9), 5947−5972.
(27) Kanakidou, M.; Seinfeld, J. H.; Pandis, S. N.; Barnes, I.; Dentener, F. J.; Facchini, M. C.; Van Dingenen, R.; Ervens, B.; Nenes, A.; Nielsen, C. J.; Swietlicki, E.; Putaud, J. P.; Balkanski, Y.; Fuzzi, S.; Horth, J.; Moortgat, G. K.; Winterhalter, R.; Myhre, C. E. L.; Tsigaridis, K.; Vignati, E.; Stephanou, E. G.; Wilson, J. Organic aerosol and global climate modelling: a review. *Atmos. Chem. Phys.* **2005**, *5*, 1053−1123.
(28) Hallquist, M.; Wenger, J. C.; Baltensperger, U.; Rudich, Y.; Simpson, D.; Claeys, M.; Dommen, J.; Donahue, N. M.; George, C.; Goldstein, A. H.; Hamilton, J. F.; Herrmann, H.; Hoffmann, T.; Iinuma, Y.; Jang, M.; Jenkin, M. E.; Jimenez, J. L.; Kiendler-Scharr, A.; Maenhaut, W.; McFiggans, G.; Mentel, T. F.; Monod, A.; Prevot, A. S. H.; Seinfeld, J. H.; Surratt, J. D.; Szmigielski, R.; Wildt, J. The formation, properties and impact of secondary organic aerosol: current and emerging issues. *Atmos. Chem. Phys.* **2009**, *9* (14), 5155−5236.
(29) Jimenez, J. L.; Canagaratna, M. R.; Donahue, N. M.; Prevot, A. S. H.; Zhang, Q.; Kroll, J. H.; DeCarlo, P. F.; Allan, J. D.; Coe, H.; Ng, N. L.; Aiken, A. C.; Docherty, K. S.; Ulbrich, I. M.; Grieshop, A. P.; Robinson, A. L.; Duplissy, J.; Smith, J. D.; Wilson, K. R.; Lanz, V. A.; Hueglin, C.; Sun, Y. L.; Tian, J.; Laaksonen, A.; Raatikainen, T.; Rautiainen, J.; Vaattovaara, P.; Ehn, M.; Kulmala, M.; Tomlinson, J. M.; Collins, D. R.; Cubison, M. J.; Dunlea, E. J.; Huffman, J. A.; Onasch, T. B.; Alfarra, M. R.; Williams, P. I.; Bower, K.; Kondo, Y.; Schneider, J.; Drewnick, F.; Borrmann, S.; Weimer, S.; Demerjian, K.; Salcedo, D.; Cottrell, L.; Griffin, R.; Takami, A.; Miyoshi, T.; Hatakeyama, S.; Shimono, A.; Sun, J. Y.; Zhang, Y. M.; Dzepina, K.; Kimmel, J. R.; Sueper, D.; Jayne, J. T.; Herndon, S. C.; Trimborn, A. M.; Williams, L. R.; Wood, E. C.; Middlebrook, A. M.; Kolb, C. E.; Baltensperger, U.; Worsnop, D. R. Evolution of Organic Aerosols in the Atmosphere. *Science* **2009**, *326* (5959), 1525−1529.
(30) Heald, C. L.; Goldstein, A. H.; Allan, J. D.; Aiken, A. C.; Apel, E.; Atlas, E. L.; Baker, A. K.; Bates, T. S.; Beyersdorf, A. J.; Blake, D. R.; Campos, T.; Coe, H.; Crounse, J. D.; DeCarlo, P. F.; de Gouw, J. A.; Dunlea, E. J.; Flocke, F. M.; Fried, A.; Goldan, P.; Griffin, R. J.;

DOI: 10.1021/acsearthspacechem.7b00120
ACS Earth Space Chem. 2018, 2, 168−202

Herndon, S. C.; Holloway, J. S.; Holzinger, R.; Jimenez, J. L.; Junkermann, W.; Kuster, W. C.; Lewis, A. C.; Meinardi, S.; Millet, D. B.; Onasch, T.; Polidori, A.; Quinn, P. K.; Riemer, D. D.; Roberts, J. M.; Salcedo, D.; Sive, B.; Swanson, A. L.; Talbot, R.; Warneke, C.; Weber, R. J.; Weibring, P.; Wennberg, P. O.; Worsnop, D. R.; Wittig, A. E.; Zhang, R.; Zheng, J.; Zheng, W. Total observed organic carbon (TOOC) in the atmosphere: a synthesis of North American observations. *Atmos. Chem. Phys.* **2008**, *8* (7), 2007−2025.

(31) Zhang, Q.; Jimenez, J. L.; Canagaratna, M. R.; Allan, J. D.; Coe, H.; Ulbrich, I.; Alfarra, M. R.; Takami, A.; Middlebrook, A. M.; Sun, Y. L.; Dzepina, K.; Dunlea, E.; Docherty, K.; DeCarlo, P. F.; Salcedo, D.; Onasch, T.; Jayne, J. T.; Miyoshi, T.; Shimono, A.; Hatakeyama, S.; Takegawa, N.; Kondo, Y.; Schneider, J.; Drewnick, F.; Borrmann, S.; Weimer, S.; Demerjian, K.; Williams, P.; Bower, K.; Bahreini, R.; Cottrell, L.; Griffin, R. J.; Rautiainen, J.; Sun, J. Y.; Zhang, Y. M.; Worsnop, D. R. Ubiquity and dominance of oxygenated species in organic aerosols in anthropogenically-influenced Northern Hemisphere midlatitudes. *Geophys. Res. Lett.* **2007**, *34* (13), L13801.

(32) Ehn, M.; Thornton, J. A.; Kleist, E.; Sipila, M.; Junninen, H.; Pullinen, I.; Springer, M.; Rubach, F.; Tillmann, R.; Lee, B.; Lopez-Hilfiker, F.; Andres, S.; Acir, I. H.; Rissanen, M.; Jokinen, T.; Schobesberger, S.; Kangasluoma, J.; Kontkanen, J.; Nieminen, T.; Kurten, T.; Nielsen, L. B.; Jorgensen, S.; Kjaergaard, H. G.; Canagaratna, M.; Dal Maso, M.; Berndt, T.; Petaja, T.; Wahner, A.; Kerminen, V. M.; Kulmala, M.; Worsnop, D. R.; Wildt, J.; Mentel, T. F. A large source of low-volatility secondary organic aerosol. *Nature* **2014**, *506* (7489), 476−479.

(33) Shrivastava, M.; Cappa, C. D.; Fan, J. W.; Goldstein, A. H.; Guenther, A. B.; Jimenez, J. L.; Kuang, C.; Laskin, A.; Martin, S. T.; Ng, N. L.; Petaja, T.; Pierce, J. R.; Rasch, P. J.; Roldin, P.; Seinfeld, J. H.; Shilling, J.; Smith, J. N.; Thornton, J. A.; Volkamer, R.; Wang, J.; Worsnop, D. R.; Zaveri, R. A.; Zelenyuk, A.; Zhang, Q. Recent advances in understanding secondary organic aerosol: Implications for global climate forcing. *Rev. Geophys.* **2017**, *55* (2), 509−559.

(34) Turpin, B. J.; Lim, H. J. Species contributions to PM2.5 mass concentrations: Revisiting common assumptions for estimating organic mass. *Aerosol Sci. Technol.* **2001**, *35* (1), 602−610.

(35) Murphy, D. M.; Cziczo, D. J.; Froyd, K. D.; Hudson, P. K.; Matthew, B. M.; Middlebrook, A. M.; Peltier, R. E.; Sullivan, A.; Thomson, D. S.; Weber, R. J. Single-particle mass spectrometry of tropospheric aerosol particles. *J. Geophys. Res.* **2006**, *111* (D23), D23S32.

(36) Heald, C. L.; Jacob, D. J.; Park, R. J.; Russell, L. M.; Huebert, B. J.; Seinfeld, J. H.; Liao, H.; Weber, R. J. A large organic aerosol source in the free troposphere missing from current models. *Geophys. Res. Lett.* **2005**, *32* (18), L18809.

(37) Volkamer, R.; Jimenez, J. L.; San Martini, F.; Dzepina, K.; Zhang, Q.; Salcedo, D.; Molina, L. T.; Worsnop, D. R.; Molina, M. J. Secondary organic aerosol formation from anthropogenic air pollution: Rapid and higher than expected. *Geophys. Res. Lett.* **2006**, *33* (17), L17811.

(38) Goldstein, A. H.; Galbally, I. E. Known and unexplored organic constituents in the earth's atmosphere. *Environ. Sci. Technol.* **2007**, *41* (5), 1514−1521.

(39) de Gouw, J. A.; Middlebrook, A. M.; Warneke, C.; Goldan, P. D.; Kuster, W. C.; Roberts, J. M.; Fehsenfeld, F. C.; Worsnop, D. R.; Canagaratna, M. R.; Pszenny, A. A. P.; Keene, W. C.; Marchewka, M.; Bertman, S. B.; Bates, T. S. Budget of organic carbon in a polluted atmosphere: Results from the New England Air Quality Study in 2002. *J. Geophys. Res.* **2005**, *110* (D16), D16305.

(40) Pruppacher, H. R.; Klett, J. D. *Microphysics of Clouds and Precipitation*; Kluwer Academic Publishers: Dordrecht, The Netherlands, 1997.

(41) Morris, C. E.; Georgakopoulos, D. G.; Sands, D. C. Ice nucleation active bacteria and their potential role in precipitation. *J. Phys. IV* **2004**, *121*, 87−103.

(42) Schnell, R. C.; Vali, G. Biogenic Ice Nuclei: Part I. Terrestrial and Marine Sources. *J. Atmos. Sci.* **1976**, *33* (8), 1554−1564.

(43) Vali, G.; Christensen, M.; Fresh, R. W.; Galyan, E. L.; Maki, L. R.; Schnell, R. C. Biogenic Ice Nuclei. Part II: Bacterial Sources. *J. Atmos. Sci.* **1976**, *33* (8), 1565−1570.

(44) Fröhlich-Nowoisky, J.; Kampf, C. J.; Weber, B.; Huffman, J. A.; Pöhlker, C.; Andreae, M. O.; Lang-Yona, N.; Burrows, S. M.; Gunthe, S. S.; Elbert, W.; Su, H.; Hoor, P.; Thines, E.; Hoffmann, T.; Despres, V. R.; Poschl, U. Bioaerosols in the Earth system: Climate, health, and ecosystem interactions. *Atmos. Res.* **2016**, *182*, 346−376.

(45) Huffman, J. A.; Prenni, A. J.; DeMott, P. J.; Pöhlker, C.; Mason, R. H.; Robinson, N. H.; Fröhlich-Nowoisky, J.; Tobo, Y.; Despres, V. R.; Garcia, E.; Gochis, D. J.; Harris, E.; Mueller-Germann, I.; Ruzene, C.; Schmer, B.; Sinha, B.; Day, D. A.; Andreae, M. O.; Jimenez, J. L.; Gallagher, M.; Kreidenweis, S. M.; Bertram, A. K.; Pöschl, U. High concentrations of biological aerosol particles and ice nuclei during and after rain. *Atmos. Chem. Phys.* **2013**, *13* (13), 6151−6164.

(46) Despres, V. R.; Huffman, J. A.; Burrows, S. M.; Hoose, C.; Safatov, A. S.; Buryak, G.; Fröhlich-Nowoisky, J.; Elbert, W.; Andreae, M. O.; Pöschl, U.; Jaenicke, R. Primary biological aerosol particles in the atmosphere: a review. *Tellus, Ser. B* **2012**, *64*, 1−58.

(47) Fröhlich-Nowoisky, J.; Burrows, S. M.; Xie, Z.; Engling, G.; Solomon, P. A.; Fraser, M. P.; Mayol-Bracero, O. L.; Artaxo, P.; Begerow, D.; Conrad, R.; Andreae, M. O.; Despres, V. R.; Pöschl, U. Biogeography in the air: fungal diversity over land and oceans. *Biogeosciences* **2012**, *9* (3), 1125−1136.

(48) Hegg, D. A.; Baker, M. B. Nucleation in the atmosphere. *Rep. Prog. Phys.* **2009**, *72* (5), 056801.

(49) Murray, B. J.; O'Sullivan, D.; Atkinson, J. D.; Webb, M. E. Ice nucleation by particles immersed in supercooled cloud droplets. *Chem. Soc. Rev.* **2012**, *41* (19), 6519−6554.

(50) Hoose, C.; Möhler, O. Heterogeneous ice nucleation on atmospheric aerosols: a review of results from laboratory experiments. *Atmos. Chem. Phys.* **2012**, *12* (20), 9817−9854.

(51) Cantrell, W.; Heymsfield, A. Production of ice in tropospheric clouds - A review. *Bull. Am. Meteorol. Soc.* **2005**, *86* (6), 795−807.

(52) DeMott, P. J.; Möhler, O.; Stetzer, O.; Vali, G.; Levin, Z.; Petters, M. D.; Murakami, M.; Leisner, T.; Bundke, U.; Klein, H.; Kanji, Z. A.; Cotton, R.; Jones, H.; Benz, S.; Brinkmann, M.; Rzesanke, D.; Saathoff, H.; Nicolet, M.; Saito, A.; Nillius, B.; Bingemer, H.; Abbatt, J.; Ardon, K.; Ganor, E.; Georgakopoulos, D. G.; Saunders, C. Resurgence in ice nuclei measurement research. *Bull. Am. Meteorol. Soc.* **2011**, *92* (12), 1623−1635.

(53) Kanji, Z. A.; Ladino, L. A.; Wex, H.; Boose, Y.; Burkert-Kohn, M.; Cziczo, D. J.; Krämer, M. Overview of Ice Nucleating Particles. In *Ice Formation and Evolution in Clouds and Precipitation: Measurement and Modeling Challenges*; American Meteorological Society, 2017; Vol. *58*, pp 1.1−1.33.

(54) Cziczo, D. J.; Ladino, L. A.; Boose, Y.; Kanji, Z. A.; Kupiszewski, P.; Lance, S.; Mertes, S.; Wex, H. Measurements of Ice Nucleating Particles and Ice Residuals. In *Ice Formation and Evolution in Clouds and Precipitation: Measurement and Modeling Challenges*; American Meteorological Society, 2017; Vol. *58*, pp 8.1−8.13.

(55) Coluzza, I.; Creamean, J.; Rossi, M. J.; Wex, H.; Alpert, P. A.; Bianco, V.; Boose, Y.; Dellago, C.; Felgitsch, L.; Fröhlich-Nowoisky, J.; Herrmann, H.; Jungblut, S.; Kanji, Z. A.; Menzl, G.; Moffett, B.; Moritz, C.; Mutzel, A.; Pöschl, U.; Schauperl, M.; Scheel, J.; Stopelli, E.; Stratmann, F.; Grothe, H.; Schmale, D. G., III Perspectives on the Future of Ice Nucleation Research: Research Needs and Unanswered Questions Identified from Two International Workshops. *Atmosphere* **2017**, *8*, 138.

(56) Ariya, P. A.; Sun, J.; Eltouny, N. A.; Hudson, E. D.; Hayes, C. T.; Kos, G. Physical and chemical characterization of bioaerosols - Implications for nucleation processes. *Int. Rev. Phys. Chem.* **2009**, *28* (1), 1−32.

(57) Salameh, A.; Daskalakis, V. Atmospheric Ice Nucleation by Glassy Organic Compounds: A Review. *Chemi. Compol. J.* **2017**, *1*, 13−23.

(58) Vali, G.; DeMott, P. J.; Möhler, O.; Whale, T. F. Technical Note: A proposal for ice nucleation terminology. *Atmos. Chem. Phys.* **2015**, *15* (18), 10263−10270.

DOI: 10.1021/acsearthspacechem.7b00120
ACS Earth Space Chem. 2018, 2, 168−202

(59) Heald, C. L.; Coe, H.; Jimenez, J. L.; Weber, R. J.; Bahreini, R.; Middlebrook, A. M.; Russell, L. M.; Jolleys, M.; Fu, T.-M.; Allan, J. D.; Bower, K. N.; Capes, G.; Crosier, J.; Morgan, W. T.; Robinson, N. H.; Williams, P. I.; Cubison, M. J.; DeCarlo, P. F.; Dunlea, E. J. Exploring the vertical profile of atmospheric organic aerosol: comparing 17 aircraft field campaigns with a global model. *Atmos. Chem. Phys.* **2011**, *11* (24), 12673.
(60) Donahue, N. M.; Epstein, S. A.; Pandis, S. N.; Robinson, A. L. A two-dimensional volatility basis set: 1. organic-aerosol mixing thermodynamics. *Atmos. Chem. Phys.* **2011**, *11* (7), 3303−3318.
(61) Kroll, J. H.; Donahue, N. M.; Jimenez, J. L.; Kessler, S. H.; Canagaratna, M. R.; Wilson, K. R.; Altieri, K. E.; Mazzoleni, L. R.; Wozniak, A. S.; Bluhm, H.; Mysak, E. R.; Smith, J. D.; Kolb, C. E.; Worsnop, D. R. Carbon oxidation state as a metric for describing the chemistry of atmospheric organic aerosol. *Nat. Chem.* **2011**, *3* (2), 133−139.
(62) Li, Y.; Pöschl, U.; Shiraiwa, M. Molecular corridors and parameterizations of volatility in the chemical evolution of organic aerosols. *Atmos. Chem. Phys.* **2016**, *16* (5), 3327−3344.
(63) Hoyle, C. R.; Boy, M.; Donahue, N. M.; Fry, J. L.; Glasius, M.; Guenther, A.; Hallar, A. G.; Hartz, K. H.; Petters, M. D.; Petaja, T.; Rosenoern, T.; Sullivan, A. P. A review of the anthropogenic influence on biogenic secondary organic aerosol. *Atmos. Chem. Phys.* **2011**, *11* (1), 321−343.
(64) Ervens, B.; Turpin, B. J.; Weber, R. J. Secondary organic aerosol formation in cloud droplets and aqueous particles (aqSOA): a review of laboratory, field and model studies. *Atmos. Chem. Phys.* **2011**, *11* (21), 11069−11102.
(65) Lim, Y. B.; Tan, Y.; Perri, M. J.; Seitzinger, S. P.; Turpin, B. J. Aqueous chemistry and its role in secondary organic aerosol (SOA) formation. *Atmos. Chem. Phys.* **2010**, *10* (21), 10521−10539.
(66) Altieri, K. E.; Carlton, A. G.; Lim, H. J.; Turpin, B. J.; Seitzinger, S. P. Evidence for oligomer formation in clouds: Reactions of isoprene oxidation products. *Environ. Sci. Technol.* **2006**, *40* (16), 4956−4960.
(67) Lim, H. J.; Carlton, A. G.; Turpin, B. J. Isoprene forms secondary organic aerosol through cloud processing: Model simulations. *Environ. Sci. Technol.* **2005**, *39* (12), 4441−4446.
(68) Ervens, B. Modeling the Processing of Aerosol and Trace Gases in Clouds and Fogs. *Chem. Rev.* **2015**, *115* (10), 4157−4198.
(69) Moffet, R. C.; O'Brien, R. E.; Alpert, P. A.; Kelly, S. T.; Pham, D. Q.; Gilles, M. K.; Knopf, D. A.; Laskin, A. Morphology and mixing of black carbon particles collected in central California during the CARES field study. *Atmos. Chem. Phys.* **2016**, *16* (22), 14515−14525.
(70) Laskin, A.; Gilles, M. K.; Knopf, D. A.; Wang, B.; China, S. Progress in the Analysis of Complex Atmospheric Particles. *Annu. Rev. Anal. Chem.* **2016**, *9* (1), 117−143.
(71) Pöhlker, C.; Wiedemann, K. T.; Sinha, B.; Shiraiwa, M.; Gunthe, S. S.; Smith, M.; Su, H.; Artaxo, P.; Chen, Q.; Cheng, Y. F.; Elbert, W.; Gilles, M. K.; Kilcoyne, A. L. D.; Moffet, R. C.; Weigand, M.; Martin, S. T.; Pöschl, U.; Andreae, M. O. Biogenic Potassium Salt Particles as Seeds for Secondary Organic Aerosol in the Amazon. *Science* **2012**, *337* (6098), 1075−1078.
(72) Moffet, R. C.; Tivanski, A. V.; Gilles, M. K., Scanning X-ray Transmission Microscopy: Applications in Atmospheric Aerosol Research. In *Fundamentals and Applications in Aerosol Spectroscopy*; Signorell, R., Reid, J. P., Eds.; Taylor and Francis Books, Inc., 2010; pp 419−462.
(73) Gilles, M. K.; Moffet, R. C.; Laskin, A. Spectro-microscopy of carbonaceous particulates. *Geochim. Cosmochim. Ac.* **2010**, *74* (12), A332−A332.
(74) Moffet, R. C.; Henn, T. R.; Tivanski, A. V.; Hopkins, R. J.; Desyaterik, Y.; Kilcoyne, A. L. D.; Tyliszczak, T.; Fast, J.; Barnard, J.; Shutthanandan, V.; Cliff, S. S.; Perry, K. D.; Laskin, A.; Gilles, M. K. Microscopic characterization of carbonaceous aerosol particle aging in the outflow from Mexico City. *Atmos. Chem. Phys.* **2010**, *10*, 961−976.
(75) Adachi, K.; Freney, E. J.; Buseck, P. R. Shapes of internally mixed hygroscopic aerosol particles after deliquescence, and their effect on light scattering. *Geophys. Res. Lett.* **2011**, *38*, L13804.
(76) Posfai, M.; Gelencser, A.; Simonics, R.; Arato, K.; Li, J.; Hobbs, P. V.; Buseck, P. R. Atmospheric tar balls: Particles from biomass and biofuel burning. *J. Geophys. Res.* **2004**, *109* (D6), D06213.
(77) Li, J.; Posfai, M.; Hobbs, P. V.; Buseck, P. R. Individual aerosol particles from biomass burning in southern Africa: 2, Compositions and aging of inorganic particles. *J. Geophys. Res.* **2003**, *108* (D13), 8484.
(78) Buseck, P. R.; Posfai, M. Airborne minerals and related aerosol particles: Effects on climate and the environment. *Proc. Natl. Acad. Sci. U. S. A.* **1999**, *96* (7), 3372−3379.
(79) Laskin, A.; Laskin, J.; Nizkorodov, S. A. Chemistry of Atmospheric Brown Carbon. *Chem. Rev.* **2015**, *115* (10), 4335−4382.
(80) Solomon, P. A.; Sioutas, C. Continuous and semicontinuous monitoring techniques for particulate matter mass and chemical components: A synthesis of findings from EPA's particulate matter supersites program and related studies. *J. Air Waste Manage. Assoc.* **2008**, *58* (2), 164−195.
(81) Hersey, S. P.; Craven, J. S.; Metcalf, A. R.; Lin, J.; Lathem, T.; Suski, K. J.; Cahill, J. F.; Duong, H. T.; Sorooshian, A.; Jonsson, H. H.; Shiraiwa, M.; Zuend, A.; Nenes, A.; Prather, K. A.; Flagan, R. C.; Seinfeld, J. H. Composition and hygroscopicity of the Los Angeles Aerosol: CalNex. *J. Geophys. Res.* **2013**, *118* (7), 3016−3036.
(82) Hidy, G. M. Surface-Level Fine Particle Mass Concentrations: From Hemispheric Distributions to Megacity Sources. *J. Air Waste Manage. Assoc.* **2009**, *59* (7), 770−789.
(83) Bond, T. C.; Doherty, S. J.; Fahey, D. W.; Forster, P. M.; Berntsen, T.; DeAngelo, B. J.; Flanner, M. G.; Ghan, S.; Karcher, B.; Koch, D.; Kinne, S.; Kondo, Y.; Quinn, P. K.; Sarofim, M. C.; Schultz, M. G.; Schulz, M.; Venkataraman, C.; Zhang, H.; Zhang, S.; Bellouin, N.; Guttikunda, S. K.; Hopke, P. K.; Jacobson, M. Z.; Kaiser, J. W.; Klimont, Z.; Lohmann, U.; Schwarz, J. P.; Shindell, D.; Storelvmo, T.; Warren, S. G.; Zender, C. S. Bounding the role of black carbon in the climate system: A scientific assessment. *J. Geophys. Res.* **2013**, *118* (11), 5380−5552.
(84) Farmer, D. K.; Cappa, C. D.; Kreidenweis, S. M. Atmospheric Processes and Their Controlling Influence on Cloud Condensation Nuclei Activity. *Chem. Rev.* **2015**, *115* (10), 4199−4217.
(85) Sullivan, R. C.; Petters, M. D.; DeMott, P. J.; Kreidenweis, S. M.; Wex, H.; Niedermeier, D.; Hartmann, S.; Clauss, T.; Stratmann, F.; Reitz, P.; Schneider, J.; Sierau, B. Irreversible loss of ice nucleation active sites in mineral dust particles caused by sulphuric acid condensation. *Atmos. Chem. Phys.* **2010**, *10* (23), 11471−11487.
(86) Sullivan, R. C.; Minambres, L.; DeMott, P. J.; Prenni, A. J.; Carrico, C. M.; Levin, E. J. T.; Kreidenweis, S. M. Chemical processing does not always impair heterogeneous ice nucleation of mineral dust particles. *Geophys. Res. Lett.* **2010**, *37*, L24805.
(87) Niedermeier, D.; Hartmann, S.; Clauss, T.; Wex, H.; Kiselev, A.; Sullivan, R. C.; DeMott, P. J.; Petters, M. D.; Reitz, P.; Schneider, J.; Mikhailov, E.; Sierau, B.; Stetzer, O.; Reimann, B.; Bundke, U.; Shaw, R. A.; Buchholz, A.; Mentel, T. F.; Stratmann, F. Experimental study of the role of physicochemical surface processing on the IN ability of mineral dust particles. *Atmos. Chem. Phys.* **2011**, *11* (21), 11131−11144.
(88) Sihvonen, S. K.; Schill, G. P.; Lyktey, N. A.; Veghte, D. P.; Tolbert, M. A.; Freedman, M. A. Chemical and Physical Transformations of Aluminosilicate Clay Minerals Due to Acid Treatment and Consequences for Heterogeneous Ice Nucleation. *J. Phys. Chem. A* **2014**, *118* (38), 8787−8796.
(89) Fierce, L.; Riemer, N.; Bond, T. C. Toward reduced representation of mixing state for simulating aerosol effects on climate. *Bull. Am. Meteorol. Soc.* **2017**, *98* (5), 971−980.
(90) Ching, J.; Zaveri, R. A.; Easter, R. C.; Riemer, N.; Fast, J. D. A three-dimensional sectional representation of aerosol mixing state for simulating optical properties and cloud condensation nuclei. *J. Geophys. Res.* **2016**, *121* (10), 5912−5929.
(91) Riemer, N.; West, M. Quantifying aerosol mixing state with entropy and diversity measures. *Atmos. Chem. Phys.* **2013**, *13* (22), 11423−11439.

DOI: 10.1021/acsearthspacechem.7b00120
ACS Earth Space Chem. 2018, 2, 168−202

(92) Riemer, N.; West, M.; Zaveri, R. A.; Easter, R. C. Simulating the evolution of soot mixing state with a particle-resolved aerosol model. *J. Geophys. Res.* **2009**, *114*, D09202.
(93) Cziczo, D. J.; Froyd, K. D.; Hoose, C.; Jensen, E. J.; Diao, M. H.; Zondlo, M. A.; Smith, J. B.; Twohy, C. H.; Murphy, D. M. Clarifying the Dominant Sources and Mechanisms of Cirrus Cloud Formation. *Science* **2013**, *340* (6138), 1320−1324.
(94) Froyd, K. D.; Cziczo, D. J.; Hoose, C.; Jensen, E. J.; Diao, M. H.; Zondlo, M. A.; Smith, J. B.; Twohy, C. H.; Murphy, D. M., Cirrus cloud formation and the role of heterogeneous ice nuclei. In *Nucleation and Atmospheric Aerosols*; DeMott, P. J., Odowd, C. D., Eds.; Amer. Inst. Physics: Melville, NY, 2013; Vol. *1527*, pp 976−978.
(95) O'Brien, R. E.; Wang, B. B.; Laskin, A.; Riemer, N.; West, M.; Zhang, Q.; Sun, Y. L.; Yu, X. Y.; Alpert, P.; Knopf, D. A.; Gilles, M. K.; Moffet, R. C. Chemical imaging of ambient aerosol particles: Observational constraints on mixing state parameterization. *J. Geophys. Res.* **2015**, *120* (18), 9591−9605.
(96) Knopf, D. A.; Alpert, P. A.; Wang, B.; O'Brien, R. E.; Kelly, S. T.; Laskin, A.; Gilles, M. K.; Moffet, R. C. Microspectroscopic imaging and characterization of individually identified ice nucleating particles from a case field study. *J. Geophys. Res.* **2014**, *119*, 10365−10381.
(97) Moffet, R. C.; Rodel, T. C.; Kelly, S. T.; Yu, X. Y.; Carroll, G. T.; Fast, J.; Zaveri, R. A.; Laskin, A.; Gilles, M. K. Spectro-microscopic measurements of carbonaceous aerosol aging in Central California. *Atmos. Chem. Phys.* **2013**, *13* (20), 10445−10459.
(98) Wang, B.; Laskin, A.; Roedel, T.; Gilles, M. K.; Moffet, R. C.; Tivanski, A. V.; Knopf, D. A. Heterogeneous ice nucleation and water uptake by field-collected atmospheric particles below 273 K. *J. Geophys. Res.* **2012**, *117*, D00V19.
(99) Laskin, A.; Moffet, R. C.; Gilles, M. K.; Fast, J. D.; Zaveri, R. A.; Wang, B. B.; Nigge, P.; Shutthanandan, J. Tropospheric chemistry of internally mixed sea salt and organic particles: Surprising reactivity of NaCl with weak organic acids. *J. Geophys. Res.* **2012**, *117*, D15302.
(100) Moffet, R. C.; Henn, T.; Laskin, A.; Gilles, M. K. Automated Chemical Analysis of Internally Mixed Aerosol Particles Using X-ray Spectromicroscopy at the Carbon K-Edge. *Anal. Chem.* **2010**, *82* (19), 7906−7914.
(101) Knopf, D. A.; Wang, B.; Laskin, A.; Moffet, R. C.; Gilles, M. K. Heterogeneous nucleation of ice on anthropogenic organic particles collected in Mexico City. *Geophys. Res. Lett.* **2010**, *37*, L11803.
(102) China, S.; Alpert, P. A.; Zhang, B.; Schum, S.; Dzepina, K.; Wright, K.; Owen, R. C.; Fialho, P.; Mazzoleni, L. R.; Mazzoleni, C.; Knopf, D. A. Ice cloud formation potential by free tropospheric particles from long-range transport over the Northern Atlantic Ocean. *J. Geophys. Res.* **2017**, *122* (5), 3065−3079.
(103) Collier, K. N.; Brooks, S. D. Role of organic hydrocarbons in atmospheric ice formation via contact freezing. *J. Phys. Chem. A* **2016**, *120* (51), 10169−10180.
(104) Pummer, B. G.; Budke, C.; Augustin-Bauditz, S.; Niedermeier, D.; Felgitsch, L.; Kampf, C. J.; Huber, R. G.; Liedl, K. R.; Loerting, T.; Moschen, T.; Schauperl, M.; Tollinger, M.; Morris, C. E.; Wex, H.; Grothe, H.; Pöschl, U.; Koop, T.; Fröhlich-Nowoisky, J. Ice nucleation by water-soluble macromolecules. *Atmos. Chem. Phys.* **2015**, *15* (8), 4077−4091.
(105) Wang, B. B.; Lambe, A. T.; Massoli, P.; Onasch, T. B.; Davidovits, P.; Worsnop, D. R.; Knopf, D. A. The deposition ice nucleation and immersion freezing potential of amorphous secondary organic aerosol: Pathways for ice and mixed-phase cloud formation. *J. Geophys. Res.* **2012**, *117*, D16209.
(106) Cantrell, W.; Robinson, C. Heterogeneous freezing of ammonium sulfate and sodium chloride solutions by long chain alcohols. *Geophys. Res. Lett.* **2006**, *33* (7), L07802.
(107) Ochshorn, E.; Cantrell, W. Towards understanding ice nucleation by long chain alcohols. *J. Chem. Phys.* **2006**, *124* (5), 054714.
(108) Zobrist, B.; Koop, T.; Luo, B. P.; Marcolli, C.; Peter, T. Heterogeneous ice nucleation rate coefficient of water droplets coated by a nonadecanol monolayer. *J. Phys. Chem. C* **2007**, *111* (5), 2149−2155.
(109) Knopf, D. A.; Forrester, S. M. Freezing of Water and Aqueous NaCl Droplets Coated by Organic Monolayers as a Function of Surfactant Properties and Water Activity. *J. Phys. Chem. A* **2011**, *115* (22), 5579−5591.
(110) Dreischmeier, K.; Budke, C.; Wiehemeier, L.; Kottke, T.; Koop, T. Boreal pollen contain ice-nucleating as well as ice-binding 'antifreeze' polysaccharides. *Sci. Rep.* **2017**, *7*, 41890.
(111) Gavish, M.; Popovitzbiro, R.; Lahav, M.; Leiserowitz, L. Ice Nucleation by Alcohols Arranged in Monolayers at the Surface of Water Drops. *Science* **1990**, *250* (4983), 973−975.
(112) Charnawskas, J. C.; Alpert, P. A.; Lambe, A. T.; Berkemeier, T.; O'Brien, R. E.; Massoli, P.; Onasch, T. B.; Shiraiwa, M.; Moffet, R. C.; Gilles, M. K.; Davidovits, P.; Worsnop, D. R.; Knopf, D. A. Condensed-phase biogenic-anthropogenic interactions with implications for cold cloud formation. *Faraday Discuss.* **2017**, *200*, 164−195.
(113) Koop, T.; Bookhold, J.; Shiraiwa, M.; Pöschl, U. Glass transition and phase state of organic compounds: dependency on molecular properties and implications for secondary organic aerosols in the atmosphere. *Phys. Chem. Chem. Phys.* **2011**, *13* (43), 19238−19255.
(114) Saukko, E.; Lambe, A. T.; Massoli, P.; Koop, T.; Wright, J. P.; Croasdale, D. R.; Pedernera, D. A.; Onasch, T. B.; Laaksonen, A.; Davidovits, P.; Worsnop, D. R.; Virtanen, A. Humidity-dependent phase state of SOA particles from biogenic and anthropogenic precursors. *Atmos. Chem. Phys.* **2012**, *12* (16), 7517−7529.
(115) Virtanen, A.; Kannosto, J.; Kuuluvainen, H.; Arffman, A.; Joutsensaari, J.; Saukko, E.; Hao, L.; Yli-Pirila, P.; Tiitta, P.; Holopainen, J. K.; Keskinen, J.; Worsnop, D. R.; Smith, J. N.; Laaksonen, A. Bounce behavior of freshly nucleated biogenic secondary organic aerosol particles. *Atmos. Chem. Phys.* **2011**, *11* (16), 8759−8766.
(116) Virtanen, A.; Joutsensaari, J.; Koop, T.; Kannosto, J.; Yli-Pirila, P.; Leskinen, J.; Makela, J. M.; Holopainen, J. K.; Pöschl, U.; Kulmala, M.; Worsnop, D. R.; Laaksonen, A. An amorphous solid state of biogenic secondary organic aerosol particles. *Nature* **2010**, *467* (7317), 824−827.
(117) Martin, S. T. Phase transitions of aqueous atmospheric particles. *Chem. Rev.* **2000**, *100* (9), 3403−3453.
(118) Lienhard, D. M.; Huisman, A. J.; Krieger, U. K.; Rudich, Y.; Marcolli, C.; Luo, B. P.; Bones, D. L.; Reid, J. P.; Lambe, A. T.; Canagaratna, M. R.; Davidovits, P.; Onasch, T. B.; Worsnop, D. R.; Steimer, S. S.; Koop, T.; Peter, T. Viscous organic aerosol particles in the upper troposphere: diffusivity-controlled water uptake and ice nucleation? *Atmos. Chem. Phys.* **2015**, *15* (23), 13599−13613.
(119) Berkemeier, T.; Shiraiwa, M.; Pöschl, U.; Koop, T. Competition between water uptake and ice nucleation by glassy organic aerosol particles. *Atmos. Chem. Phys.* **2014**, *14* (22), 12513−12531.
(120) Angell, C. A. Formation of Glasses from Liquids and Biopolymers. *Science* **1995**, *267* (5206), 1924−1935.
(121) Zobrist, B.; Soonsin, V.; Luo, B. P.; Krieger, U. K.; Marcolli, C.; Peter, T.; Koop, T. Ultra-slow water diffusion in aqueous sucrose glasses. *Phys. Chem. Chem. Phys.* **2011**, *13* (8), 3514−3526.
(122) Shiraiwa, M.; Li, Y.; Tsimpidi, A. P.; Karydis, V. A.; Berkemeier, T.; Pandis, S. N.; Lelieveld, J.; Koop, T.; Pöschl, U. Global distribution of particle phase state in atmospheric secondary organic aerosols. *Nat. Commun.* **2017**, *8*, 15002.
(123) Wylie, D.; Jackson, D. L.; Menzel, W. P.; Bates, J. J. Trends in global cloud cover in two decades of HIRS observations. *J. Clim.* **2005**, *18* (15), 3021−3031.
(124) Yang, S.; Zou, X. Lapse rate characteristics in ice clouds inferred from GPS RO and CloudSat observations. *Atmos. Res.* **2017**, *197*, 105−112.
(125) McFarquhar, G. M.; Ghan, S.; Verlinde, J.; Korolev, A.; Strapp, J. W.; Schmid, B.; Tomlinson, J. M.; Wolde, M.; Brooks, S. D.; Cziczo, D.; Dubey, M. K.; Fan, J.; Flynn, C.; Gultepe, I.; Hubbe, J.; Gilles, M. K.; Laskin, A.; Lawson, P.; Leaitch, W. R.; Liu, P.; Liu, X.; Lubin, D.; Mazzoleni, C.; Macdonald, A.-M.; Moffet, R. C.; Morrison, H.; Ovchinnikov, M.; Shupe, M. D.; Turner, D. D.; Xie, S.; Zelenyuk, A.;

DOI: 10.1021/acsearthspacechem.7b00120
ACS Earth Space Chem. 2018, 2, 168−202

Bae, K.; Freer, M.; Glen, A. Indirect and Semi-Direct Aerosol Campaign: The Impact of Arctic Aerosols on Clouds. *Bull. Am. Meteorol. Soc.* **2011**, *92* (2), 183−201.
(126) Verlinde, J.; Harrington, J. Y.; McFarquhar, G. M.; Yannuzzi, V. T.; Avramov, A.; Greenberg, S.; Johnson, N.; Zhang, G.; Poellot, M. R.; Mather, J. H.; Turner, D. D.; Eloranta, E. W.; Zak, B. D.; Prenni, A. J.; Daniel, J. S.; Kok, G. L.; Tobin, D. C.; Holz, R.; Sassen, K.; Spangenberg, D.; Minnis, P.; Tooman, T. P.; Ivey, M. D.; Richardson, S. J.; Bahrmann, C. P.; Shupe, M.; DeMott, P. J.; Heymsfield, A. J.; Schofield, R. The mixed-phase Arctic cloud experiment. *Bull. Am. Meteorol. Soc.* **2007**, *88* (2), 205−221.
(127) Lawson, R. P.; Baker, B. A.; Schmitt, C. G.; Jensen, T. L. An overview of microphysical properties of Arctic clouds observed in May and July 1998 during FIRE ACE. *J. Geophys. Res.* **2001**, *106* (D14), 14989−15014.
(128) Morrison, H.; de Boer, G.; Feingold, G.; Harrington, J.; Shupe, M. D.; Sulia, K. Resilience of persistent Arctic mixed-phase clouds. *Nat. Geosci.* **2011**, *5* (1), 11−17.
(129) Shiraiwa, M.; Seinfeld, J. H. Equilibration timescale of atmospheric secondary organic aerosol partitioning. *Geophys. Res. Lett.* **2012**, *39*, L24801.
(130) Mikhailov, E.; Vlasenko, S.; Martin, S. T.; Koop, T.; Pöschl, U. Amorphous and crystalline aerosol particles interacting with water vapor: conceptual framework and experimental evidence for restructuring, phase transitions and kinetic limitations. *Atmos. Chem. Phys.* **2009**, *9* (24), 9491−9522.
(131) Moreno, L. A. L.; Stetzer, O.; Lohmann, U. Contact freezing: a review of experimental studies. *Atmos. Chem. Phys.* **2013**, *13* (19), 9745−9769.
(132) Durant, A. J.; Shaw, R. A. Evaporation freezing by contact nucleation inside-out. *Geophys. Res. Lett.* **2005**, *32* (20), L20814.
(133) Wex, H.; DeMott, P. J.; Tobo, Y.; Hartmann, S.; Roesch, M.; Clauss, T.; Tomsche, L.; Niedermeier, D.; Stratmann, F. Kaolinite particles as ice nuclei: learning from the use of different kaolinite samples and different coatings. *Atmos. Chem. Phys.* **2014**, *14* (11), 5529−5546.
(134) Ansmann, A.; Baars, H.; Tesche, M.; Mueller, D.; Althausen, D.; Engelmann, R.; Pauliquevis, T.; Artaxo, P. Dust and smoke transport from Africa to South America: Lidar profiling over Cape Verde and the Amazon rainforest. *Geophys. Res. Lett.* **2009**, *36*, L11802.
(135) de Boer, G.; Morrison, H.; Shupe, M. D.; Hildner, R. Evidence of liquid dependent ice nucleation in high-latitude stratiform clouds from surface remote sensors. *Geophys. Res. Lett.* **2011**, *38*, L01803.
(136) Wiacek, A.; Peter, T.; Lohmann, U. The potential influence of Asian and African mineral dust on ice, mixed-phase and liquid water clouds. *Atmos. Chem. Phys.* **2010**, *10* (18), 8649−8667.
(137) Hande, L. B.; Hoose, C. Partitioning the primary ice formation modes in large eddy simulations of mixed-phase clouds. *Atmos. Chem. Phys.* **2017**, *17* (22), 14105−14118.
(138) Shaw, R. A.; Durant, A. J.; Mi, Y. Heterogeneous surface crystallization observed in undercooled water. *J. Phys. Chem. B* **2005**, *109* (20), 9865−9868.
(139) Hoffmann, N.; Duft, D.; Kiselev, A.; Leisner, T. Contact freezing efficiency of mineral dust aerosols studied in an electrodynamic balance: quantitative size and temperature dependence for Illite particles. *Faraday Discuss.* **2013**, *165*, 383−390.
(140) Zobrist, B.; Marcolli, C.; Pedernera, D. A.; Koop, T. Do atmospheric aerosols form glasses? *Atmos. Chem. Phys.* **2008**, *8* (17), 5221−5244.
(141) Price, H. C.; Mattsson, J.; Zhang, Y.; Bertram, A. K.; Davies, J. F.; Grayson, J. W.; Martin, S. T.; O'Sullivan, D.; Reid, J. P.; Rickards, A. M. J.; Murray, B. J. Water diffusion in atmospherically relevant α-pinene secondary organic material. *Chem. Sci.* **2015**, *6* (8), 4876−4883.
(142) Herrmann, H.; Schaefer, T.; Tilgner, A.; Styler, S. A.; Weller, C.; Teich, M.; Otto, T. Tropospheric Aqueous-Phase Chemistry: Kinetics, Mechanisms, and Its Coupling to a Changing Gas Phase. *Chem. Rev.* **2015**, *115* (10), 4259−4334.
(143) Thomson, W. On the equilibrium of vapour at a curved surface of liquid. *Philos. Mag.* **1871**, *42* (282), 448−452.
(144) Hatch, C. D.; Greenaway, A. L.; Christie, M. J.; Baltrusaitis, J. Water adsorption constrained Frenkel-Halsey-Hill adsorption activation theory: Montmorillonite and Illite. *Atmos. Environ.* **2014**, *87*, 26−33.
(145) Hatch, C. D.; Gierlus, K. M.; Schuttlefield, J. D.; Grassian, V. H. Water adsorption and cloud condensation nuclei activity of calcite and calcite coated with model humic and fulvic acids. *Atmos. Environ.* **2008**, *42* (22), 5672−5684.
(146) Vlasenko, A.; Sjogren, S.; Weingartner, E.; Gaggeler, H. W.; Ammann, M. Generation of submicron Arizona test dust aerosol: Chemical and hygroscopic properties. *Aerosol Sci. Technol.* **2005**, *39* (5), 452−460.
(147) Gustafsson, R. J.; Orlov, A.; Badger, C. L.; Griffiths, P. T.; Cox, R. A.; Lambert, R. M. A comprehensive evaluation of water uptake on atmospherically relevant mineral surfaces: DRIFT spectroscopy, thermogravimetric analysis and aerosol growth measurements. *Atmos. Chem. Phys.* **2005**, *5*, 3415−3421.
(148) Herich, H.; Tritscher, T.; Wiacek, A.; Gysel, M.; Weingartner, E.; Lohmann, U.; Baltensperger, U.; Cziczo, D. J. Water uptake of clay and desert dust aerosol particles at sub- and supersaturated water vapor conditions. *Phys. Chem. Chem. Phys.* **2009**, *11* (36), 7804−7809.
(149) Koehler, K. A.; Kreidenweis, S. M.; DeMott, P. J.; Petters, M. D.; Prenni, A. J.; Carrico, C. M. Hygroscopicity and cloud droplet activation of mineral dust aerosol. *Geophys. Res. Lett.* **2009**, *36*, L08805.
(150) Koehler, K. A.; Kreidenweis, S. M.; DeMott, P. J.; Prenni, A. J.; Petters, M. D. Potential impact of Owens (dry) Lake dust on warm and cold cloud formation. *J. Geophys. Res.* **2007**, *112* (D12), D12210.
(151) Kumar, P.; Sokolik, I. N.; Nenes, A. Measurements of cloud condensation nuclei activity and droplet activation kinetics of fresh unprocessed regional dust samples and minerals. *Atmos. Chem. Phys.* **2011**, *11* (7), 3527−3541.
(152) Kumar, P.; Nenes, A.; Sokolik, I. N. Importance of adsorption for CCN activity and hygroscopic properties of mineral dust aerosol. *Geophys. Res. Lett.* **2009**, *36*, L24804.
(153) Sullivan, R. C.; Moore, M. J. K.; Petters, M. D.; Kreidenweis, S. M.; Qafoku, O.; Laskin, A.; Roberts, G. C.; Prather, K. A. Impact of Particle Generation Method on the Apparent Hygroscopicity of Insoluble Mineral Particles. *Aerosol Sci. Technol.* **2010**, *44* (10), 830−846.
(154) Garimella, S.; Huang, Y. W.; Seewald, J. S.; Cziczo, D. J. Cloud condensation nucleus activity comparison of dry- and wet-generated mineral dust aerosol: the significance of soluble material. *Atmos. Chem. Phys.* **2014**, *14* (12), 6003−6019.
(155) Hung, H. M.; Wang, K. C.; Chen, J. P. Adsorption of nitrogen and water vapor by insoluble particles and the implication on cloud condensation nuclei activity. *J. Aerosol Sci.* **2015**, *86*, 24−31.
(156) Gibson, E. R.; Gierlus, K. M.; Hudson, P. K.; Grassian, V. H. Generation of internally mixed insoluble and soluble aerosol particles to investigate the impact of atmospheric aging and heterogeneous processing on the CCN activity of mineral dust aerosol. *Aerosol Sci. Technol.* **2007**, *41* (10), 914−924.
(157) Tang, M. J.; Whitehead, J.; Davidson, N. M.; Pope, F. D.; Alfarra, M. R.; McFiggans, G.; Kalberer, M. Cloud condensation nucleation activities of calcium carbonate and its atmospheric ageing products. *Phys. Chem. Chem. Phys.* **2015**, *17* (48), 32194−32203.
(158) Cziczo, D. J.; Froyd, K. D.; Gallavardin, S. J.; Möhler, O.; Benz, S.; Saathoff, H.; Murphy, D. M. Deactivation of ice nuclei due to atmospherically relevant surface coatings. *Environ. Res. Lett.* **2009**, *4* (4), 044013.
(159) Knopf, D. A.; Koop, T. Heterogeneous nucleation of ice on surrogates of mineral dust. *J. Geophys. Res.* **2006**, *111* (D12), D12201.
(160) Bogdan, A.; Molina, M. J. Physical Chemistry of the Freezing Process of Atmospheric Aqueous Drops. *J. Phys. Chem. A* **2017**, *121* (16), 3109−3116.
(161) Bogdan, A.; Molina, M. J.; Tenhu, H. Freezing and glass transitions upon cooling and warming and ice/freeze-concentration-solution morphology of emulsified aqueous citric acid. *Eur. J. Pharm. Biopharm.* **2016**, *109*, 49−60.

DOI: 10.1021/acsearthspacechem.7b00120
ACS Earth Space Chem. 2018, 2, 168−202

(162) Bogdan, A.; Molina, M. J.; Tenhu, H.; Loerting, T. Multiple glass transitions and freezing events of aqueous citric acid. *J. Phys. Chem. A* **2015**, *119* (19), 4515−4523.
(163) Bogdan, A.; Loerting, T. Phase separation during freezing upon warming of aqueous solutions. *J. Chem. Phys.* **2014**, *141* (18), 4.
(164) Bogdan, A.; Molina, M. J.; Tenhu, H.; Bertel, E.; Bogdan, N.; Loerting, T. Visualization of Freezing Process in situ upon Cooling and Warming of Aqueous Solutions. *Sci. Rep.* **2015**, *4*, 6.
(165) Adler, G.; Koop, T.; Haspel, C.; Taraniuk, I.; Moise, T.; Koren, I.; Heiblum, R. H.; Rudich, Y. Formation of highly porous aerosol particles by atmospheric freeze-drying in ice clouds. *Proc. Natl. Acad. Sci. U. S. A.* **2013**, *110* (51), 20414−20419.
(166) Adler, G.; Haspel, C.; Moise, T.; Rudich, Y. Optical extinction of highly porous aerosol following atmospheric freeze drying. *Journal of Geophysical Research* **2014**, *119* (11), 6768−6787.
(167) Wagner, R.; Höhler, K.; Huang, W.; Kiselev, A.; Möhler, O.; Mohr, C.; Pajunoja, A.; Saathoff, H.; Schiebel, T.; Shen, X.; Virtanen, A. Heterogeneous ice nucleation of α-pinene SOA particles before and after ice cloud processing. *J. Geophys. Res.* **2017**, *122* (9), 4924−4943.
(168) Wagner, R.; Möhler, O.; Saathoff, H.; Schnaiter, M.; Skrotzki, J.; Leisner, T.; Wilson, T. W.; Malkin, T. L.; Murray, B. J. Ice cloud processing of ultra-viscous/glassy aerosol particles leads to enhanced ice nucleation ability. *Atmos. Chem. Phys.* **2012**, *12* (18), 8589−8610.
(169) Wagner, R.; Mohler, O.; Saathoff, H.; Schnaiter, M. Enhanced high-temperature ice nucleation ability of crystallized aerosol particles after preactivation at low temperature. *J. Geophys. Res.* **2014**, *119* (13), 8212−8230.
(170) Nangia, A. Conformational polymorphism in organic crystals. *Acc. Chem. Res.* **2008**, *41* (5), 595−604.
(171) Stahly, G. P. Diversity in single- and multiple-component crystals. The search for and prevalence of polymorphs and cocrystals. *Cryst. Growth Des.* **2007**, *7* (6), 1007−1026.
(172) Davey, R. J.; Schroeder, S. L. M.; ter Horst, J. H. Nucleation of Organic Crystals − A Molecular Perspective. *Angew. Chem., Int. Ed.* **2013**, *52* (8), 2166−2179.
(173) Threlfall, T. L. Analysis of organic polymorphs - a review. *Analyst* **1995**, *120* (10), 2435−2460.
(174) Suzuki, M.; Ogaki, T.; Sato, K. Crystallization and transformation mechanisms of α,β-polymorphs and γ-polymorphs of ultrapure oleic-acid. *J. Am. Oil Chem. Soc.* **1985**, *62* (11), 1600−1604.
(175) Inoue, T.; Hisatsugu, Y.; Yamamoto, R.; Suzuki, M. Solid-liquid phase behavior of binary fatty acid mixtures 1. Oleic acid stearic acid and oleic acid behenic acid mixtures. *Chem. Phys. Lipids* **2004**, *127* (2), 143−152.
(176) Inoue, T.; Hisatsugu, Y.; Ishikawa, R.; Suzuki, M. Solid-liquid phase behavior of binary fatty acid mixtures 2. Mixtures of oleic acid with lauric acid, myristic acid, and palmitic acid. *Chem. Phys. Lipids* **2004**, *127* (2), 161−173.
(177) Knopf, D. A.; Anthony, L. M.; Bertram, A. K. Reactive uptake of O-3 by multicomponent and multiphase mixtures containing oleic acid. *J. Phys. Chem. A* **2005**, *109* (25), 5579−5589.
(178) Marcolli, C.; Luo, B. P.; Peter, T. Mixing of the organic aerosol fractions: Liquids as the thermodynamically stable phases. *J. Phys. Chem. A* **2004**, *108* (12), 2216−2224.
(179) Pöhlker, C.; Saturno, J.; Kruger, M. L.; Forster, J. D.; Weigand, M.; Wiedemann, K. T.; Bechtel, M.; Artaxo, P.; Andreae, M. O. Efflorescence upon humidification? X-ray microspectroscopic in situ observation of changes in aerosol microstructure and phase state upon hydration. *Geophys. Res. Lett.* **2014**, *41* (10), 3681−3689.
(180) Bertram, A. K.; Martin, S. T.; Hanna, S. J.; Smith, M. L.; Bodsworth, A.; Chen, Q.; Kuwata, M.; Liu, A.; You, Y.; Zorn, S. R. Predicting the relative humidities of liquid-liquid phase separation, efflorescence, and deliquescence of mixed particles of ammonium sulfate, organic material, and water using the organic-to-sulfate mass ratio of the particle and the oxygen-to-carbon elemental ratio of the organic component. *Atmos. Chem. Phys.* **2011**, *11* (21), 10995−11006.
(181) You, Y.; Bertram, A. K. Effects of molecular weight and temperature on liquid-liquid phase separation in particles containing organic species and inorganic salts. *Atmos. Chem. Phys.* **2015**, *15* (3), 1351−1365.
(182) O'Brien, R. E.; Wang, B. B.; Kelly, S. T.; Lundt, N.; You, Y.; Bertram, A. K.; Leone, S. R.; Laskin, A.; Gilles, M. K. Liquid-Liquid Phase Separation in Aerosol Particles: Imaging at the Nanometer Scale. *Environ. Sci. Technol.* **2015**, *49* (8), 4995−5002.
(183) Zuend, A.; Marcolli, C.; Peter, T.; Seinfeld, J. H. Computation of liquid-liquid equilibria and phase stabilities: implications for RH-dependent gas/particle partitioning of organic-inorganic aerosols. *Atmos. Chem. Phys.* **2010**, *10* (16), 7795−7820.
(184) Renbaum-Wolff, L.; Song, M. J.; Marcolli, C.; Zhang, Y.; Liu, P. F. F.; Grayson, J. W.; Geiger, F. M.; Martin, S. T.; Bertram, A. K. Observations and implications of liquid-liquid phase separation at high relative humidities in secondary organic material produced by α-pinene ozonolysis without inorganic salts. *Atmos. Chem. Phys.* **2016**, *16* (12), 7969−7979.
(185) Song, M.; Liu, P.; Martin, S. T.; Bertram, A. K. Liquid−liquid phase separation in particles containing secondary organic material free of inorganic salts. *Atmos. Chem. Phys.* **2017**, *17*, 11261−11271.
(186) Song, M.; Marcolli, C.; Krieger, U. K.; Zuend, A.; Peter, T. Liquid-liquid phase separation in aerosol particles: Dependence on O:C, organic functionalities, and compositional complexity. *Geophys. Res. Lett.* **2012**, *39*, L19801.
(187) Ovadnevaite, J.; Zuend, A.; Laaksonen, A.; Sanchez, K. J.; Roberts, G.; Ceburnis, D.; Decesari, S.; Rinaldi, M.; Hodas, N.; Facchini, M. C.; Seinfeld, J. H.; O'Dowd, C. Surface tension prevails over solute effect in organic-influenced cloud droplet activation. *Nature* **2017**, *546*, 637−641.
(188) Rasmussen, D. H. Ice Formation in Aqueous Systems. *J. Microsc.* **1982**, *128* (NOV), 167−174.
(189) Rasmussen, D. H. Thermodynamics and Nucleation Phenomena - a Set of Experimental Observations. *J. Cryst. Growth* **1982**, *56* (1), 56−66.
(190) Koop, T. Homogeneous Ice Nucleation in Water and Aqueous Solutions. *Z. Phys. Chem.* **2004**, *218*, 1231−1258.
(191) Koop, T.; Murray, B. J. A physically constrained classical description of the homogeneous nucleation of ice in water. *J. Chem. Phys.* **2016**, *145* (21), 211915.
(192) Herbert, R. J.; Murray, B. J.; Dobbie, S. J.; Koop, T. Sensitivity of liquid clouds to homogenous freezing parameterizations. *Geophys. Res. Lett.* **2015**, *42* (5), 1599−1605.
(193) Lupi, L.; Hudait, A.; Peters, B.; Grunwald, M.; Mullen, R. G.; Nguyen, A. H.; Molinero, V. Role of stacking disorder in ice nucleation. *Nature* **2017**, *551*, 218−222.
(194) Murray, B. J.; Knopf, D. A.; Bertram, A. K. The formation of cubic ice under conditions relevant to Earth's atmosphere. *Nature* **2005**, *434* (7030), 202−205.
(195) Malkin, T. L.; Murray, B. J.; Brukhno, A. V.; Anwar, J.; Salzmann, C. G. Structure of ice crystallized from supercooled water. *Proc. Natl. Acad. Sci. U. S. A.* **2012**, *109* (4), 1041−1045.
(196) Zobrist, B.; Weers, U.; Koop, T. Ice nucleation in aqueous solutions of poly[ethylene glycol] with different molar mass. *J. Chem. Phys.* **2003**, *118* (22), 10254−10261.
(197) Koop, T.; Luo, B. P.; Tsias, A.; Peter, T. Water activity as the determinant for homogeneous ice nucleation in aqueous solutions. *Nature* **2000**, *406* (6796), 611−614.
(198) Knopf, D. A.; Rigg, Y. J. Homogeneous Ice Nucleation From Aqueous Inorganic/Organic Particles Representative of Biomass Burning: Water Activity, Freezing Temperatures, Nucleation Rates. *J. Phys. Chem. A* **2011**, *115* (5), 762−773.
(199) Knopf, D. A.; Lopez, M. D. Homogeneous ice freezing temperatures and ice nucleation rates of aqueous ammonium sulfate and aqueous levoglucosan particles for relevant atmospheric conditions. *Phys. Chem. Chem. Phys.* **2009**, *11* (36), 8056−8068.
(200) Bullock, G.; Molinero, V. Low-density liquid water is the mother of ice: on the relation between mesostructure, thermodynamics and ice crystallization in solutions. *Faraday Discuss.* **2014**, *167*, 371−388.

DOI: 10.1021/acsearthspacechem.7b00120
ACS Earth Space Chem. 2018, 2, 168−202

(201) Murata, K.; Tanaka, H. General nature of liquid-liquid transition in aqueous organic solutions. *Nat. Commun.* **2013**, *4*, 2844.
(202) Baker, M. B.; Baker, M. A new look at homogeneous freezing of water. *Geophys. Res. Lett.* **2004**, *31* (19), L19102.
(203) Ganbavale, G.; Marcolli, C.; Krieger, U. K.; Zuend, A.; Stratmann, G.; Peter, T. Experimental determination of the temperature dependence of water activities for a selection of aqueous organic solutions. *Atmos. Chem. Phys.* **2014**, *14* (18), 9993−10012.
(204) Wexler, A. S.; Clegg, S. L. Atmospheric aerosol models for systems including the ions H^+, NH_4^+, Na^+, SO_4^{2-}, NO_3^-, Cl^-, Br^-, and H_2O. *J. Geophys. Res.* **2002**, *107* (D14), 4207.
(205) Carslaw, K. S.; Clegg, S. L.; Brimblecombe, P. A Thermodynamic Model of the System HCl-HNO_3-H_2SO_4-H_2O, Including Solubilities of HBr, from <200 to 328 K. *J. Phys. Chem.* **1995**, *99* (29), 11557−11574.
(206) Clegg, S. L.; Brimblecombe, P. Comment on the "Thermodynamic dissociation constant of the bisulfate ion from Raman and ion interaction modeling studies of aqueous sulfuric acid at low temperatures". *J. Phys. Chem. A* **2005**, *109* (11), 2703−2706.
(207) Massucci, M.; Clegg, S. L.; Brimblecombe, P. Equilibrium partial pressures, thermodynamic properties of aqueous and solid phases, and Cl_2 production from aqueous HCl and HNO_3 and their mixtures. *J. Phys. Chem. A* **1999**, *103* (21), 4209−4226.
(208) Knopf, D. A.; Luo, B. P.; Krieger, U. K.; Koop, T. Reply to "Comment on the 'Thermodynamic dissociation constant of the bisulfate ion from Raman and ion interaction modeling studies of aqueous sulfuric acid at low temperatures'". *J. Phys. Chem. A* **2005**, *109* (11), 2707−2709.
(209) Knopf, D. A.; Luo, B. P.; Krieger, U. K.; Koop, T. Thermodynamic dissociation constant of the bisulfate ion from Raman and ion interaction modeling studies of aqueous sulfuric acid at low temperatures. *J. Phys. Chem. A* **2003**, *107* (21), 4322−4332.
(210) Friese, E.; Ebel, A. Temperature Dependent Thermodynamic Model of the System H^+-NH_4^+-Na^+-SO_4^{2-}-NO_3^--Cl^--H_2O. *J. Phys. Chem. A* **2010**, *114* (43), 11595−11631.
(211) Ganbavale, G.; Zuend, A.; Marcolli, C.; Peter, T. Improved AIOMFAC model parameterisation of the temperature dependence of activity coefficients for aqueous organic mixtures. *Atmos. Chem. Phys.* **2015**, *15* (1), 447−493.
(212) Tabazadeh, A.; Djikaev, Y. S.; Reiss, H. Surface crystallization of supercooled water in clouds. *Proc. Natl. Acad. Sci. U. S. A.* **2002**, *99* (25), 15873−15878.
(213) Djikaev, Y. S.; Tabazadeh, A.; Hamill, P.; Reiss, H. Thermodynamic conditions for the surface-stimulated crystallization of atmospheric droplets. *J. Phys. Chem. A* **2002**, *106* (43), 10247−10253.
(214) Duft, D.; Leisner, T. Laboratory evidence for volume-dominated nucleation of ice in supercooled water microdroplets. *Atmos. Chem. Phys.* **2004**, *4*, 1997−2000.
(215) Djikaev, Y. S.; Ruckenstein, E. Dependence of homogeneous crystal nucleation in water droplets on their radii and its implication for modeling the formation of ice particles in cirrus clouds. *Phys. Chem. Chem. Phys.* **2017**, *19*, 20075−20081.
(216) Pluharova, E.; Vrbka, L.; Jungwirth, P. Effect of Surface Pollution on Homogeneous Ice Nucleation: A Molecular Dynamics Study. *J. Phys. Chem. C* **2010**, *114* (17), 7831−7838.
(217) Vrbka, L.; Jungwirth, P. Homogeneous freezing of water starts in the subsurface. *J. Phys. Chem. B* **2006**, *110* (37), 18126−18129.
(218) Haji-Akbari, A.; Debenedetti, P. G. Computational investigation of surface freezing in a molecular model of water. *Proc. Natl. Acad. Sci. U. S. A.* **2017**, *114* (13), 3316−3321.
(219) Wang, B.; Knopf, D. A.; China, S.; Arey, B. W.; Harder, T. H.; Gilles, M. K.; Laskin, A. Direct observation of ice nucleation events on individual atmospheric particles. *Phys. Chem. Chem. Phys.* **2016**, *18* (43), 29721−29731.
(220) Kiselev, A.; Bachmann, F.; Pedevilla, P.; Cox, S. J.; Michaelides, A.; Gerthsen, D.; Leisner, T. Active sites in heterogeneous ice nucleation—the example of K-rich feldspars. *Science* **2017**, *355*, 367−371.
(221) Marcolli, C. Deposition nucleation viewed as homogeneous or immersion freezing in pores and cavities. *Atmos. Chem. Phys.* **2014**, *14* (4), 2071−2104.
(222) Layton, R. G.; Harris, F. S. Nucleation of ice on mica. *J. Atmos. Sci.* **1963**, *20* (2), 142−148.
(223) Campbell, J. M.; Meldrum, F. C.; Christenson, H. K. Observing the formation of ice and organic crystals in active sites. *Proc. Natl. Acad. Sci. U. S. A.* **2017**, *114* (5), 810−815.
(224) Campbell, J. M.; Meldrum, F. C.; Christenson, H. K. Characterization of Preferred Crystal Nucleation Sites on Mica Surfaces. *Cryst. Growth Des.* **2013**, *13* (5), 1915−1925.
(225) Christenson, H. K. Two-step crystal nucleation via capillary condensation. *CrystEngComm* **2013**, *15* (11), 2030−2039.
(226) Kovacs, T.; Christenson, H. K. A two-step mechanism for crystal nucleation without supersaturation. *Faraday Discuss.* **2012**, *159*, 123−138.
(227) Hofmann, S. *Auger- and X-Ray Photoelectron Spectroscopy in Materials Science A User-Oriented Guide*; Springer Berlin Heidelberg: Berlin, Germany, 2013; Vol. *49*.
(228) Barr, T. L.; Seal, S. Nature of the use of adventitious carbon as a binding energy standard. *J. Vac. Sci. Technol., A* **1995**, *13* (3), 1239−1246.
(229) Bzdek, B. R.; Power, R. M.; Simpson, S. H.; Reid, J. P.; Royall, C. P. Precise, contactless measurements of the surface tension of picolitre aerosol droplets. *Chem. Sci.* **2016**, *7* (1), 274−285.
(230) Kirkby, J.; Curtius, J.; Almeida, J.; Dunne, E.; Duplissy, J.; Ehrhart, S.; Franchin, A.; Gagne, S.; Ickes, L.; Kurten, A.; Kupc, A.; Metzger, A.; Riccobono, F.; Rondo, L.; Schobesberger, S.; Tsagkogeorgas, G.; Wimmer, D.; Amorim, A.; Bianchi, F.; Breitenlechner, M.; David, A.; Dommen, J.; Downard, A.; Ehn, M.; Flagan, R. C.; Haider, S.; Hansel, A.; Hauser, D.; Jud, W.; Junninen, H.; Kreissl, F.; Kvashin, A.; Laaksonen, A.; Lehtipalo, K.; Lima, J.; Lovejoy, E. R.; Makhmutov, V.; Mathot, S.; Mikkila, J.; Minginette, P.; Mogo, S.; Nieminen, T.; Onnela, A.; Pereira, P.; Petaja, T.; Schnitzhofer, R.; Seinfeld, J. H.; Sipila, M.; Stozhkov, Y.; Stratmann, F.; Tome, A.; Vanhanen, J.; Viisanen, Y.; Vrtala, A.; Wagner, P. E.; Walther, H.; Weingartner, E.; Wex, H.; Winkler, P. M.; Carslaw, K. S.; Worsnop, D. R.; Baltensperger, U.; Kulmala, M. Role of sulphuric acid, ammonia and galactic cosmic rays in atmospheric aerosol nucleation. *Nature* **2011**, *476*, 429−433.
(231) Bianchi, F.; Dommen, J.; Mathot, S.; Baltensperger, U. On-line determination of ammonia at low pptv mixing ratios in the CLOUD chamber. *Atmos. Meas. Tech.* **2012**, *5* (7), 1719−1725.
(232) Schnitzhofer, R.; Metzger, A.; Breitenlechner, M.; Jud, W.; Heinritzi, M.; De Menezes, L. P.; Duplissy, J.; Guida, R.; Haider, S.; Kirkby, J.; Mathot, S.; Minginette, P.; Onnela, A.; Walther, H.; Wasem, A.; Hansel, A.; Team, C. Characterisation of organic contaminants in the CLOUD chamber at CERN. *Atmos. Meas. Tech.* **2014**, *7* (7), 2159−2168.
(233) Wang, B.; Knopf, D. A. Heterogeneous ice nucleation on particles composed of humic-like substances impacted by O_3. *J. Geophys. Res.* **2011**, *116*, D03205.
(234) Riechers, B.; Wittbracht, F.; Hutten, A.; Koop, T. The homogeneous ice nucleation rate of water droplets produced in a microfluidic device and the role of temperature uncertainty. *Phys. Chem. Chem. Phys.* **2013**, *15* (16), 5873−5887.
(235) Sosso, G. C.; Chen, J.; Cox, S. J.; Fitzner, M.; Pedevilla, P.; Zen, A.; Michaelides, A. Crystal Nucleation in Liquids: Open Questions and Future Challenges in Molecular Dynamics Simulations. *Chem. Rev.* **2016**, *116* (12), 7078−7116.
(236) Zielke, S. A.; Bertram, A. K.; Patey, G. N. Simulations of Ice Nucleation by Model AgI Disks and Plates. *J. Phys. Chem. B* **2016**, *120* (9), 2291−2299.
(237) Zielke, S. A.; Bertram, A. K.; Patey, G. N. Simulations of Ice Nucleation by Kaolinite (001) with Rigid and Flexible Surfaces. *J. Phys. Chem. B* **2016**, *120* (8), 1726−1734.
(238) Zielke, S. A.; Bertram, A. K.; Patey, G. N. A Molecular Mechanism of Ice Nucleation on Model AgI Surfaces. *J. Phys. Chem. B* **2015**, *119* (29), 9049−9055.

DOI: 10.1021/acsearthspacechem.7b00120
ACS Earth Space Chem. 2018, 2, 168−202

(239) Croteau, T.; Bertram, A. K.; Patey, G. N. Water Adsorption on Kaolinite Surfaces Containing Trenches. *J. Phys. Chem. A* **2010**, *114* (5), 2171−2178.
(240) Croteau, T.; Bertram, A. K.; Patey, G. N. Simulation of Water Adsorption on Kaolinite under Atmospheric Conditions. *J. Phys. Chem. A* **2009**, *113* (27), 7826−7833.
(241) Croteau, T.; Bertram, A. K.; Patey, G. N. Adsorption and Structure of Water on Kaolinite Surfaces: Possible Insight into Ice Nucleation from Grand Canonical Monte Carlo Calculations. *J. Phys. Chem. A* **2008**, *112* (43), 10708−10712.
(242) Cox, S. J.; Kathmann, S. M.; Slater, B.; Michaelides, A. Molecular simulations of heterogeneous ice nucleation. II. Peeling back the layers. *J. Chem. Phys.* **2015**, *142* (18), 184705.
(243) Cox, S. J.; Kathmann, S. M.; Slater, B.; Michaelides, A. Molecular simulations of heterogeneous ice nucleation. I. Controlling ice nucleation through surface hydrophilicity. *J. Chem. Phys.* **2015**, *142* (18), 184704.
(244) Cox, S. J.; Raza, Z.; Kathmann, S. M.; Slater, B.; Michaelides, A. The microscopic features of heterogeneous ice nucleation may affect the macroscopic morphology of atmospheric ice crystals. *Faraday Discuss.* **2014**, *167*, 389−403.
(245) Sosso, G. C.; Tribello, G. A.; Zen, A.; Pedevilla, P.; Michaelides, A. Ice formation on kaolinite: Insights from molecular dynamics simulations. *J. Chem. Phys.* **2016**, *145* (21), 10.
(246) Liu, J.; Zhu, C.; Liu, K.; Jiang, Y.; Song, Y.; Francisco, J. S.; Cheng, X. C.; Wang, J. Distinct ice patterns on solid surfaces with various wettabilities. *Proc. Natl. Acad. Sci. U. S. A.* **2017**, *114*, 11285.
(247) Yan, J. Y.; Overduin, S. D.; Patey, G. N. Understanding electrofreezing in water simulations. *J. Chem. Phys.* **2014**, *141* (7), 074501.
(248) Yan, J. Y.; Patey, G. N. Ice nucleation by electric surface fields of varying range and geometry. *J. Chem. Phys.* **2013**, *139* (14), 144501.
(249) Yan, J. Y.; Patey, G. N. Molecular Dynamics Simulations of Ice Nucleation by Electric Fields. *J. Phys. Chem. A* **2012**, *116* (26), 7057−7064.
(250) Yan, J. Y.; Patey, G. N. Heterogeneous Ice Nucleation Induced by Electric Fields. *J. Phys. Chem. Lett.* **2011**, *2* (20), 2555−2559.
(251) Pedevilla, P.; Cox, S. J.; Slater, B.; Michaelides, A. Can Ice-Like Structures Form on Non-Ice-Like Substrates? The Example of the K-feldspar Microcline. *J. Phys. Chem. C* **2016**, *120* (12), 6704−6713.
(252) Fitzner, M.; Sosso, G. C.; Cox, S. J.; Michaelides, A. The Many Faces of Heterogeneous Ice Nucleation: Interplay Between Surface Morphology and Hydrophobicity. *J. Am. Chem. Soc.* **2015**, *137* (42), 13658−13669.
(253) Cox, S. J.; Kathmann, S. M.; Purton, J. A.; Gillan, M. J.; Michaelides, A. Non-hexagonal ice at hexagonal surfaces: the role of lattice mismatch. *Phys. Chem. Chem. Phys.* **2012**, *14* (22), 7944−7949.
(254) Fitzner, M.; Sosso, G. C.; Pietrucci, F.; Pipolo, S.; Michaelides, A. Pre-critical fluctuations and what they disclose about heterogeneous crystal nucleation. *Nat. Commun.* **2017**, *8*, 2257.
(255) Lupi, L.; Peters, B.; Molinero, V. Pre-ordering of interfacial water in the pathway of heterogeneous ice nucleation does not lead to a two-step crystallization mechanism. *J. Chem. Phys.* **2016**, *145* (21), 10.
(256) Lupi, L.; Kastelowitz, N.; Molinero, V. Vapor deposition of water on graphitic surfaces: Formation of amorphous ice, bilayer ice, ice I, and liquid water. *J. Chem. Phys.* **2014**, *141* (18), 11.
(257) Lupi, L.; Molinero, V. Does Hydrophilicity of Carbon Particles Improve Their Ice Nucleation Ability? *J. Phys. Chem. A* **2014**, *118* (35), 7330−7337.
(258) Lupi, L.; Hudait, A.; Molinero, V. Heterogeneous Nucleation of Ice on Carbon Surfaces. *J. Am. Chem. Soc.* **2014**, *136* (8), 3156−3164.
(259) Cabriolu, R.; Li, T. S. Ice nucleation on carbon surface supports the classical theory for heterogeneous nucleation. *Phys. Rev. E* **2015**, *91* (5), 052402.
(260) Dymarska, M.; Murray, B. J.; Sun, L. M.; Eastwood, M. L.; Knopf, D. A.; Bertram, A. K. Deposition ice nucleation on soot at temperatures relevant for the lower troposphere. *J. Geophys. Res.* **2006**, *111* (D4), D04204.
(261) Pedevilla, P.; Fitzner, M.; Michaelides, A. What makes a good descriptor for heterogeneous ice nucleation on OH-patterned surfaces. *Phys. Rev. B: Condens. Matter Mater. Phys.* **2017**, *96* (11), 115441.
(262) Seeley, L. H.; Seidler, G. T. Two-dimensional nucleation of ice from supercooled water. *Phys. Rev. Lett.* **2001**, *8705* (5), 055702.
(263) Seeley, L. H.; Seidler, G. T. Preactivation in the nucleation of ice by Langmuir films of aliphatic alcohols. *J. Chem. Phys.* **2001**, *114* (23), 10464−10470.
(264) Qiu, Y. Q.; Odendahl, N.; Hudait, A.; Mason, R.; Bertram, A. K.; Paesani, F.; DeMott, P. J.; Molinero, V. Ice Nucleation Efficiency of Hydroxylated Organic Surfaces Is Controlled by Their Structural Fluctuations and Mismatch to Ice. *J. Am. Chem. Soc.* **2017**, *139* (8), 3052−3064.
(265) Zou, A.; Chanana, A.; Agrawal, A.; Wayner, P. C.; Maroo, S. C. Steady State Vapor Bubble in Pool Boiling. *Sci. Rep.* **2016**, *6*, 20240.
(266) Sear, R. P. Nucleation at contact lines where fluid-fluid interfaces meet solid surfaces. *J. Phys.: Condens. Matter* **2007**, *19* (46), 466106.
(267) Yang, F.; Shaw, R. A.; Gurganus, C. W.; Chong, S. K.; Yap, Y. K. Ice nucleation at the contact line triggered by transient electrowetting fields. *Appl. Phys. Lett.* **2015**, *107* (26), 264101.
(268) Gurganus, C. W.; Charnawskas, J. C.; Kostinski, A. B.; Shaw, R. A. Nucleation at the Contact Line Observed on Nanotextured Surfaces. *Phys. Rev. Lett.* **2014**, *113* (23), 235701.
(269) Gurganus, C.; Kostinski, A. B.; Shaw, R. A. High-Speed Imaging of Freezing Drops: Still No Preference for the Contact Line. *J. Phys. Chem. C* **2013**, *117* (12), 6195−6200.
(270) Gurganus, C.; Kostinski, A. B.; Shaw, R. A. Fast Imaging of Freezing Drops: No Preference for Nucleation at the Contact Line. *J. Phys. Chem. Lett.* **2011**, *2* (12), 1449−1454.
(271) Pandey, R.; Usui, K.; Livingstone, R. A.; Fischer, S. A.; Pfaendtner, J.; Backus, E. H. G.; Nagata, Y.; Fröhlich-Nowoisky, J.; Schmuser, L.; Mauri, S.; Scheel, J. F.; Knopf, D. A.; Pöschl, U.; Bonn, M.; Weidner, T. Ice-nucleating bacteria control the order and dynamics of interfacial water. *Sci. Adv.* **2016**, *2* (4), e1501630.
(272) Djikaev, Y. S.; Ruckenstein, E. Thermodynamics of Heterogeneous Crystal Nucleation in Contact and Immersion Modes. *J. Phys. Chem. A* **2008**, *112* (46), 11677−11687.
(273) Fu, Q. T.; Liu, E. J.; Wilson, P.; Chen, Z. Ice nucleation behaviour on sol-gel coatings with different surface energy and roughness. *Phys. Chem. Chem. Phys.* **2015**, *17* (33), 21492−21500.
(274) Carvalho, J. L.; Dalnoki-Veress, K. Homogeneous Bulk, Surface, and Edge Nucleation in Crystalline Nanodroplets. *Phys. Rev. Lett.* **2010**, *105* (23), 237801.
(275) Abdelmonem, A.; Backus, E. H. G.; Hoffmann, N.; Sanchez, M. A.; Cyran, J. D.; Kiselev, A.; Bonn, M. Surface-charge-induced orientation of interfacial water suppresses heterogeneous ice nucleation on α-alumina (0001). *Atmos. Chem. Phys.* **2017**, *17* (12), 7827−7837.
(276) Abdelmonem, A.; Lutzenkirchen, J.; Leisner, T. Probing ice-nucleation processes on the molecular level using second harmonic generation spectroscopy. *Atmos. Meas. Tech.* **2015**, *8* (8), 3519−3526.
(277) DeMott, P. J.; Prenni, A. J.; Liu, X.; Kreidenweis, S. M.; Petters, M. D.; Twohy, C. H.; Richardson, M. S.; Eidhammer, T.; Rogers, D. C. Predicting global atmospheric ice nuclei distributions and their impacts on climate. *Proc. Natl. Acad. Sci. U. S. A.* **2010**, *107* (25), 11217−11222.
(278) DeMott, P. J.; Cziczo, D. J.; Prenni, A. J.; Murphy, D. M.; Kreidenweis, S. M.; Thomson, D. S.; Borys, R.; Rogers, D. C. Measurements of the concentration and composition of nuclei for cirrus formation. *Proc. Natl. Acad. Sci. U. S. A.* **2003**, *100* (25), 14655−14660.
(279) DeMott, P. J.; Hill, T. C. J.; McCluskey, C. S.; Prather, K. A.; Collins, D. B.; Sullivan, R. C.; Ruppel, M. J.; Mason, R. H.; Irish, V. E.; Lee, T.; Hwang, C. Y.; Rhee, T. S.; Snider, J. R.; McMeeking, G. R.; Dhaniyala, S.; Lewis, E. R.; Wentzell, J. J. B.; Abbatt, J.; Lee, C.; Sultana, C. M.; Ault, A. P.; Axson, J. L.; Diaz Martinez, M.; Venero, I.;

DOI: 10.1021/acsearthspacechem.7b00120
ACS Earth Space Chem. 2018, 2, 168−202

Santos-Figueroa, G.; Stokes, M. D.; Deane, G. B.; Mayol-Bracero, O. L.; Grassian, V. H.; Bertram, T. H.; Bertram, A. K.; Moffett, B. F.; Franc, G. D. Sea spray aerosol as a unique source of ice nucleating particles. *Proc. Natl. Acad. Sci. U. S. A.* **2016**, *113* (21), 5797−5803.
(280) Schrod, J.; Weber, D.; Drücke, J.; Keleshis, C.; Pikridas, M.; Ebert, M.; Cvetković, B.; Nickovic, S.; Marinou, E.; Baars, H.; Ansmann, A.; Vrekoussis, M.; Mihalopoulos, N.; Sciare, J.; Curtius, J.; Bingemer, H. G. Ice nucleating particles over the Eastern Mediterranean measured by unmanned aircraft systems. *Atmos. Chem. Phys.* **2017**, *17* (7), 4817−4835.
(281) DeMott, P. J.; Hill, T. C. J.; Petters, M. D.; Bertram, A. K.; Tobo, Y.; Mason, R. H.; Suski, K. J.; McCluskey, C. S.; Levin, E. J. T.; Schill, G. P.; Boose, Y.; Rauker, A. M.; Miller, A. J.; Zaragoza, J.; Rocci, K.; Rothfuss, N. E.; Taylor, H. P.; Hader, J. D.; Chou, C.; Huffman, J. A.; Pöschl, U.; Prenni, A. J.; Kreidenweis, S. M. Comparative measurements of ambient atmospheric concentrations of ice nucleating particles using multiple immersion freezing methods and a continuous flow diffusion chamber. *Atmos. Chem. Phys.* **2017**, *17* (18), 11227−11245.
(282) Conen, F.; Eckhardt, S.; Gundersen, H.; Stohl, A.; Yttri, K. E. Rainfall drives atmospheric ice-nucleating particles in the coastal climate of southern Norway. *Atmos. Chem. Phys.* **2017**, *17* (18), 11065−11073.
(283) Belosi, F.; Rinaldi, M.; Decesari, S.; Tarozzi, L.; Nicosia, A.; Santachiara, G. Ground level ice nuclei particle measurements including Saharan dust events at a Po Valley rural site (San Pietro Capofiume, Italy). *Atmos. Res.* **2017**, *186*, 116−126.
(284) Jiang, H.; Yin, Y.; Wang, X.; Gao, R.; Yuan, L.; Chen, K.; Shan, Y. The measurement and parameterization of ice nucleating particles in different backgrounds of China. *Atmos. Res.* **2016**, *181*, 72−80.
(285) Yin, J.; Wang, D.; Zhai, G. An Evaluation of Ice Nuclei Characteristics from the Long-term Measurement Data over North China. *Asia-Pac. J. Atmos. Sci.* **2012**, *48* (2), 197−204.
(286) Twohy, C. H.; Poellot, M. R. Chemical characteristics of ice residual nuclei in anvil cirrus clouds: evidence for homogeneous and heterogeneous ice formation. *Atmos. Chem. Phys.* **2005**, *5*, 2289−2297.
(287) Baustian, K. J.; Cziczo, D. J.; Wise, M. E.; Pratt, K. A.; Kulkarni, G.; Hallar, A. G.; Tolbert, M. A. Importance of aerosol composition, mixing state, and morphology for heterogeneous ice nucleation: A combined field and laboratory approach. *J. Geophys. Res.* **2012**, *117*, D06217.
(288) Hiranuma, N.; Brooks, S. D.; Moffet, R. C.; Glen, A.; Laskin, A.; Gilles, M. K.; Liu, P.; Macdonald, A. M.; Strapp, J. W.; McFarquhar, G. M. Chemical characterization of individual particles and residuals of cloud droplets and ice crystals collected on board research aircraft in the ISDAC 2008 study. *J. Geophys. Res.* **2013**, *118* (12), 6564−6579.
(289) Chen, Y. L.; Kreidenweis, S. M.; McInnes, L. M.; Rogers, D. C.; DeMott, P. J. Single particle analyses of ice nucleating aerosols in the upper troposphere and lower stratosphere. *Geophys. Res. Lett.* **1998**, *25* (9), 1391−1394.
(290) Froyd, K. D.; Murphy, D. M.; Lawson, P.; Baumgardner, D.; Herman, R. L. Aerosols that form subvisible cirrus at the tropical tropopause. *Atmos. Chem. Phys.* **2010**, *10* (1), 209−218.
(291) Cziczo, D. J.; Froyd, K. D. Sampling the composition of cirrus ice residuals. *Atmos. Res.* **2014**, *142*, 15−31.
(292) McCluskey, C. S.; DeMott, P. J.; Prenni, A. J.; Levin, E. J. T.; McMeeking, G. R.; Sullivan, A. P.; Hill, T. C. J.; Nakao, S.; Carrico, C. M.; Kreidenweis, S. M. Characteristics of atmospheric ice nucleating particles associated with biomass burning in the US: Prescribed burns and wildfires. *J. Geophys. Res.* **2014**, *119* (17), 10458−10470.
(293) Pratt, K. A.; DeMott, P. J.; French, J. R.; Wang, Z.; Westphal, D. L.; Heymsfield, A. J.; Twohy, C. H.; Prenni, A. J.; Prather, K. A. In situ detection of biological particles in cloud ice-crystals. *Nat. Geosci.* **2009**, *2* (6), 397−400.
(294) Pratt, K. A.; Murphy, S. M.; Subramanian, R.; DeMott, P. J.; Kok, G. L.; Campos, T.; Rogers, D. C.; Prenni, A. J.; Heymsfield, A. J.; Seinfeld, J. H.; Prather, K. A. Flight-based chemical characterization of biomass burning aerosols within two prescribed burn smoke plumes. *Atmos. Chem. Phys.* **2011**, *11* (24), 12549−12565.
(295) Prenni, A. J.; DeMott, P. J.; Sullivan, A. P.; Sullivan, R. C.; Kreidenweis, S. M.; Rogers, D. C. Biomass burning as a potential source for atmospheric ice nuclei: Western wildfires and prescribed burns. *Geophys. Res. Lett.* **2012**, *39*, L11805.
(296) Prenni, A. J.; Petters, M. D.; Kreidenweis, S. M.; Heald, C. L.; Martin, S. T.; Artaxo, P.; Garland, R. M.; Wollny, A. G.; Pöschl, U. Relative roles of biogenic emissions and Saharan dust as ice nuclei in the Amazon basin. *Nat. Geosci.* **2009**, *2* (6), 401−404.
(297) Prenni, A. J.; Demott, P. J.; Rogers, D. C.; Kreidenweis, S. M.; McFarquhar, G. M.; Zhang, G.; Poellot, M. R. Ice nuclei characteristics from M-PACE and their relation to ice formation in clouds. *Tellus, Ser. B* **2009**, *61* (2), 436−448.
(298) Rogers, D. C.; DeMott, P. J.; Kreidenweis, S. M. Airborne measurements of tropospheric ice-nucleating aerosol particles in the Arctic spring. *J. Geophys. Res.* **2001**, *106* (D14), 15053−15063.
(299) Schmidt, S.; Schneider, J.; Klimach, T.; Mertes, S.; Schenk, L. P.; Kupiszewski, P.; Curtius, J.; Borrmann, S. Online single particle analysis of ice particle residuals from mountain-top mixed-phase clouds using laboratory derived particle type assignment. *Atmos. Chem. Phys.* **2017**, *17* (1), 575−594.
(300) Ebert, M.; Worringen, A.; Benker, N.; Mertes, S.; Weingartner, E.; Weinbruch, S. Chemical composition and mixing-state of ice residuals sampled within mixed phase clouds. *Atmos. Chem. Phys.* **2011**, *11* (6), 2805−2816.
(301) Worringen, A.; Kandler, K.; Benker, N.; Dirsch, T.; Mertes, S.; Schenk, L.; Kastner, U.; Frank, F.; Nillius, B.; Bundke, U.; Rose, D.; Curtius, J.; Kupiszewski, P.; Weingartner, E.; Vochezer, P.; Schneider, J.; Schmidt, S.; Weinbruch, S.; Ebert, M. Single-particle characterization of ice-nucleating particles and ice particle residuals sampled by three different techniques. *Atmos. Chem. Phys.* **2015**, *15* (8), 4161−4178.
(302) Kupiszewski, P.; Zanatta, M.; Mertes, S.; Vochezer, P.; Lloyd, G.; Schneider, J.; Schenk, L.; Schnaiter, M.; Baltensperger, U.; Weingartner, E.; Gysel, M. Ice residual properties in mixed-phase clouds at the high-alpine Jungfraujoch site. *J. Geophys. Res.* **2016**, *121* (20), 12343−12362.
(303) Corbin, J. C.; Rehbein, P. J. G.; Evans, G. J.; Abbatt, J. P. D. Combustion particles as ice nuclei in an urban environment: Evidence from single-particle mass spectrometry. *Atmos. Environ.* **2012**, *51*, 286−292.
(304) Froyd, K. D.; Murphy, S. M.; Murphy, D. M.; de Gouw, J. A.; Eddingsaas, N. C.; Wennberg, P. O. Contribution of isoprene-derived organosulfates to free tropospheric aerosol mass. *Proc. Natl. Acad. Sci. U. S. A.* **2010**, *107* (50), 21360−21365.
(305) Surratt, J. D.; Chan, A. W. H.; Eddingsaas, N. C.; Chan, M.; Loza, C. L.; Kwan, A. J.; Hersey, S. P.; Flagan, R. C.; Wennberg, P. O.; Seinfeld, J. H. Reactive intermediates revealed in secondary organic aerosol formation from isoprene. *Proc. Natl. Acad. Sci. U. S. A.* **2010**, *107* (15), 6640−6645.
(306) Claeys, M. Comment on "Unexpected Epoxide Formation in the Gas-Phase Photooxidation of Isoprene". *Science* **2010**, *327*, 644−645.
(307) Paulot, F.; Crounse, J. D.; Kjaergaard, H. G.; Kuerten, A.; St; St. Clair, J. M.; Seinfeld, J. H.; Wennberg, P. O. Unexpected Epoxide Formation in the Gas-Phase Photooxidation of Isoprene. *Science* **2009**, *325*, 730−733.
(308) Molina, L. T.; Madronich, S.; Gaffney, J. S.; Apel, E.; de Foy, B.; Fast, J.; Ferrare, R.; Herndon, S.; Jimenez, J. L.; Lamb, B.; Osornio-Vargas, A. R.; Russell, P.; Schauer, J. J.; Stevens, P. S.; Volkamer, R.; Zavala, M. An overview of the MILAGRO 2006 Campaign: Mexico City emissions and their transport and transformation. *Atmos. Chem. Phys.* **2010**, *10* (18), 8697−8760.
(309) Ryerson, T. B.; Andrews, A. E.; Angevine, W. M.; Bates, T. S.; Brock, C. A.; Cairns, B.; Cohen, R. C.; Cooper, O. R.; de Gouw, J. A.; Fehsenfeld, F. C.; Ferrare, R. A.; Fischer, M. L.; Flagan, R. C.; Goldstein, A. H.; Hair, J. W.; Hardesty, R. M.; Hostetler, C. A.; Jimenez, J. L.; Langford, A. O.; McCauley, E.; McKeen, S. A.; Molina,

DOI: 10.1021/acsearthspacechem.7b00120
ACS Earth Space Chem. 2018, 2, 168−202

L. T.; Nenes, A.; Oltmans, S. J.; Parrish, D. D.; Pederson, J. R.; Pierce, R. B.; Prather, K.; Quinn, P. K.; Seinfeld, J. H.; Senff, C. J.; Sorooshian, A.; Stutz, J.; Surratt, J. D.; Trainer, M.; Volkamer, R.; Williams, E. J.; Wofsy, S. C. The 2010 California Research at the Nexus of Air Quality and Climate Change (CalNex) field study. *J. Geophys. Res.* **2013**, *118* (11), 5830−5866.

(310) Rogers, D. C. Measurements of natural ice nuclei with a continuous flow diffusion chamber. *Atmos. Res.* **1993**, *29* (3−4), 209−228.

(311) Aiken, A. C.; McMeeking, G. R.; Levin, E. J. T.; Dubey, M. K.; DeMott, P. J.; Kreidenweis, S. M. Quantification of online removal of refractory black carbon using laser-induced incandescence in the single particle soot photometer. *Aerosol Sci. Technol.* **2016**, *50* (7), 679−692.

(312) Levin, E. J. T.; McMeeking, G. R.; DeMott, P. J.; McCluskey, C. S.; Stockwell, C. E.; Yokelson, R. J.; Kreidenweis, S. M. A New Method to Determine the Number Concentrations of Refractory Black Carbon Ice Nucleating Particles. *Aerosol Sci. Technol.* **2014**, *48* (12), 1264−1275.

(313) McFarquhar, G. M.; Ghan, S.; Verlinde, J.; Korolev, A.; Strapp, J. W.; Schmid, B.; Tomlinson, J. M.; Wolde, M.; Brooks, S. D.; Cziczo, D.; Dubey, M. K.; Fan, J. W.; Flynn, C.; Gultepe, I.; Hubbe, J.; Gilles, M. K.; Laskin, A.; Lawson, P.; Leaitch, W. R.; Liu, P.; Liu, X. H.; Lubin, D.; Mazzoleni, C.; Macdonald, A. M.; Moffet, R. C.; Morrison, H.; Ovchinnikov, M.; Shupe, M. D.; Turner, D. D.; Xie, S. C.; Zelenyuk, A.; Bae, K.; Freer, M.; Glen, A. Indirect and Semi-Direct Aerosol Campaign: The Impact of Arctic Aerosols on Clouds. *Bull. Am. Meteorol. Soc.* **2011**, *92* (2), 183−201.

(314) Zaveri, R. A.; Shaw, W. J.; Cziczo, D. J.; Schmid, B.; Ferrare, R. A.; Alexander, M. L.; Alexandrov, M.; Alvarez, R. J.; Arnott, W. P.; Atkinson, D. B.; Baidar, S.; Banta, R. M.; Barnard, J. C.; Beranek, J.; Berg, L. K.; Brechtel, F.; Brewer, W. A.; Cahill, J. F.; Cairns, B.; Cappa, C. D.; Chand, D.; China, S.; Comstock, J. M.; Dubey, M. K.; Easter, R. C.; Erickson, M. H.; Fast, J. D.; Floerchinger, C.; Flowers, B. A.; Fortner, E.; Gaffney, J. S.; Gilles, M. K.; Gorkowski, K.; Gustafson, W. I.; Gyawali, M.; Hair, J.; Hardesty, R. M.; Harworth, J. W.; Herndon, S.; Hiranuma, N.; Hostetler, C.; Hubbe, J. M.; Jayne, J. T.; Jeong, H.; Jobson, B. T.; Kassianov, E. I.; Kleinman, L. I.; Kluzek, C.; Knighton, B.; Kolesar, K. R.; Kuang, C.; Kubatova, A.; Langford, A. O.; Laskin, A.; Laulainen, N.; Marchbanks, R. D.; Mazzoleni, C.; Mei, F.; Moffet, R. C.; Nelson, D.; Obland, M. D.; Oetjen, H.; Onasch, T. B.; Ortega, I.; Ottaviani, M.; Pekour, M.; Prather, K. A.; Radney, J. G.; Rogers, R. R.; Sandberg, S. P.; Sedlacek, A.; Senff, C. J.; Senum, G.; Setyan, A.; Shilling, J. E.; Shrivastava, M.; Song, C.; Springston, S. R.; Subramanian, R.; Suski, K.; Tomlinson, J.; Volkamer, R.; Wallace, H. W.; Wang, J.; Weickmann, A. M.; Worsnop, D. R.; Yu, X. Y.; Zelenyuk, A.; Zhang, Q. Overview of the 2010 Carbonaceous Aerosols and Radiative Effects Study (CARES). *Atmos. Chem. Phys.* **2012**, *12* (16), 7647−7687.

(315) Mason, R. H.; Si, M.; Li, J.; Chou, C.; Dickie, R.; Toom-Sauntry, D.; Pöhlker, C.; Yakobi-Hancock, J. D.; Ladino, L. A.; Jones, K.; Leaitch, W. R.; Schiller, C. L.; Abbatt, J. P. D.; Huffman, J. A.; Bertram, A. K. Ice nucleating particles at a coastal marine boundary layer site: correlations with aerosol type and meteorological conditions. *Atmos. Chem. Phys.* **2015**, *15* (21), 12547−12566.

(316) Mason, R. H.; Chou, C.; McCluskey, C. S.; Levin, E. J. T.; Schiller, C. L.; Hill, T. C. J.; Huffman, J. A.; DeMott, P. J.; Bertram, A. K. The micro-orifice uniform deposit impactor-droplet freezing technique (MOUDI-DFT) for measuring concentrations of ice nucleating particles as a function of size: improvements and initial validation. *Atmos. Meas. Tech.* **2015**, *8* (6), 2449−2462.

(317) Mason, R. H.; Si, M.; Chou, C.; Irish, V. E.; Dickie, R.; Elizondo, P.; Wong, R.; Brintnell, M.; Elsasser, M.; Lassar, W. M.; Pierce, K. M.; Leaitch, W. R.; MacDonald, A. M.; Platt, A.; Toom-Sauntry, D.; Sarda-Esteve, R.; Schiller, C. L.; Suski, K. J.; Hill, T. C. J.; Abbatt, J. P. D.; Huffman, J. A.; DeMott, P. J.; Bertram, A. K. Size-resolved measurements of ice-nucleating particles at six locations in North America and one in Europe. *Atmos. Chem. Phys.* **2016**, *16* (3), 1637−1651.

(318) Jiang, H.; Yin, Y.; Su, H.; Shan, Y. P.; Gao, R. J. The characteristics of atmospheric ice nuclei measured at the top of Huangshan (the Yellow Mountains) in Southeast China using a newly built static vacuum water vapor diffusion chamber. *Atmos. Res.* **2015**, *153*, 200−208.

(319) Jiang, H.; Yin, Y.; Yang, L.; Yang, S. Z.; Su, H.; Chen, K. The Characteristics of Atmospheric Ice Nuclei Measured at Different Altitudes in the Huangshan Mountains in Southeast China. *Adv. Atmos. Sci.* **2014**, *31* (2), 396−406.

(320) Rinaldi, M.; Santachiara, G.; Nicosia, A.; Piazza, M.; Decesari, S.; Gilardoni, S.; Paglione, M.; Cristofanelli, P.; Marinoni, A.; Bonasoni, P.; Belosi, F. Atmospheric Ice Nucleating Particle measurements at the high mountain observatory Mt. Cimone (2165 m a.s.l., Italy). *Atmos. Environ.* **2017**, *171*, 173.

(321) Möhler, O.; Benz, S.; Saathoff, H.; Schnaiter, M.; Wagner, R.; Schneider, J.; Walter, S.; Ebert, V.; Wagner, S. The effect of organic coating on the heterogeneous ice nucleation efficiency of mineral dust aerosols. *Environ. Res. Lett.* **2008**, *3* (2), 025007.

(322) Murray, B. J.; Wilson, T. W.; Dobbie, S.; Cui, Z. Q.; Al-Jumur, S. M. R. K.; Möhler, O.; Schnaiter, M.; Wagner, R.; Benz, S.; Niemand, M.; Saathoff, H.; Ebert, V.; Wagner, S.; Kärcher, B. Heterogeneous nucleation of ice particles on glassy aerosols under cirrus conditions. *Nat. Geosci.* **2010**, *3* (4), 233−237.

(323) Baustian, K. J.; Wise, M. E.; Jensen, E. J.; Schill, G. P.; Freedman, M. A.; Tolbert, M. A. State transformations and ice nucleation in amorphous (semi-)solid organic aerosol. *Atmos. Chem. Phys.* **2013**, *13* (11), 5615−5628.

(324) Schill, G. P.; Tolbert, M. A. Heterogeneous ice nucleation on phase-separated organic-sulfate particles: effect of liquid vs. glassy coatings. *Atmos. Chem. Phys.* **2013**, *13* (9), 4681−4695.

(325) Schill, G. P.; De Haan, D. O.; Tolbert, M. A. Heterogeneous Ice Nucleation on Simulated Secondary Organic Aerosol. *Environ. Sci. Technol.* **2014**, *48* (3), 1675−1682.

(326) Ladino, L. A.; Zhou, S.; Yakobi-Hancock, J. D.; Aljawhary, D.; Abbatt, J. P. D. Factors controlling the ice nucleating abilities of α-pinene SOA particles. *J. Geophys. Res.* **2014**, *119* (14), 9041−9051.

(327) Ignatius, K.; Kristensen, T. B.; Jarvinen, E.; Nichman, L.; Fuchs, C.; Gordon, H.; Herenz, P.; Hoyle, C. R.; Duplissy, J.; Garimella, S.; Dias, A.; Frege, C.; Hoppel, N.; Troestl, J.; Wagner, R.; Yan, C.; Amorim, A.; Baltensperger, U.; Curtius, J.; Donahue, N. M.; Gallagher, M. W.; Kirkby, J.; Kulmala, M.; Möhler, O.; Saathoff, H.; Schnaiter, M.; Tome, A.; Virtanen, A.; Worsnop, D.; Stratmann, F. Heterogeneous ice nucleation of viscous secondary organic aerosol produced from ozonolysis of α-pinene. *Atmos. Chem. Phys.* **2016**, *16* (10), 6495−6509.

(328) Alpert, P. A.; Knopf, D. A. Analysis of isothermal and cooling-rate-dependent immersion freezing by a unifying stochastic ice nucleation model. *Atmos. Chem. Phys.* **2016**, *16* (4), 2083−2107.

(329) Riechers, B.; Wittbracht, F.; Hutten, A.; Koop, T. The homogeneous ice nucleation rate of water droplets produced in a microfluidic device and the role of temperature uncertainty. *Phys. Chem. Chem. Phys.* **2013**, *15* (16), 5873−5887.

(330) Hiranuma, N.; Augustin-Bauditz, S.; Bingemer, H.; Budke, C.; Curtius, J.; Danielczok, A.; Diehl, K.; Dreischmeier, K.; Ebert, M.; Frank, F.; Hoffmann, N.; Kandler, K.; Kiselev, A.; Koop, T.; Leisner, T.; Möhler, O.; Nillius, B.; Peckhaus, A.; Rose, D.; Weinbruch, S.; Wex, H.; Boose, Y.; DeMott, P. J.; Hader, J. D.; Hill, T. C. J.; Kanji, Z. A.; Kulkarni, G.; Levin, E. J. T.; McCluskey, C. S.; Murakami, M.; Murray, B. J.; Niedermeier, D.; Petters, M. D.; O'Sullivan, D.; Saito, A.; Schill, G. P.; Tajiri, T.; Tolbert, M. A.; Welti, A.; Whale, T. F.; Wright, T. P.; Yamashita, K. A comprehensive laboratory study on the immersion freezing behavior of Illite NX particles: a comparison of 17 ice nucleation measurement techniques. *Atmos. Chem. Phys.* **2015**, *15* (5), 2489−2518.

(331) Barahona, D. Thermodynamic derivation of the activation energy for ice nucleation. *Atmos. Chem. Phys.* **2015**, *15* (24), 13819−13831.

DOI: 10.1021/acsearthspacechem.7b00120
ACS Earth Space Chem. 2018, 2, 168−202

(332) Barahona, D. Analysis of the effect of water activity on ice formation using a new thermodynamic framework. *Atmos. Chem. Phys.* **2014**, *14* (14), 7665−7680.
(333) Barahona, D. On the ice nucleation spectrum. *Atmos. Chem. Phys.* **2012**, *12* (8), 3733−3752.
(334) Lovering, K. A.; Bertram, A. K.; Chou, K. C. Transient Phase of Ice Observed by Sum Frequency Generation at the Water/Mineral Interface During Freezing. *J. Phys. Chem. Lett.* **2017**, *8* (4), 871−875.
(335) Zimmermann, F.; Ebert, M.; Worringen, A.; Schutz, L.; Weinbruch, S. Environmental scanning electron microscopy (ESEM) as a new technique to determine the ice nucleation capability of individual atmospheric aerosol particles. *Atmos. Environ.* **2007**, *41* (37), 8219−8227.
(336) Magee, N. B.; Miller, A.; Amaral, M.; Cumiskey, A. Mesoscopic surface roughness of ice crystals pervasive across a wide range of ice crystal conditions. *Atmos. Chem. Phys.* **2014**, *14* (22), 12357−12371.
(337) Wilson, T. W.; Ladino, L. A.; Alpert, P. A.; Breckels, M. N.; Brooks, I. M.; Browse, J.; Burrows, S. M.; Carslaw, K. S.; Huffman, J. A.; Judd, C.; Kilthau, W. P.; Mason, R. H.; McFiggans, G.; Miller, L. A.; Najera, J. J.; Polishchuk, E.; Rae, S.; Schiller, C. L.; Si, M.; Temprado, J. V.; Whale, T. F.; Wong, J. P. S.; Wurl, O.; Yakobi-Hancock, J. D.; Abbatt, J. P. D.; Aller, J. Y.; Bertram, A. K.; Knopf, D. A.; Murray, B. J. A marine biogenic source of atmospheric ice-nucleating particles. *Nature* **2015**, *525*, 234−238.
(338) von Blohn, N.; Mitra, S. K.; Diehl, K.; Borrmann, S. The ice nucleating ability of pollen. Part III: New laboratory studies in immersion and contact freezing modes including more pollen types. *Atmos. Res.* **2005**, *78* (3), 182−189.
(339) Tong, H. J.; Ouyang, B.; Nikolovski, N.; Lienhard, D. M.; Pope, F. D.; Kalberer, M. A new electrodynamic balance (EDB) design for low-temperature studies: application to immersion freezing of pollen extract bioaerosols. *Atmos. Meas. Tech.* **2015**, *8* (3), 1183−1195.
(340) Pummer, B. G.; Bauer, H.; Bernardi, J.; Bleicher, S.; Grothe, H. Suspendable macromolecules are responsible for ice nucleation activity of birch and conifer pollen. *Atmos. Chem. Phys.* **2012**, *12* (5), 2541−2550.
(341) Hader, J. D.; Wright, T. P.; Petters, M. D. Contribution of pollen to atmospheric ice nuclei concentrations. *Atmos. Chem. Phys.* **2014**, *14* (11), 5433−5449.
(342) Augustin, S.; Wex, H.; Niedermeier, D.; Pummer, B.; Grothe, H.; Hartmann, S.; Tomsche, L.; Clauss, T.; Voigtländer, J.; Ignatius, K.; Stratmann, F. Immersion freezing of birch pollen washing water. *Atmos. Chem. Phys.* **2013**, *13* (21), 10989−11003.
(343) Augustin-Bauditz, S.; Wex, H.; Denjean, C.; Hartmann, S.; Schneider, J.; Schmidt, S.; Ebert, M.; Stratmann, F. Laboratory-generated mixtures of mineral dust particles with biological substances: characterization of the particle mixing state and immersion freezing behavior. *Atmos. Chem. Phys.* **2016**, *16* (9), 5531−5543.
(344) O'Sullivan, D.; Murray, B. J.; Ross, J. F.; Whale, T. F.; Price, H. C.; Atkinson, J. D.; Umo, N. S.; Webb, M. E. The relevance of nanoscale biological fragments for ice nucleation in clouds. *Sci. Rep.* **2015**, *5*, 8082.
(345) Tobo, Y.; DeMott, P. J.; Hill, T. C. J.; Prenni, A. J.; Swoboda-Colberg, N. G.; Franc, G. D.; Kreidenweis, S. M. Organic matter matters for ice nuclei of agricultural soil origin. *Atmos. Chem. Phys.* **2014**, *14* (16), 8521−8531.
(346) Steinke, I.; Funk, R.; Busse, J.; Iturri, A.; Kirchen, S.; Leue, M.; Möhler, O.; Schwartz, T.; Schnaiter, M.; Sierau, B.; Toprak, E.; Ullrich, R.; Ulrich, A.; Hoose, C.; Leisner, T. Ice nucleation activity of agricultural soil dust aerosols from Mongolia, Argentina, and Germany. *J. Geophys. Res.* **2016**, *121* (22), 13559−13576.
(347) O'Sullivan, D.; Murray, B. J.; Malkin, T. L.; Whale, T. F.; Umo, N. S.; Atkinson, J. D.; Price, H. C.; Baustian, K. J.; Browse, J.; Webb, M. E. Ice nucleation by fertile soil dusts: relative importance of mineral and biogenic components. *Atmos. Chem. Phys.* **2014**, *14* (4), 1853−1867.
(348) Hill, T. C. J.; DeMott, P. J.; Tobo, Y.; Fröhlich-Nowoisky, J.; Moffett, B. F.; Franc, G. D.; Kreidenweis, S. M. Sources of organic ice nucleating particles in soils. *Atmos. Chem. Phys.* **2016**, *16* (11), 7195−7211.
(349) Fornea, A. P.; Brooks, S. D.; Dooley, J. B.; Saha, A. Heterogeneous freezing of ice on atmospheric aerosols containing ash, soot, and soil. *J. Geophys. Res.* **2009**, *114*, D13201.
(350) Schnell, R. C.; Vali, G. World-wide source of leaf derived freezing nuclei. *Nature* **1973**, *246* (5430), 212−213.
(351) Schnell, R. C.; Vali, G. Atmospheric ice nuclei from decomposing vegetation. *Nature* **1972**, *236* (5343), 163−165.
(352) Hiranuma, N.; Möhler, O.; Yamashita, K.; Tajiri, T.; Saito, A.; Kiselev, A.; Hoffmann, N.; Hoose, C.; Jantsch, E.; Koop, T.; Murakami, M. Ice nucleation by cellulose and its potential contribution to ice formation in clouds. *Nat. Geosci.* **2015**, *8* (4), 273−277.
(353) Du, R.; Ariya, P. A. The test freezing temperature of C(2)-C(6) dicarboxylic acid: The important indicator for ice nucleation processes. *Chin. Sci. Bull.* **2008**, *53* (17), 2685−2691.
(354) Prenni, A. J.; DeMott, P. J.; Kreidenweis, S. M.; Sherman, D. E.; Russell, L. M.; Ming, Y. The effects of low molecular weight dicarboxylic acids on cloud formation. *J. Phys. Chem. A* **2001**, *105* (50), 11240−11248.
(355) Koop, T.; Zobrist, B. Parameterizations for ice nucleation in biological and atmospheric systems. *Phys. Chem. Chem. Phys.* **2009**, *11* (46), 10839−10850.
(356) Zobrist, B.; Marcolli, C.; Peter, T.; Koop, T. Heterogeneous ice nucleation in aqueous solutions: the role of water activity. *J. Phys. Chem. A* **2008**, *112* (17), 3965−3975.
(357) Kanji, Z. A.; Florea, O.; Abbatt, J. P. D. Ice formation via deposition nucleation on mineral dust and organics: dependence of onset relative humidity on total particulate surface area. *Environ. Res. Lett.* **2008**, *3*, 025004.
(358) Wilson, T. W.; Murray, B. J.; Wagner, R.; Möhler, O.; Saathoff, H.; Schnaiter, M.; Skrotzki, J.; Price, H. C.; Malkin, T. L.; Dobbie, S.; Al-Jumur, S. M. R. K. Glassy aerosols with a range of compositions nucleate ice heterogeneously at cirrus temperatures. *Atmos. Chem. Phys.* **2012**, *12* (18), 8611−8632.
(359) Schill, G. P.; Tolbert, M. A. Depositional Ice Nucleation on Monocarboxylic Acids: Effect of the O:C Ratio. *J. Phys. Chem. A* **2012**, *116* (25), 6817−6822.
(360) Rigg, Y. J.; Alpert, P. A.; Knopf, D. A. Immersion freezing of water and aqueous ammonium sulfate droplets initiated by humic-like substances as a function of water activity. *Atmos. Chem. Phys.* **2013**, *13* (13), 6603−6622.
(361) Primm, K. M.; Schill, G. P.; Veghte, D. P.; Freedman, M. A.; Tolbert, M. A. Depositional ice nucleation on NX Illite and mixtures of NX Illite with organic acids. *J. Atmos. Chem.* **2017**, *74* (1), 55−69.
(362) Murray, B. J. Inhibition of ice crystallisation in highly viscous aqueous organic acid droplets. *Atmos. Chem. Phys.* **2008**, *8* (17), 5423−5433.
(363) Zobrist, B.; Marcolli, C.; Koop, T.; Luo, B. P.; Murphy, D. M.; Lohmann, U.; Zardini, A. A.; Krieger, U. K.; Corti, T.; Cziczo, D. J.; Fueglistaler, S.; Hudson, P. K.; Thomson, D. S.; Peter, T. Oxalic acid as a heterogeneous ice nucleus in the upper troposphere and its indirect aerosol effect. *Atmos. Chem. Phys.* **2006**, *6*, 3115−3129.
(364) DeMott, P. J.; Petters, M. D.; Prenni, A. J.; Carrico, C. M.; Kreidenweis, S. M.; Collett, J. L.; Moosmuller, H. Ice nucleation behavior of biomass combustion particles at cirrus temperatures. *J. Geophys. Res.* **2009**, *114*, D16205.
(365) Petters, M. D.; Parsons, M. T.; Prenni, A. J.; DeMott, P. J.; Kreidenweis, S. M.; Carrico, C. M.; Sullivan, A. P.; McMeeking, G. R.; Levin, E.; Wold, C. E.; Collett, J. L.; Moosmuller, H. Ice nuclei emissions from biomass burning. *J. Geophys. Res.* **2009**, *114*, D07209.
(366) Levin, E. J. T.; McMeeking, G. R.; DeMott, P. J.; McCluskey, C. S.; Carrico, C. M.; Nakao, S.; Jayarathne, T.; Stone, E. A.; Stockwell, C. E.; Yokelson, R. J.; Kreidenweis, S. M. Ice-nucleating particle emissions from biomass combustion and the potential importance of soot aerosol. *J. Geophys. Res.* **2016**, *121* (10), 5888−5903.
(367) Prenni, A. J.; Petters, M. D.; Faulhaber, A.; Carrico, C. M.; Ziemann, P. J.; Kreidenweis, S. M.; DeMott, P. J. Heterogeneous ice

DOI: 10.1021/acsearthspacechem.7b00120
ACS Earth Space Chem. 2018, 2, 168−202

nucleation measurements of secondary organic aerosol generated from ozonolysis of alkenes. *Geophys. Res. Lett.* **2009**, *36* (6), L06808.
(368) Wagner, R.; Hohler, K.; Huang, W.; Kiselev, A.; Möhler, O.; Mohr, C.; Pajunoja, A.; Saathoff, H.; Schiebel, T.; Shen, X. L.; Virtanen, A. Heterogeneous ice nucleation of α-pinene SOA particles before and after ice cloud processing. *J. Geophys. Res.-Atmos.* **2017**, *122* (9), 4924−4943.
(369) Gao, S.; Ng, N. L.; Keywood, M.; Varutbangkul, V.; Bahreini, R.; Nenes, A.; He, J. W.; Yoo, K. Y.; Beauchamp, J. L.; Hodyss, R. P.; Flagan, R. C.; Seinfeld, J. H. Particle phase acidity and oligomer formation in secondary organic aerosol. *Environ. Sci. Technol.* **2004**, *38* (24), 6582−6589.
(370) Tolocka, M. P.; Jang, M.; Ginter, J. M.; Cox, F. J.; Kamens, R. M.; Johnston, M. V. Formation of oligomers in secondary organic aerosol. *Environ. Sci. Technol.* **2004**, *38* (5), 1428−1434.
(371) Graber, E. R.; Rudich, Y. Atmospheric HULIS: How humic-like are they? A comprehensive and critical review. *Atmos. Chem. Phys.* **2006**, *6* (3), 729−753.
(372) Kanji, Z. A.; Florea, O.; Abbatt, J. P. D. Ice formation via deposition nucleation on mineral dust and organics: dependence of onset relative humidity on total particulate surface area. *Environ. Res. Lett.* **2008**, *3* (2), 025004.
(373) Knopf, D. A.; Alpert, P. A. Water Activity Based Model of Heterogeneous Ice Nucleation Kinetics for Freezing of Water and Aqueous Solution Droplets. *Faraday Discuss.* **2013**, *165*, 513−534.
(374) Rudich, Y.; Donahue, N. M.; Mentel, T. F. Aging of organic aerosol: Bridging the gap between laboratory and field studies. *Annu. Rev. Phys. Chem.* **2007**, *58*, 321−352.
(375) Rudich, Y. Laboratory perspectives on the chemical transformations of organic matter in atmospheric particles. *Chem. Rev.* **2003**, *103* (12), 5097−5124.
(376) Taraniuk, I.; Rudich, Y.; Graber, E. R. Hydration-Influenced Sorption of Organic Compounds by Model and Atmospheric Humic-Like Substances (HULIS). *Environ. Sci. Technol.* **2009**, *43* (6), 1811−1817.
(377) Slade, J. H.; Shiraiwa, M.; Arangio, A.; Su, H.; Pöschl, U.; Wang, J.; Knopf, D. A. Cloud droplet activation through oxidation of organic aerosol influenced by temperature and particle phase state. *Geophys. Res. Lett.* **2017**, *44* (3), 1583−1591.
(378) Augustin, S.; Wex, H.; Niedermeier, D.; Pummer, B.; Grothe, H.; Hartmann, S.; Tomsche, L.; Clauss, T.; Voigtlaender, J.; Ignatius, K.; Stratmann, F. Immersion freezing of birch pollen washing water. *Atmos. Chem. Phys.* **2013**, *13* (21), 10989−11003.
(379) Fröhlich-Nowoisky, J.; Hill, T. C. J.; Pummer, B. G.; Yordanova, P.; Franc, G. D.; Pöschl, U. Ice nucleation activity in the widespread soil fungus Mortierella alpina. *Biogeosciences* **2015**, *12* (4), 1057−1071.
(380) Pummer, B. G.; Bauer, H.; Bernardi, J.; Chazallon, B.; Facq, S.; Lendl, B.; Whitmore, K.; Grothe, H. Chemistry and morphology of dried-up pollen suspension residues. *J. Raman Spectrosc.* **2013**, *44* (12), 1654−1658.
(381) Sicard, M.; Izquierdo, R.; Alarcon, M.; Belmonte, J.; Comeron, A.; Baldasano, J. M. Near-surface and columnar measurements with a micro pulse lidar of atmospheric pollen in Barcelona, Spain. *Atmos. Chem. Phys.* **2016**, *16* (11), 6805−6821.
(382) Yttri, K. E.; Dye, C.; Kiss, G. Ambient aerosol concentrations of sugars and sugar-alcohols at four different sites in Norway. *Atmos. Chem. Phys.* **2007**, *7* (16), 4267−4279.
(383) Rathnayake, C. M.; Metwali, N.; Jayarathne, T.; Kettler, J.; Huang, Y. F.; Thorne, P. S.; O'Shaughnessy, P. T.; Stone, E. A. Influence of rain on the abundance of bioaerosols in fine and coarse particles. *Atmos. Chem. Phys.* **2017**, *17* (3), 2459−2475.
(384) Hawkins, L. N.; Russell, L. M. Polysaccharides, Proteins, and Phytoplankton Fragments: Four Chemically Distinct Types of Marine Primary Organic Aerosol Classified by Single Particle Spectromicroscopy. *Adv. Meteol.* **2010**, *2010*, 612132.
(385) Burrows, S. M.; Hoose, C.; Pöschl, U.; Lawrence, M. G. Ice nuclei in marine air: biogenic particles or dust? *Atmos. Chem. Phys.* **2013**, *13* (1), 245−267.
(386) Yun, Y. X.; Penner, J. E. An evaluation of the potential radiative forcing and climatic impact of marine organic aerosols as heterogeneous ice nuclei. *Geophys. Res. Lett.* **2013**, *40* (15), 4121−4126.
(387) Alpert, P. A.; Aller, J. Y.; Knopf, D. A. Ice nucleation from aqueous NaCl droplets with and without marine diatoms. *Atmos. Chem. Phys.* **2011**, *11* (12), 5539−5555.
(388) Alpert, P. A.; Aller, J. Y.; Knopf, D. A. Initiation of the ice phase by marine biogenic surfaces in supersaturated gas and supercooled aqueous phases. *Phys. Chem. Chem. Phys.* **2011**, *13* (44), 19882−19894.
(389) Knopf, D. A.; Alpert, P. A.; Wang, B.; Aller, J. Y. Stimulation of ice nucleation by marine diatoms. *Nat. Geosci.* **2011**, *4* (2), 88−90.
(390) Ladino, L. A.; Yakobi-Hancock, J. D.; Kilthau, W. P.; Mason, R. H.; Si, M.; Li, J.; Miller, L. A.; Schiller, C. L.; Huffman, J. A.; Aller, J. Y.; Knopf, D. A.; Bertram, A. K.; Abbatt, J. P. D. Addressing the ice nucleating abilities of marine aerosol: A combination of deposition mode laboratory and field measurements. *Atmos. Environ.* **2016**, *132*, 1−10.
(391) Aller, J. Y.; Radway, J. C.; Kilthau, W. P.; Bothe, D. W.; Wilson, T. W.; Vaillancourt, R. D.; Quinn, P. K.; Coffman, D. J.; Murray, B. J.; Knopf, D. A. Size-resolved characterization of the polysaccharidic and proteinaceous components of sea spray aerosol. *Atmos. Environ.* **2017**, *154*, 331−347.
(392) McCluskey, C. S.; Hill, T. C. J.; Malfatti, F.; Sultana, C. M.; Lee, C.; Santander, M. V.; Beall, C. M.; Moore, K. A.; Cornwell, G. C.; Collins, D. B.; Prather, K. A.; Jayarathne, T.; Stone, E. A.; Azam, F.; Kreidenweis, S. M.; DeMott, P. J. A Dynamic Link between Ice Nucleating Particles Released in Nascent Sea Spray Aerosol and Oceanic Biological Activity during Two Mesocosm Experiments. *J. Atmos. Sci.* **2017**, *74* (1), 151−166.
(393) Archuleta, C. M.; DeMott, P. J.; Kreidenweis, S. M. Ice nucleation by surrogates for atmospheric mineral dust and mineral dust/sulfate particles at cirrus temperatures. *Atmos. Chem. Phys.* **2005**, *5* (10), 2617−2634.
(394) Augustin-Bauditz, S.; Wex, H.; Kanter, S.; Ebert, M.; Niedermeier, D.; Stolz, F.; Prager, A.; Stratmann, F. The immersion mode ice nucleation behavior of mineral dusts: A comparison of different pure and surface modified dusts. *Geophys. Res. Lett.* **2014**, *41* (20), 7375−7382.
(395) Kulkarni, G.; Sanders, C.; Zhang, K.; Liu, X.; Zhao, C. Ice nucleation of bare and sulfuric acid-coated mineral dust particles and implication for cloud properties. *J. Geophys. Res.* **2014**, *119* (16), 9993−10011.
(396) Kulkarni, G.; Zhang, K.; Zhao, C.; Nandasiri, M.; Shutthanandan, V.; Liu, X.; Fast, J.; Berg, L. Ice formation on nitric acid-coated dust particles: Laboratory and modeling studies. *J. Geophys. Res.* **2015**, *120* (15), 7682−7698.
(397) Reitz, P.; Spindler, C.; Mentel, T. F.; Poulain, L.; Wex, H.; Mildenberger, K.; Niedermeier, D.; Hartmann, S.; Clauss, T.; Stratmann, F.; Sullivan, R. C.; DeMott, P. J.; Petters, M. D.; Sierau, B.; Schneider, J. Surface modification of mineral dust particles by sulphuric acid processing: implications for ice nucleation abilities. *Atmos. Chem. Phys.* **2011**, *11* (15), 7839−7858.
(398) Tobo, Y.; DeMott, P. J.; Raddatz, M.; Niedermeier, D.; Hartmann, S.; Kreidenweis, S. M.; Stratmann, F.; Wex, H. Impacts of chemical reactivity on ice nucleation of kaolinite particles: A case study of levoglucosan and sulfuric acid. *Geophys. Res. Lett.* **2012**, *39* (19), L19803.
(399) Wex, H.; DeMott, P. J.; Tobo, Y.; Hartmann, S.; Rösch, M.; Clauss, T.; Tomsche, L.; Niedermeier, D.; Stratmann, F. Kaolinite particles as ice nuclei: learning from the use of different kaolinite samples and different coatings. *Atmos. Chem. Phys.* **2014**, *14* (11), 5529−5546.
(400) Tang, M. J.; Cziczo, D. J.; Grassian, V. H. Interactions of Water with Mineral Dust Aerosol: Water Adsorption, Hygroscopicity, Cloud Condensation, and Ice Nucleation. *Chem. Rev.* **2016**, *116* (7), 4205−4259.

DOI: 10.1021/acsearthspacechem.7b00120
ACS Earth Space Chem. 2018, 2, 168−202

(401) Eastwood, M. L.; Cremel, S.; Wheeler, M.; Murray, B. J.; Girard, E.; Bertram, A. K. Effects of sulfuric acid and ammonium sulfate coatings on the ice nucleation properties of kaolinite particles. *Geophys. Res. Lett.* **2009**, *36*, L02811.
(402) Chernoff, D. I.; Bertram, A. K. Effects of sulfate coatings on the ice nucleation properties of a biological ice nucleus and several types of minerals. *J. Geophys. Res.* **2010**, *115*, D20205.
(403) Bond, T. C.; Doherty, S. J.; Fahey, D. W.; Forster, P. M.; Berntsen, T.; DeAngelo, B. J.; Flanner, M. G.; Ghan, S.; Kärcher, B.; Koch, D.; Kinne, S.; Kondo, Y.; Quinn, P. K.; Sarofim, M. C.; Schultz, M. G.; Schulz, M.; Venkataraman, C.; Zhang, H.; Zhang, S.; Bellouin, N.; Guttikunda, S. K.; Hopke, P. K.; Jacobson, M. Z.; Kaiser, J. W.; Klimont, Z.; Lohmann, U.; Schwarz, J. P.; Shindell, D.; Storelvmo, T.; Warren, S. G.; Zender, C. S. Bounding the role of black carbon in the climate system: A scientific assessment. *J. Geophys. Res.* **2013**, *118* (11), 5380−5552.
(404) China, S.; Scarnato, B.; Owen, R. C.; Zhang, B.; Ampadu, M. T.; Kumar, S.; Dzepina, K.; Dziobak, M. P.; Fialho, P.; Perlinger, J. A.; Hueber, J.; Helmig, D.; Mazzoleni, L. R.; Mazzoleni, C. Morphology and mixing state of aged soot particles at a remote marine free troposphere site: Implications for optical properties. *Geophys. Res. Lett.* **2015**, *42* (4), 1243−1250.
(405) China, S.; Mazzoleni, C.; Gorkowski, K.; Aiken, A. C.; Dubey, M. K. Morphology and mixing state of individual freshly emitted wildfire carbonaceous particles. *Nat. Commun.* **2013**, *4*, 2122.
(406) Dzepina, K.; Mazzoleni, C.; Fialho, P.; China, S.; Zhang, B.; Owen, R. C.; Helmig, D.; Hueber, J.; Kumar, S.; Perlinger, J. A.; Kramer, L. J.; Dziobak, M. P.; Ampadu, M. T.; Olsen, S.; Wuebbles, D. J.; Mazzoleni, L. R. Molecular characterization of free tropospheric aerosol collected at the Pico Mountain Observatory: a case study with a long-range transported biomass burning plume. *Atmos. Chem. Phys.* **2015**, *15* (9), 5047−5068.
(407) China, S.; Kulkarni, G.; Scarnato, B. V.; Sharma, N.; Pekour, M.; Shilling, J. E.; Wilson, J.; Zelenyuk, A.; Chand, D.; Liu, S.; Aiken, A. C.; Dubey, M.; Laskin, A.; Zaveri, R. A.; Mazzoleni, C. Morphology of diesel soot residuals from supercooled water droplets and ice crystals: implications for optical properties. *Environ. Res. Lett.* **2015**, *10* (11), 114010.
(408) Ullrich, R.; Hoose, C.; Möhler, O.; Niemand, M.; Wagner, R.; Hohler, K.; Hiranuma, N.; Saathoff, H.; Leisner, T. A New Ice Nucleation Active Site Parameterization for Desert Dust and Soot. *J. Atmos. Sci.* **2017**, *74* (3), 699−717.
(409) Friedman, B.; Kulkarni, G.; Beranek, J.; Zelenyuk, A.; Thornton, J. A.; Cziczo, D. J. Ice nucleation and droplet formation by bare and coated soot particles. *J. Geophys. Res.* **2011**, *116*, D17203.
(410) Chou, C.; Kanji, Z. A.; Stetzer, O.; Tritscher, T.; Chirico, R.; Heringa, M. F.; Weingartner, E.; Prévôt, A. S. H.; Baltensperger, U.; Lohmann, U. Effect of photochemical ageing on the ice nucleation properties of diesel and wood burning particles. *Atmos. Chem. Phys.* **2013**, *13* (2), 761−772.
(411) Kulkarni, G.; China, S.; Liu, S.; Nandasiri, M.; Sharma, N.; Wilson, J.; Aiken, A. C.; Chand, D.; Laskin, A.; Mazzoleni, C.; Pekour, M.; Shilling, J.; Shutthanandan, V.; Zelenyuk, A.; Zaveri, R. A. Ice nucleation activity of diesel soot particles at cirrus relevant temperature conditions: Effects of hydration, secondary organics coating, soot morphology, and coagulation. *Geophys. Res. Lett.* **2016**, *43* (7), 3580−3588.
(412) Schill, G. P.; Jathar, S. H.; Kodros, J. K.; Levin, E. J. T.; Galang, A. M.; Friedman, B.; Link, M. F.; Farmer, D. K.; Pierce, J. R.; Kreidenweis, S. M.; DeMott, P. J. Ice-nucleating particle emissions from photochemically aged diesel and biodiesel exhaust. *Geophys. Res. Lett.* **2016**, *43* (10), 5524−5531.
(413) Liu, P. F.; Li, Y. J.; Wang, Y.; Gilles, M. K.; Zaveri, R. A.; Bertram, A. K.; Martin, S. T. Lability of secondary organic particulate matter. *Proc. Natl. Acad. Sci. U. S. A.* **2016**, *113* (45), 12643−12648.
(414) Yli-Juuti, T.; Pajunoja, A.; Tikkanen, O. P.; Buchholz, A.; Faiola, C.; Vaisanen, O.; Hao, L. Q.; Kari, E.; Perakyla, O.; Garmash, O.; Shiraiwa, M.; Ehn, M.; Lehtinen, K.; Virtanen, A. Factors controlling the evaporation of secondary organic aerosol from α-pinene ozonolysis. *Geophys. Res. Lett.* **2017**, *44* (5), 2562−2570.
(415) Saha, P. K.; Khlystov, A.; Yahya, K.; Zhang, Y.; Xu, L.; Ng, N. L.; Grieshop, A. P. Quantifying the volatility of organic aerosol in the southeastern US. *Atmos. Chem. Phys.* **2017**, *17* (1), 501−520.
(416) Giorio, C.; Monod, A.; Bregonzio-Rozier, L.; DeWitt, H. L.; Cazaunau, M.; Temime-Roussel, B.; Gratien, A.; Michoud, V.; Pangui, E.; Ravier, S.; Zielinski, A. T.; Tapparo, A.; Vermeylen, R.; Claeys, M.; Voisin, D.; Kalberer, M.; Doussin, J. F. Cloud Processing of Secondary Organic Aerosol from Isoprene and Methacrolein Photooxidation. *J. Phys. Chem. A* **2017**, *121* (40), 7641−7654.
(417) Boyd, C. M.; Nah, T.; Xu, L.; Berkemeier, T.; Ng, N. L. Secondary Organic Aerosol (SOA) from Nitrate Radical Oxidation of Monoterpenes: Effects of Temperature, Dilution, and Humidity on Aerosol Formation, Mixing, and Evaporation. *Environ. Sci. Technol.* **2017**, *51* (14), 7831−7841.
(418) Wilson, J.; Imre, D.; Beranek, J.; Shrivastava, M.; Zelenyuk, A. Evaporation Kinetics of Laboratory-Generated Secondary Organic Aerosols at Elevated Relative Humidity. *Environ. Sci. Technol.* **2015**, *49* (1), 243−249.
(419) Moise, T.; Flores, J. M.; Rudich, Y. Optical properties of secondary organic aerosols and their changes by chemical processes. *Chem. Rev.* **2015**, *115* (10), 4400−4439.
(420) Pöschl, U.; Shiraiwa, M. Multiphase Chemistry at the Atmosphere-Biosphere Interface Influencing Climate and Public Health in the Anthropocene. *Chem. Rev.* **2015**, *115* (10), 4440−4475.
(421) Pöschl, U. Atmospheric aerosols: Composition, transformation, climate and health effects. *Angew. Chem., Int. Ed.* **2005**, *44* (46), 7520−7540.
(422) Slade, J. H.; Knopf, D. A. Heterogeneous OH oxidation of biomass burning organic aerosol surrogate compounds: assessment of volatilisation products and the role of OH concentration on the reactive uptake kinetics. *Phys. Chem. Chem. Phys.* **2013**, *15* (16), 5898−5915.
(423) Shiraiwa, M.; Pöschl, U.; Knopf, D. A. Multiphase Chemical Kinetics of NO_3 Radicals Reacting with Organic Aerosol Components from Biomass Burning. *Environ. Sci. Technol.* **2012**, *46* (12), 6630−6636.
(424) Knopf, D. A.; Forrester, S. M.; Slade, J. H. Heterogeneous oxidation kinetics of organic biomass burning aerosol surrogates by O_3, NO_2, N_2O_5, and NO_3. *Phys. Chem. Chem. Phys.* **2011**, *13* (47), 21050−21062.
(425) Brooks, S. D.; Suter, K.; Olivarez, L. Effects of Chemical Aging on the Ice Nucleation Activity of Soot and Polycyclic Aromatic Hydrocarbon Aerosols. *J. Phys. Chem. A* **2014**, *118* (43), 10036−10047.
(426) Renbaum, L. H.; Smith, G. D. The importance of phase in the radical-initiated oxidation of model organic aerosols: reactions of solid and liquid brassidic acid particles. *Phys. Chem. Chem. Phys.* **2009**, *11* (14), 2441−2451.
(427) Shiraiwa, M.; Ammann, M.; Koop, T.; Pöschl, U. Gas uptake and chemical aging of semisolid organic aerosol particles. *Proc. Natl. Acad. Sci. U. S. A.* **2011**, *108* (27), 11003−11008.
(428) Arangio, A. M.; Slade, J. H.; Berkemeier, T.; Pöschl, U.; Knopf, D. A.; Shiraiwa, M. Multiphase Chemical Kinetics of OH Radical Uptake by Molecular Organic Markers of Biomass Burning Aerosols: Humidity and Temperature Dependence, Surface Reaction, and Bulk Diffusion. *J. Phys. Chem. A* **2015**, *119* (19), 4533−4544.
(429) Slade, J. H.; Knopf, D. A. Multiphase OH oxidation kinetics of organic aerosol: The role of particle phase state and relative humidity. *Geophys. Res. Lett.* **2014**, *41* (14), 5297−5306.
(430) Kroll, J. H.; Lim, C. Y.; Kessler, S. H.; Wilson, K. R. Heterogeneous Oxidation of Atmospheric Organic Aerosol: Kinetics of Changes to the Amount and Oxidation State of Particle-Phase Organic Carbon. *J. Phys. Chem. A* **2015**, *119* (44), 10767−10783.
(431) Kessler, S. H.; Nah, T.; Daumit, K. E.; Smith, J. D.; Leone, S. R.; Kolb, C. E.; Worsnop, D. R.; Wilson, K. R.; Kroll, J. H. OH-Initiated Heterogeneous Aging of Highly Oxidized Organic Aerosol. *J. Phys. Chem. A* **2012**, *116* (24), 6358−6365.

DOI: 10.1021/acsearthspacechem.7b00120
ACS Earth Space Chem. 2018, 2, 168−202

(432) Mikhailov, E.; Vlasenko, S.; Rose, D.; Pöschl, U. Mass-based hygroscopicity parameter interaction model and measurement of atmospheric aerosol water uptake. *Atmos. Chem. Phys.* **2013**, *13* (2), 717−740.
(433) Ruehl, C. R.; Davies, J. F.; Wilson, K. R. An interfacial mechanism for cloud droplet formation on organic aerosols. *Science* **2016**, *351*, 1447−1450.
(434) Pathak, R. K.; Stanier, C. O.; Donahue, N. M.; Pandis, S. N. Ozonolysis of a-pinene at atmospherically relevant concentrations: Temperature dependence of aerosol mass fractions (yields). *J. Geophys. Res.* **2007**, *112* (D3), D03201.
(435) Warren, B.; Austin, R. L.; Cocker, D. R. Temperature dependence of secondary organic aerosol. *Atmos. Environ.* **2009**, *43* (22−23), 3548−3555.
(436) Saathoff, H.; Naumann, K. H.; Möhler, O.; Jonsson, A. M.; Hallquist, M.; Kiendler-Scharr, A.; Mentel, T. F.; Tillmann, R.; Schurath, U. Temperature dependence of yields of secondary organic aerosols from the ozonolysis of α-pinene and limonene. *Atmos. Chem. Phys.* **2009**, *9* (5), 1551−1577.
(437) Kristensen, K.; Jensen, L. N.; Glasius, M.; Bilde, M. The effect of sub-zero temperature on the formation and composition of secondary organic aerosol from ozonolysis of α-pinene. *Environ. Sci.: Processes Impacts* **2017**, *19*, 1220−1234.
(438) Hallquist, M.; Wenger, J. C.; Baltensperger, U.; Rudich, Y.; Simpson, D.; Claeys, M.; Dommen, J.; Donahue, N. M.; George, C.; Goldstein, A. H.; Hamilton, J. F.; Herrmann, H.; Hoffmann, T.; Iinuma, Y.; Jang, M.; Jenkin, M. E.; Jimenez, J. L.; Kiendler-Scharr, A.; Maenhaut, W.; McFiggans, G.; Mentel, T. F.; Monod, A.; Prevot, A. S. H.; Seinfeld, J. H.; Surratt, J. D.; Szmigielski, R.; Wildt, J. The formation, properties and impact of secondary organic aerosol: current and emerging issues. *Atmos. Chem. Phys.* **2009**, *9* (14), 5155−5236.
(439) Massoli, P.; Lambe, A. T.; Ahern, A. T.; Williams, L. R.; Ehn, M.; Mikkila, J.; Canagaratna, M. R.; Brune, W. H.; Onasch, T. B.; Jayne, J. T.; Petaja, T.; Kulmala, M.; Laaksonen, A.; Kolb, C. E.; Davidovits, P.; Worsnop, D. R. Relationship between aerosol oxidation level and hygroscopic properties of laboratory generated secondary organic aerosol (SOA) particles. *Geophys. Res. Lett.* **2010**, *37*, L24801.
(440) Pajunoja, A.; Lambe, A. T.; Hakala, J.; Rastak, N.; Cummings, M. J.; Brogan, J. F.; Hao, L. Q.; Paramonov, M.; Hong, J.; Prisle, N. L.; Malila, J.; Romakkaniemi, S.; Lehtinen, K. E. J.; Laaksonen, A.; Kulmala, M.; Massoli, P.; Onasch, T. B.; Donahue, N. M.; Riipinen, I.; Davidovits, P.; Worsnop, D. R.; Petaja, T.; Virtanen, A. Adsorptive uptake of water by semisolid secondary organic aerosols. *Geophys. Res. Lett.* **2015**, *42* (8), 3063−3068.
(441) Ickes, L.; Welti, A.; Lohmann, U. Classical nucleation theory of immersion freezing: sensitivity of contact angle schemes to thermodynamic and kinetic parameters. *Atmos. Chem. Phys.* **2017**, *17* (3), 1713−1739.
(442) Beydoun, H.; Polen, M.; Sullivan, R. C. Effect of particle surface area on ice active site densities retrieved from droplet freezing spectra. *Atmos. Chem. Phys.* **2016**, *16* (20), 13359−13378.
(443) Wheeler, M. J.; Bertram, A. K. Deposition nucleation on mineral dust particles: a case against classical nucleation theory with the assumption of a single contact angle. *Atmos. Chem. Phys.* **2012**, *12* (2), 1189−1201.
(444) Niedermeier, D.; Shaw, R. A.; Hartmann, S.; Wex, H.; Clauss, T.; Voigtlaender, J.; Stratmann, F. Heterogeneous ice nucleation: exploring the transition from stochastic to singular freezing behavior. *Atmos. Chem. Phys.* **2011**, *11* (16), 8767−8775.
(445) Murray, B. J.; Broadley, S. L.; Wilson, T. W.; Atkinson, J. D.; Wills, R. H. Heterogeneous freezing of water droplets containing kaolinite particles. *Atmos. Chem. Phys.* **2011**, *11* (9), 4191−4207.
(446) Vali, G.; Snider, J. R. Time-dependent freezing rate parcel model. *Atmos. Chem. Phys.* **2015**, *15* (4), 2071−2079.
(447) Marcolli, C.; Gedamke, S.; Peter, T.; Zobrist, B. Efficiency of immersion mode ice nucleation on surrogates of mineral dust. *Atmos. Chem. Phys.* **2007**, *7* (19), 5081−5091.
(448) Lüönd, F.; Stetzer, O.; Welti, A.; Lohmann, U. Experimental study on the ice nucleation ability of size-selected kaolinite particles in the immersion mode. *J. Geophys. Res.* **2010**, *115*, D14201.
(449) Vali, G. Quantitative evaluation of experimental results on heterogeneous freezing nucleation of supercooled liquids. *J. Atmos. Sci.* **1971**, *28* (3), 402−409.
(450) Connolly, P. J.; Möhler, O.; Field, P. R.; Saathoff, H.; Burgess, R.; Choularton, T.; Gallagher, M. Studies of heterogeneous freezing by three different desert dust samples. *Atmos. Chem. Phys.* **2009**, *9* (8), 2805−2824.
(451) Vali, G. Repeatability and randomness in heterogeneous freezing nucleation. *Atmos. Chem. Phys.* **2008**, *8* (16), 5017−5031.
(452) Ervens, B.; Feingold, G. Sensitivities of immersion freezing: Reconciling classical nucleation theory and deterministic expressions. *Geophys. Res. Lett.* **2013**, *40* (12), 3320−3324.
(453) Ervens, B.; Feingold, G. On the representation of immersion and condensation freezing in cloud models using different nucleation schemes. *Atmos. Chem. Phys.* **2012**, *12* (13), 5807−5826.
(454) Westbrook, C. D.; Illingworth, A. J. The formation of ice in a long-lived supercooled layer cloud. *Q. J. R. Meteorol. Soc.* **2013**, *139* (677), 2209−2221.
(455) Wang, Y.; Liu, X.; Hoose, C.; Wang, B. Different contact angle distributions for heterogeneous ice nucleation in the Community Atmospheric Model version 5. *Atmos. Chem. Phys.* **2014**, *14* (19), 10411−10430.
(456) English, J. M.; Kay, J. E.; Gettelman, A.; Liu, X. H.; Wang, Y.; Zhang, Y. Y.; Chepfer, H. Contributions of Clouds, Surface Albedos, and Mixed-Phase Ice Nucleation Schemes to Arctic Radiation Biases in CAM5. *J. Clim.* **2014**, *27* (13), 5174−5197.
(457) Spichtinger, P.; Cziczo, D. J. Aerosol-cloud interactions - a challenge for measurements and modeling at the cutting edge of cloud-climate interactions. *Environ. Res. Lett.* **2008**, *3* (2), 025002.
(458) Peter, T.; Marcolli, C.; Spichtinger, P.; Corti, T.; Baker, M. B.; Koop, T. When dry air is too humid. *Science* **2006**, *314*, 1399−1402.
(459) Bergeron, T. On the physics of cloud and precipitation. *Proc. 5th Assembly U.G.G.I. Lisbon* **1935**, *2*, 156.
(460) Findeisen, W. Die kolloidmeteorologischen Vorgänge bei der Niederschlagsbildung (Colloidal meteorological processes in the formation of precipitation). *Met. Z.* **1938**, *55*, 121.
(461) Wegener, A. *Thermodynamik der Atmosphäre*; Barth: Leipzig, Germany, **1911**.
(462) Broadley, S. L.; Murray, B. J.; Herbert, R. J.; Atkinson, J. D.; Dobbie, S.; Malkin, T. L.; Condliffe, E.; Neve, L. Immersion mode heterogeneous ice nucleation by an Illite rich powder representative of atmospheric mineral dust. *Atmos. Chem. Phys.* **2012**, *12* (1), 287−307.
(463) Avramov, A.; Ackerman, A. S.; Fridlind, A. M.; van Diedenhoven, B.; Botta, G.; Aydin, K.; Verlinde, J.; Korolev, A. V.; Strapp, J. W.; McFarquhar, G. M.; Jackson, R.; Brooks, S. D.; Glen, A.; Wolde, M. Toward ice formation closure in Arctic mixed-phase boundary layer clouds during ISDAC. *J. Geophys. Res.* **2011**, *116*, D00T08.
(464) Ovchinnikov, M.; Ackerman, A. S.; Avramov, A.; Cheng, A. N.; Fan, J. W.; Fridlind, A. M.; Ghan, S.; Harrington, J.; Hoose, C.; Korolev, A.; McFarquhar, G. M.; Morrison, H.; Paukert, M.; Savre, J.; Shipway, B. J.; Shupe, M. D.; Solomon, A.; Sulia, K. Intercomparison of large-eddy simulations of Arctic mixed-phase clouds: Importance of ice size distribution assumptions. *J. Adv. Model. Earth Syst.* **2014**, *6* (1), 223−248.
(465) Morrison, H.; Pinto, J. O.; Curry, J. A.; McFarquhar, G. M. Sensitivity of modeled arctic mixed-phase stratocumulus to cloud condensation and ice nuclei over regionally varying surface conditions. *J. Geophys. Res.* **2008**, *113* (D5), D05203.
(466) Niemand, M.; Möhler, O.; Vogel, B.; Vogel, H.; Hoose, C.; Connolly, P.; Klein, H.; Bingemer, H.; DeMott, P.; Skrotzki, J.; Leisner, T. A Particle-Surface-Area-Based Parameterization of Immersion Freezing on Desert Dust Particles. *J. Atmos. Sci.* **2012**, *69* (10), 3077−3092.
(467) Boose, Y.; Kanji, Z. A.; Kohn, M.; Sierau, B.; Zipori, A.; Crawford, I.; Lloyd, G.; Bukowiecki, N.; Herrmann, E.; Kupiszewski,

DOI: 10.1021/acsearthspacechem.7b00120
ACS Earth Space Chem. 2018, 2, 168−202

P.; Steinbacher, M.; Lohmann, U. Ice Nucleating Particle Measurements at 241 K during Winter Months at 3580m MSL in the Swiss Alps. *J. Atmos. Sci.* **2016**, 73 (5), 2203−2228.

DOI: 10.1021/acsearthspacechem.7b00120
ACS Earth Space Chem. 2018, 2, 168−202